Studies on a Stable Silicon–Silicon Triple Bond Species: Synthesis, Characterization, and Reactivity

Rei KINJO

February 2007

Studies on Chemistry of Silicon–Silicon Triple Bond Species: Synthesis, Characterization, and Reactivity

Rei KINJO

Submitted to the Graduate School of
Pure and Applied Sciences
in Partial Fulfillment of the Requirements
for the Degree of Doctor of Philosophy in Chemistry
at the
University of Tsukuba

A Table of Contents

Introduction

Organosilicon Chemistry

To understand the differences between carbon and heavier Group 14 elements is very important[1] since all scientific phenomena are based on the nature of element. The discovery of method to prepare Et_4Si by Friedel and Crafts established the silicon chemistry in 1863.[2] In 1904, F. S. Kipping discovered the convenient method for the preparation of organosilicon compounds by the reaction of silicon tetrachloride with various Grignard reagents.[3] This was the time to open the world of organosilicon chemistry. Furthermore, the establishment of direct process for preparation of halogenated organosilane derivatives by the reaction of methyl chloride with alloy of silicon and copper by E. G. Rochow in the second half of 1940's[4,5] made a rapid progress of silicone industry as well as fundamental organosilicon chemistry.[6] Silicon is positioned in Group 14 right under the carbon in the Periodic Table (Figure 0-1), and electronic configuration of its

1																	18
1 H	2											13	**14**	15	16	17	2 He
3 Li	4 Be											5 B	**6 C**	7 N	8 O	9 F	10 Ne
11 Na	12 Mg	3	4	5	6	7	8	9	10	11	12	13 Al	**14 Si**	15 P	16 S	17 Cl	18 Ar
19 K	20 Ca	21 Sc	22 Ti	23 V	24 Cr	25 Mn	26 Fe	27 Co	28 Ni	29 Cu	30 Zn	31 Ga	**32 Ge**	33 As	34 Se	35 Br	36 Kr
37 Rb	38 Sr	39 Y	40 Zr	41 CB	42 Mo	43 Tc	44 Ru	45 Rh	46 Pd	47 Ag	48 Cd	49 In	**50 Sn**	51 Sb	52 Te	53 I	54 Xe
55 Cs	56 Ba	57 La *	72 Hf	73 Ta	74 W	75 Re	76 Os	77 Ir	78 Pt	79 Au	80 Hg	81 Tl	**82 Pb**	83 Bi	84 Po	85 At	86 Rn
87 Fr	88 Ra	89 Ac |															

*	58 ce	59 Pr	60 Nd	61 Pm	62 Sm	63 Eu	64 Gd	65 Tb	66 Dy	67 Ho	68 Er	69 Tm	70 Yb	71 Lu
|	90 Th	91 Pa	92 U	93 Np	94 Pu	95 Am	96 Cm	97 Bk	98 Cf	99 E	100 Fm	101 Mv	102 No	103 Lw

Figure 0-1. Periodic Table.

outer shell is $3s^2 3p^2$. For this reason, silicon is expected to have similar properties to carbon. Actually, silicon forms numerous stable compounds, which have a tetrahedral structure, such as $SiMe_4$ and $SiCl_4$. However, due to the progress of organosilicon chemistry, it is became clear that there are many differences between silicon and carbon. For example, although unsaturated organic compounds, such as ethylene and acetylene, are generally stable and play an important role in organic chemistry, unsaturated species consisting of silicon atoms are highly reactive. This difference is also operating between carbon and other heavier Group 14 elements (Ge, Sn, and Pb). It is very important to have an insight into the origin of remarkable difference between them. To consider the size of valence *n*s and *n*p atomic orbitals is very useful for interpretation of this difference. The ground state electronic configuration of the Group 14 atoms is [core]ns^2np^2, with n = 2,3,4,5 and 6 for C, Si, Ge, Sn, and Pb, respectively.

As shown in Figure 0-2 and Table 0-1, there are some distinctions in the atomic properties of Group 14 elements.[7-11] Only for carbon, which is an element of the second row, 2s and 2p electrons show approximately the same spatial extension because the core electrons occupy only the 1s orbital. Meanwhile, for heavier Group 14 elements, the *n*p valence electrons (n>2) are spatially separated from *n*s valence electrons due to Pauli repulsion with the (n–1)p electrons in the inner shell. Therefore, it is difficult to hybridize between *n*s and *n*p obitals for heavier atoms. Actually, heavier Group 14 elements tend to preserve the valence *n*s electrons as core-like electrons in their compounds. In contrast, carbon shows a preference for an effective hybridization of the s and p atomic orbitals in order to take advantage of the strong overlap binding ability.

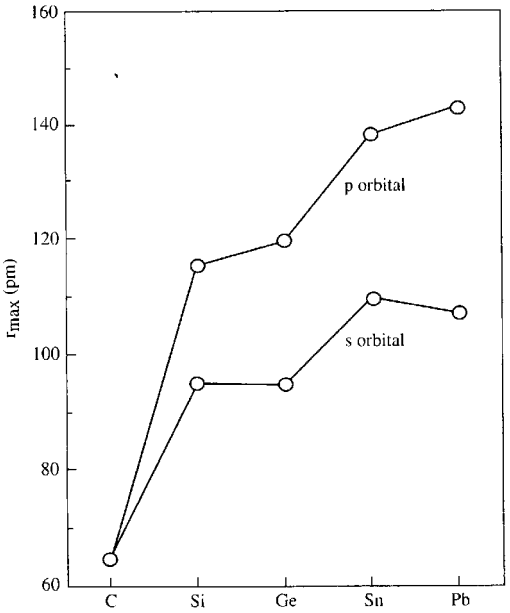

Figure 0-2. The sizes of the valence s and p orbitals of Group 14 atoms.

Table 0-1. Atomic Properties of the Group 14 Elements

Atom n	C 2	Si 3	Ge 4	Sn 5	Pb 6
Orbital energy					
ns	-19.39	-14.84	-15.52	-13.88	-15.41
np	-11.07	-7.57	-7.29	-6.71	-6.48
Ionization energy					
ns	16.60	13.64	14.43	13.49	16.04
np	11.26	8.15	7.90	7.39	7.53
Electron affinity	1.26	1.39	1.23	1.11	0.36
Polarizability	1.76	5.38	6.07	7.7	6.8
Electronegativity					
Mulliken	1.92	1.46	1.40	1.30	1.21
Pauling	2.55	1.90	2.01	1.96	2.33
Allen	2.28	1.76	1.81	1.68	1.91
Atomic radius					
ns	1.58	2.20	2.19	2.48	2.39
np	1.74	2.79	2.88	3.22	3.22

For example, carbene (CH_2) has a triplet ground state and its H-C-H bond angle is 133.84 $\pm$ 0.05 ° [12a,b] whereas carbene analogues of heavier Group 14 elements (EH_2: E = Si, Ge, Sn, Pb) possess a singlet ground state with remarkable singlet-triplet energy separation (SiH_2: 21.0 kcal/mol, GeH_2: 23 kcal/mol, SnH_2: 23-24 kcal/mol and PbH_2: 34.2-37 kcal/mol), and the H-E-H bond angle decreases with increasing atomic number (SiH_2: 92.7 °, GeH_2: 91.5 °, SnH_2: 91.1 °, PbH_2: 90.5 °).[12c,d] Thus, the lone pair electrons on the central atom E have increasing s atomic orbital character. This "reluctance to hybridize" in valence orbitals of heavier atoms offers the key to an understanding of the difference between carbon compounds and their heavier analogues, especially multiple bonded systems.

Doubly-Bonded Species Consisting of Silicon Atoms

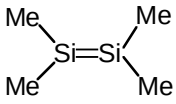

D. N. Roark and G. J. Peddle (1972)

in solution

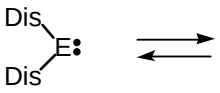

in the solid state

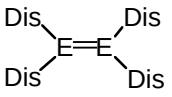

E = Ge, Sn
Dis = $(Me_3Si)_2CH$–

Lappert (1976)

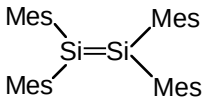

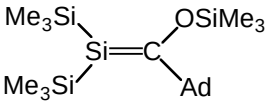

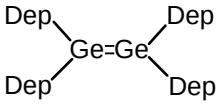

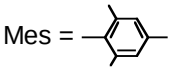

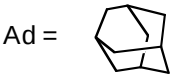

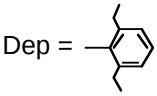

R. West (1981)

A. G. Brook (1981)

Masamune (1984)

In 1972, Roark and Peddle found out the first generation of tetramethyldisilene, which is a silicon analogue of alkene as one of the most important reactive intermediate in the organosilicon chemistry[13] Since then, it was of major interest to examine the double bond character of these reactive disilenes.[14] Such disilenes bearing sterically small substituents are generally highly reactive, and easy by polymerize in the absence of trapping reagent.

In 1976, Lappert et al. reported the method of kinetic stabilization by introducing bulky substituents for the synthesis of bis[bis(trimethylsilyl)methyl]germylene and bis[bis(trimethylsilyl)methyl]stannylene, which exist as corresponding digermene and distannene in the solid state.[15] In 1981, the introducing bulky substituents taking advantage of kinetic stabilization brought a breakthrough for the study on the chemistry of doubly-bonded compounds consisting of silicon atoms. Thus, West et al. successfully synthesized the first isolable disilene, tetramesityldisilene (mesityl = 2,4,6-trimethylphenyl), by the photolysis of

1,1,1,3,3,3-hexamethyl-2,2-dimesityltrisilane.[16] Brook et al. prepared the first silene in 1981.[17] In 1984, Masamune et al. reported the isolation, structure and reactivities of tetrakis(2,6-dimethylphenyl)digermene.[18] In contrast to carbon system, heavier Group 14 elements double bonds have inherent highly *trans*-bent structure. The unique structural features have been investigated by theoretical study.[19]

A conceptual approach to rationalizing pyramidal or bent geometries in the double bond system of the heavier Group 14 elements begins with the recognition of the electronic structure of the molecular fragments. Carbene (R_2C:) possess a triplet ground state, so that two carbenes dimerize in a manner to form a planar structure of alkene ($R_2C=CR_2$). Meanwhile, the ground state of heavier Group 14 element carbene analogues is singlet. The energy gaps between singlet and triplet of them increase with increasing atomic number. Bringing these singlet monomers together to dimerize them results in considerable repulsion between the lone pairs. This repulsion can be minimized by *trans*-bent geometry of double bond resulting from the donor-acceptor interactions between the occupied *n*s orbitals and the empty *n*p orbitals of two singlet monomers. Then, interaction occurs to bond each other strongly, as a result, affording *trans*-bent structure. Besides, the interaction to form *trans*-bent structure can be explained by molecular orbital mixing under distortion from the planar geometry. Under pyramidalization of the metal center, the E-E σ^* orbital of E_2H_4 system will mix into the π orbital (HOMO), leading to further stabilization of latter orbital. On descending the group, the degree of mixing, and hence the degree of energy lowering increase in order to the reduce the energy gap between these orbitals.

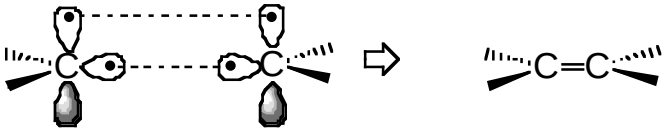

repulsion

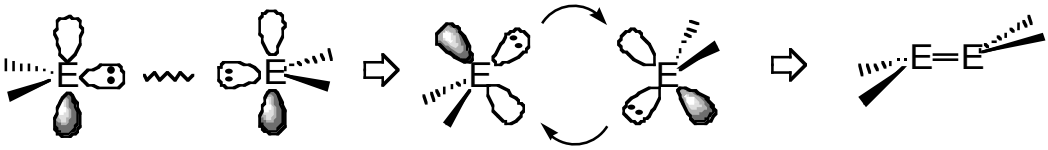

σ*-π interaction

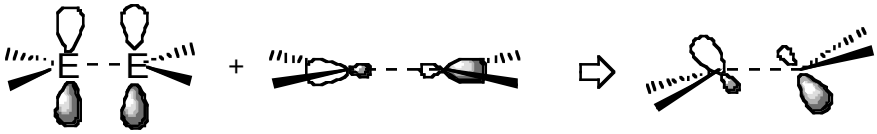

In 1986, Lappart et al. revealed the relationship between the bent angle and potential energy of double bond species of heavier Group 14 elements by theoretical calculation.[20]

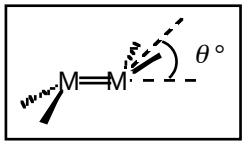

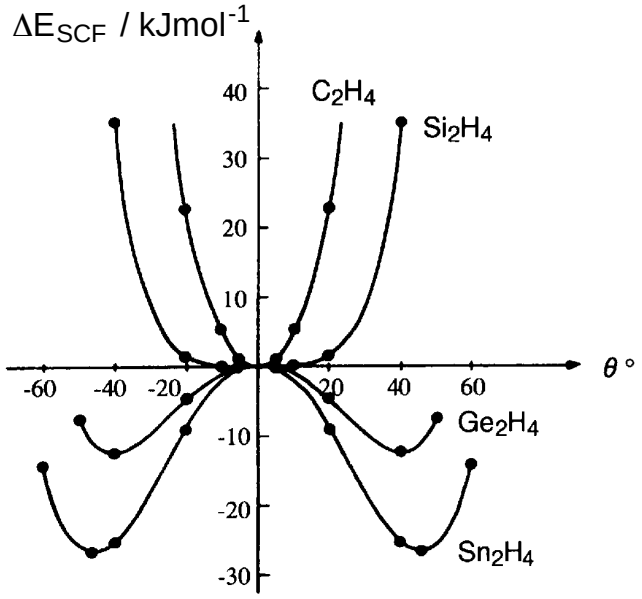

Due to the experimental and theoretical studies progress, there has been explosive growth in the area of unsaturated compounds of heavier Group 14 elements. At present, many stable disilenes have been synthesized and characterized. Now, in organosilicon chemistry, next ultimate isolable target compound remaining was silicon-silicon triple bond species, disilyne, which is a silicon alkyne analogue.

In this doctor's thesis, silicon-silicon triple bond species, disilyne, is regarded as a key compound for the chemistry of unsaturated silicon compounds, cyclic silicon compounds, silaaromatic compounds, silyl anion species, and silyl radical species.

In Chapter 1, the first synthesis, crystal structure, and characterization of silicon-silicon triple bond species, disilyne, are described. The disilyne is stabilized by two bis[bis(trimethylsilyl)methyl]isopropylsilyl substituents (denoted as *Bbi* hereafter) sterically and electronically. The nature of sp-hyblidized silicon atoms is discussed from the viewpoint of spectroscopic method and theoretical calculation.

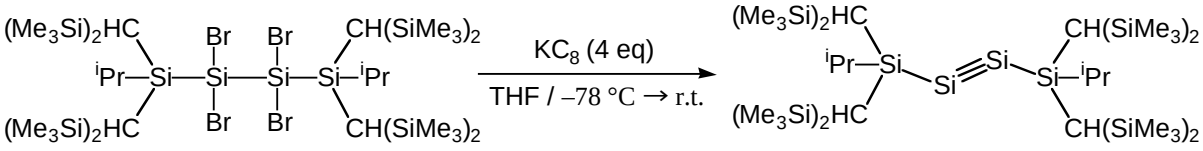

In Chapter 2, stereospecific [2+2] cycloaddition reaction of disilyne and 2-butene to give 1,2-disilacyclobutene are described. The exhaustive study on the reaction mechanism of thermally forbidden [2+2] cycloaddition reaction are achieved by theoretical calculation. The structural property on novel 1,2-disilacyclobutene is also discussed.

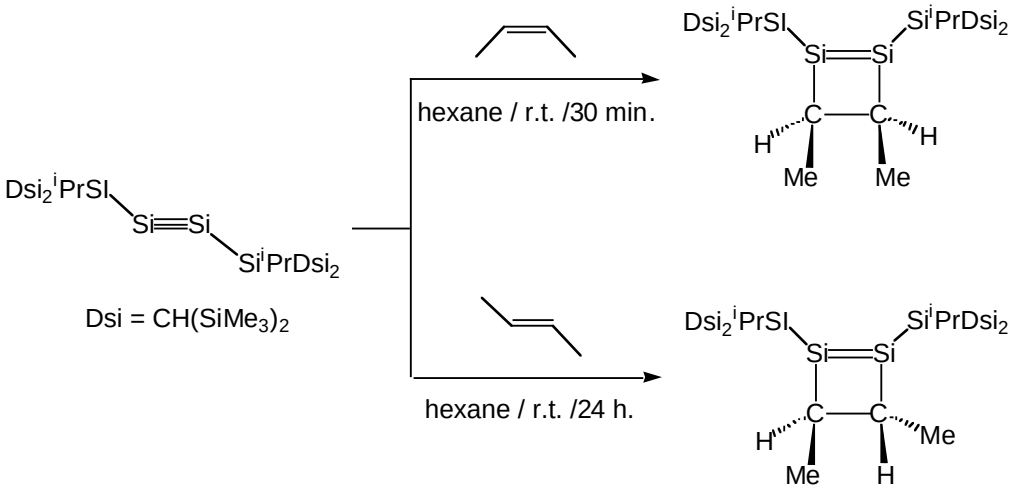

In Chapter 3, synthesis, structure, and chemical properties of stable 1,2-disilabenzenes are described. The reaction of disilyne with phenylacetylene gave two isomers of 1,2-disilabenzene as yellow crystals. The formation mechanism of 1,2-disilabenzenes is discussed on the basis of theoretical calculation. The aromaticity of 1,2-disilabenzene is also described.

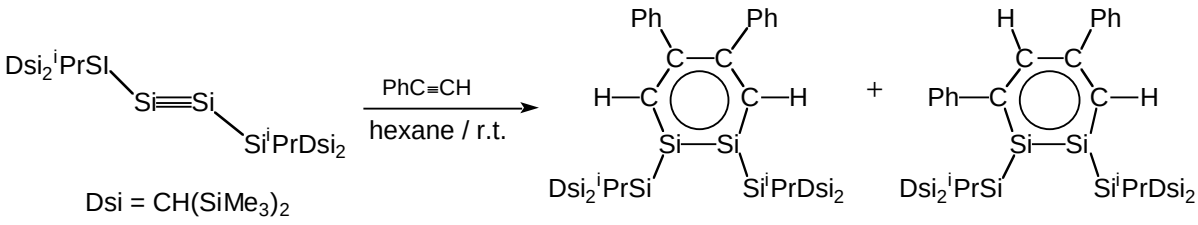

In Chapter 4, synthesis, structure and character of novel disilenide are described. The reaction of disilyne and an equivalent amount of *tert*-butyllithium resulted in formation of *trans*-1,1,4,4-tetrakis[bis(trimethylsilyl)methyl]-1,4-diisopropyl-2-lithio-2-tetrasilene. The formal addition of LiH across the Si≡Si triple bond of disilyne through a single electron transfer reaction gave the product.

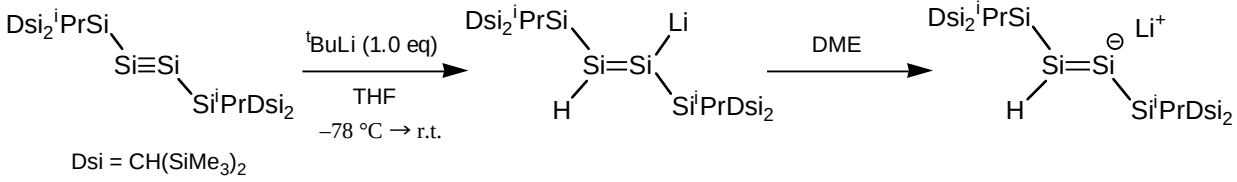

In Chapter 5, the one electron reduction to disilyne with alkali metals in various solvents is described. Synthesis, structure and chemical properties of disilyne anion radical are discussed. The reaction of disilyne and an equivalent amount of alkali metal (Li, Na, K) in THF gave metal free disilyne anion radical in which unpaired electron delocalizes between two central silicon atoms. On the other hand, the reduction of disilyne with an equivalent amount of sodium in toluene produces the first isolable silicon vinyl radical. The chemical properties are also discussed.

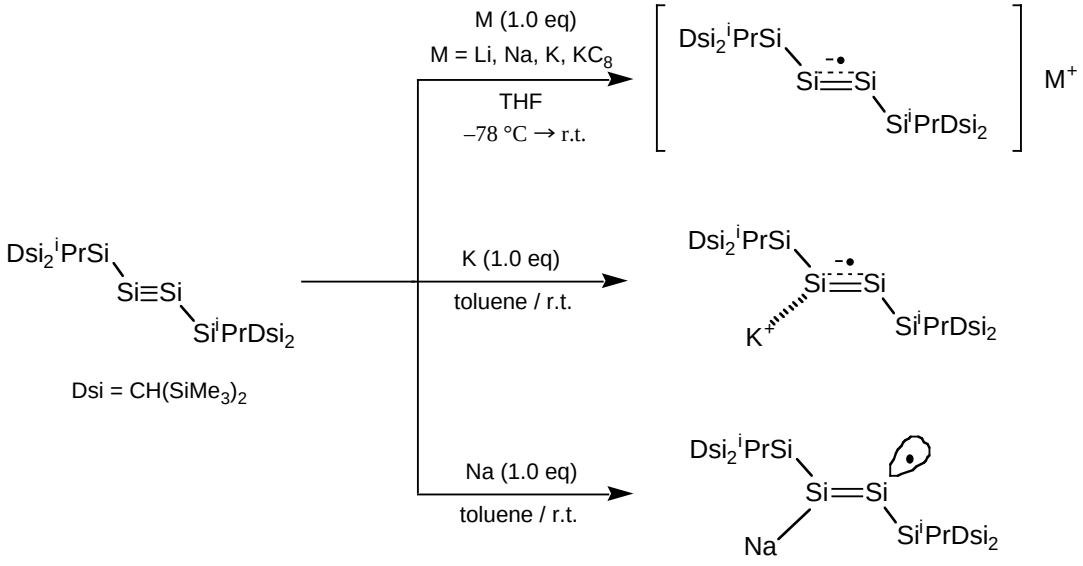

Reference

1. For reviews on heavier Group 14 elements, see: (a) *The Chemistry of Organic Silicon Compounds*, S. Patai and Z. Rappoport, Eds.; John Wiley & Sons Ltd.: 1989. (b) *The Chemistry of Organic Silicon Compounds*, Volume 2, Z. Rappoport and Y. Apeloig, Eds.; John Wiley & Sons Ltd.: 1998. (c) *The Chemistry of Organic Silicon Compounds*, Z. Rappoport and Y. Apeloig, Eds.; John Wiley & Sons Ltd.: 2001.
2. Barton, T. J. Carbacyclic Silanes, In *Comprehensive Organometallic Chemistry*, Wilkinson, G.; Stone, F. G. A.; Abel, E. W., Eds.; Pergamon, 1982, Vol. 2, Chap 9.2.
3. (a) F. S. Kipping, *Pr. Chem. Soc.*, **1904,** *20*, 15. (b) F. S. Kipping, J. E. Hackford, *J. Chem. Soc.*, **1911**, *99*, 138. (c) H. Davies, F. S. Kipping, *J. Chem. Soc.*, **1911**, *99*, 296.
4. E. G. Rochow, *J. Am. Chem. Soc.*, **1945,** *67*, 963.
5. (a) A. D. Petrov, V. F. Mironov, V. A. Ponomarenko, and E. A. Chernyshev, *Synthesis of Organosilicon Monomers*, Heywood & Co. Ltd., London, 1964. (b) R. J. H. Vorhoeve, *Organohalosilanes: Precursors to Silicones*, Elsevier, Amsterdam, 1967. (c) M. P. Clarke, *J. Organomet. Chem.*, **1989,** *376*, 165.
6. *The Chemistry of Organicgermanium, Tin, and Lead Compounds*, Z. Rappoport, Eds.; John Wiley & Sons Ltd.: 2002.
7. J. P. Desclaux, *At. Data Nucl. Data Tables*, **1984**, *12*, 311.
8. R. S. Mulliken, *J. Chem. Phys.*, **1934**, *2*, 782.
9. (a) P. L. Pauling, in *The Nature of the Chemical Bond*, 3rd ed. Cornell University Press. Ithaca, 1960. (b) A. L. Allred, *J. Inorg. Nucl. Chem.*, **1961**, *17*, 215.
10. (a) L. C. Allen, J. Am. Chem. Soc., 1989, 111, 9003; b) L. C. Allen, *J. Am. Chem. Soc.*, **1992**, *114*, 1510.
11. H. Basch and T. Hoz, in *The Chemistry of Organic Germanium, Tin and Lead Compounds*, S. Patai, Z. Rappoport, Eds. John Wiley &Sons Ltd., 1995, Chapter 1.
12. (a) P. R. Bunker, P. Jensen, *J. Chem. Phys.*, **1983**, *90*, 1124. (b) I. Shavitt, *Tetrahedron*, **1985**, *41*, 1531. (c) K. Balasubramanian, *J. Chem. Phys.*, **1988**, *89*, 5731. (d) H. Jacobsen, T. Zieglar, *J. Am. Chem. Soc.*, **1994**, *116*, 3667.
13. D. N. Roark and G. J. Peddle, *J. Am. Chem. Soc.*, **1972,** *94*, 5837.
14. For reviews on disilenes, see: (a) R. West, *Angew. Chem. Int. Ed. Engl.*, **1987**, 26, 1201. (b) J. Barrau, J. Escudie, and J. Satge, *Chem. Rev.*, **1990**, 90, 283. (c) T. Tsumuraya, S. A. Batcheller, and S. Masamune, *Angew. Chem. Int. Ed. Engl.*, **1991**, *30*, 902. (d) R. Okazaki,

15. and R. West, Adv. *Organomet. Chem.*, **1996**, *39*, 231. (e) G. Raabe and J. Michl, in *The Chemistry of Organic Silicon Compounds*, Volume 1, Part 2, Z. Rappoport, Y. Apeloig, Eds. John Wiley & Sons Ltd. 1989, Chap 17. (f) H. Sakurai, in The Chemistry of Organic Silicon Compounds, Volume 2, Part 1, Z. Rappoport, Y. Apeloig, Eds. John Wiley & Sons Ltd. 1998, Chap 15. (g) T. L. Morkin, T. R. Owens, and W. J. Leigh, in *The Chemistry of Organic Silicon Compounds*, Volume 3, Z. Rappoport, Y. Apeloig, Eds. John Wiley & Sons Ltd. 2001, Chap 17.
16. (a) D. E. Goldberg, D. H. Harris, M. F. Lappert, K. M. Thomas, *J. Chem. Soc., Chem. Commun.*, **1976**, 261. (b) P. J. Davidson, D. H. Harris, M. F. Lappert, *J. Chem. Soc., Dalton Trans.*, **1976**, 2268. (c) P. B. Hitchcock, M. F. Lappert, S. J. Miles, A. J. Thorne, *J. Chem. Soc., Chem. Commun.*, **1984**, 480. (d) D. E. Goldberg, P. B. Hitchcock, M. F. Lappert, K. M. Thomas, A. J. Thorn, T. Fjeldberg, A. Haaland, B. E. R. Schlling, *J. Chem. Soc., Dalton Trans.*, **1986**, 2387.
17. R. West, M. J. Fink, J. Michl, *Science*, **1981**, *214*, 1343.
18. A. G. Brook, F. Abdesaken, B. Gutekunst, and R. K. Kallury, *J. Chem. Soc. Chem. Commun.*, **1981**, 191.
19. (a) S. Masamune, Y. Hanazawa, D. J. Williams, *J. Am. Chem. Soc.*, **1982**, *104*, 6136. (b) J. T. Snow, S. Murakami, S. Masamune, D. J. Williams, *Tetrahedron Lett.*, **1984**, 4191.
20. Recent reviews on theoretical studies of heavier Group 14 elements, see: (a) M. Karni, J. Kapp, P. v. R. Schleyer, and Y. Apeloig, In *The Chemistry of Organi Silicon Compounds*; Z. Rappoport and Y. Apeloig, Eds.; John Wiley: Chichester,: 2001; Vol. 3, Chapter 1. (b) I. Ganzer, M. Hartmann, and G. Frenking, In *The Chemistry of Organic Germanium, Tin, and Lead Compounds*, Z. Rappoport, Eds.; John Wiley & Sons, Ltd.: 2002; Vol. 3, Chapter 3.
21. D. E. Goldberg, P. B. Hitchcok, M. F. Lappert, and K. M. Thomas, *J. Chem. Soc., Dalton. Trans*, **1986**, *11*, 2387.

Chapter 1

The First Isolable Silicon-Silicon Triple Bond Species, Disilyne. Synthesis and Structure of 1,1,4,4-tetrakis [bis(trimethylsilyl)methyl]-1,4-diisopropyl-2-tetrasilyne

Summary

The reaction of 2,2,3,3-tetrabromo-1,1,4,4-tetrakis[bis(trimethylsilyl)methyl]-1,4-diisopropyltetrasilane with four equivalents of potassium graphite (KC_8) in tetrahydrofuran produces 1,1,4,4-tetrakis[bis(trimethylsilyl)methyl]-1,4-diisopropyl-2-tetrasilyne, a stable compound with a silicon-silicon triple bond, which can be isolated as emerald green crystals stable up to 100°C in the absence of air. The Si≡Si triple-bond length is 2.0622(9) Å, which shows half the magnitude of the bond shortening of alkynes compared with that of alkenes. Unlike alkynes, the substituents at the Si≡Si group are not arranged in a linear fashion, but are trans-bent with a bond angle of 137.44(4)°.

Introduction

Hydrocarbons containing C=C double bonds (alkenes) and C≡C triple (alkynes) form an abundant and structurally diverse class of organic compounds. However, the ability of heavier congeners of carbon (where element E is Si, Ge, Sn, and Pb) to form double bond of the type >E=E< and triple bond of the type -E≡E- was for a long time doubted.[1,2,3,4] The first attempts to generate such species were unsuccessful, resulting in the formation of polymeric substances. This led to the often cited 'double-bond rule': Those elements with a principal quantum number equal to or greater than three are not capable of forming multiple bonds because of the considerable Pauli repulsion between the electrons of the inner shells.[5,6,7] Such a viewpoint prevailed despite the accumulation of a vast amount of experimental data supporting the existence of multiply bonded species as reactive intermediates.[1,2,3,4] This conflict was resolved nearly 30 years ago, since Lappert and Davidson reported in 1973 the synthesis of the stable distannene $Dis_2Sn=SnDis_2$ (Dis = $CH(SiMe_3)$), which has an Sn=Sn double bond in the solid state.[8] The next significant discoveries in the double bond chemistry of heavier group 14 elements came from research groups in 1981; West and colleagues reported the synthesis of a stable compound with a Si=Si double bond, tetramesityldisilene,[9] and Brook *et al*. synthesized a compound with a Si=C double bond.[10] Thereafter, almost every type of doubly-bonded compound having not only homo- and heteronuclear double bonds between group 14 elements of >E=E'< type (E and E' = C, Si, Ge, Sn, and Pb), but also the double bonds between the heavier group 14 elements and other main group elements (groups 13, 15, and 16) have been synthesized and structurally characterized.[11] In spite of extensive experimental efforts directed towards the synthesis of triply-bonded compounds of heavier group 14 elements, heavier analogues of alkynes, such as -E≡C- and -E≡E- (E = Si, Ge, Sn, and Pb),[12,13] had remained unknown until recently.[14,15] An epoch-making result in the chemistry of stable heavier analogues of alkynes came in 2000; Power *et al*. reported the synthesis and structural characterization of the lead

analogue of the alkyne **1** (Figure 1).[16] Subsequently, tin **2**[17] and germanium **3**[18] analogues were also synthesized by the same group in 2002. Furthermore, Tokitoh *et al*. also reported the structure of germanium analogue **4**.[19] The isolation of germanium, tin, and lead analogues of alkynes was achieved by using bulky terphenyl ligands (2,6-diarylphenyl groups) and Bbt group (C_6H_2-2,6-[$CH(SiMe_3)_2$]-4-$C(SiMe_3)_3$). The crystallographic structural determination revealed that **1**−**4** have *trans*-bent structures rather than the linear arrangement of R-E≡E-R. Having formal E≡E triple bonds, these compounds actually exhibited a highly pronounced non-bonding electron density character at the central atoms, resulting in a decrease in the bond order on descending group 14 (Figure 2).[14a,20] Thus, the bond orders in the *trans*-bent structures of heavier analogues of alkynes are estimated to be 2.32-1.74 (Ge), 1.87-1.73 (Sn), and 1.65-1.51 (Pb) for the model compounds of R-E≡E-R (R = H, Me, and Ph).[14a,21] Higher bond orders (2.20-2.37) were expected for the silicon species.[14a,21]

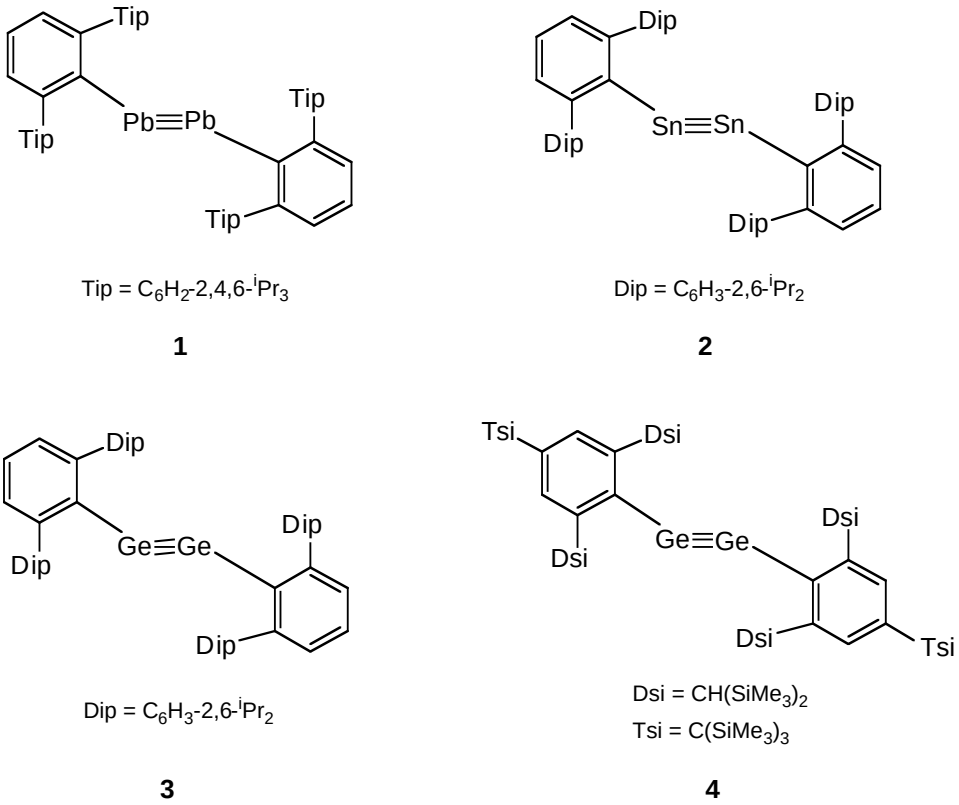

Figure 1-1. Stable lead, tin, and germanium analogues of alkyne drawn with a formal triple bond structure.

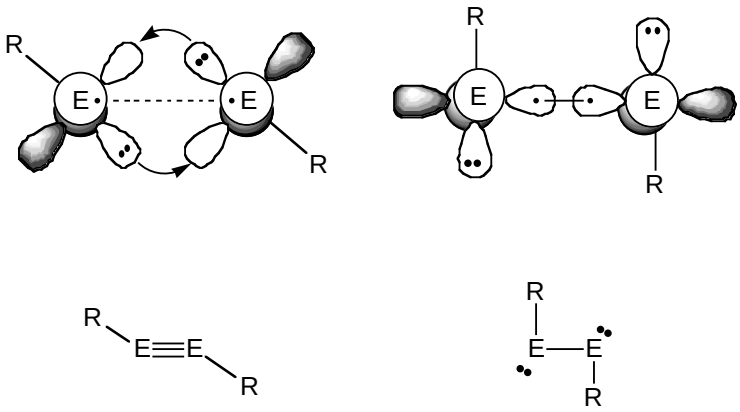

Figure 1-2. Bonding model in the *trans*-bent structure of a heavy alkyne. Arrow line, dashed line, and normal line indicate donor-acceptor dative bond, π-bond, and σ-bond, respectively.

The first experimental approach to a silicon-silicon triple bond was reported by West and Sekiguchi *et al*. in 1986.[12a,b] The compound **5** was synthesized as a possible precursor of dimethyldisilyne **6** by the retro-Diels－Alder reaction. When **5** was heated in the presence of anthracene at 350 °C, the anthracene adduct **7** of MeSi≡SiMe was produced together with 1,2,3,4-tetraphenylnaphthalene (Scheme 1-1). The anthracene adduct **7** is also a possible dimethyldisilyne precursor. In this connection, the mass spectrum of **7** (EI, 30 eV) is suggestive; peaks were observed at *m*/*z* 442 (M+, relative intensity 35), 264 (M+ – anthracene, 100), 249 (M+ – anthracene – Me, 36), and 178 (anthracene+, 50). In addition to these, a peak with a relative intensity of 15 was found at *m*/*z* 86. The exact mass and isotope ratios of this peak show that it has the molecular formula $C_2H_6Si_2^+$.

Scheme 1-1.

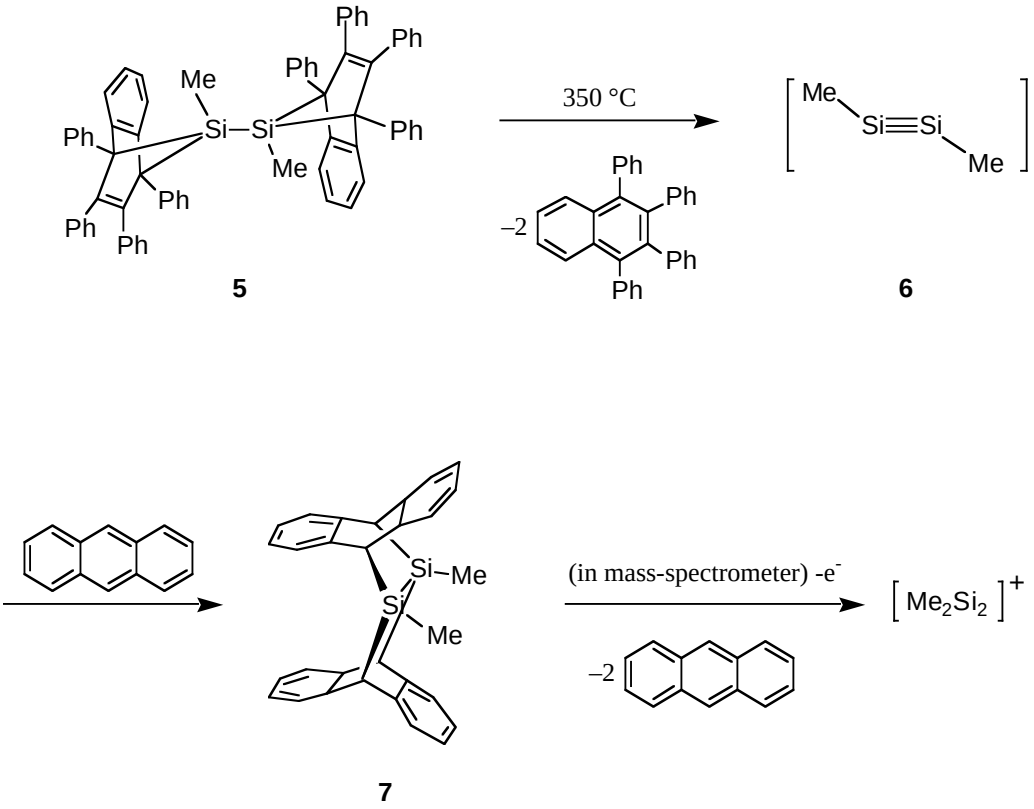

5 **6** **7**

Scheme 1-2.

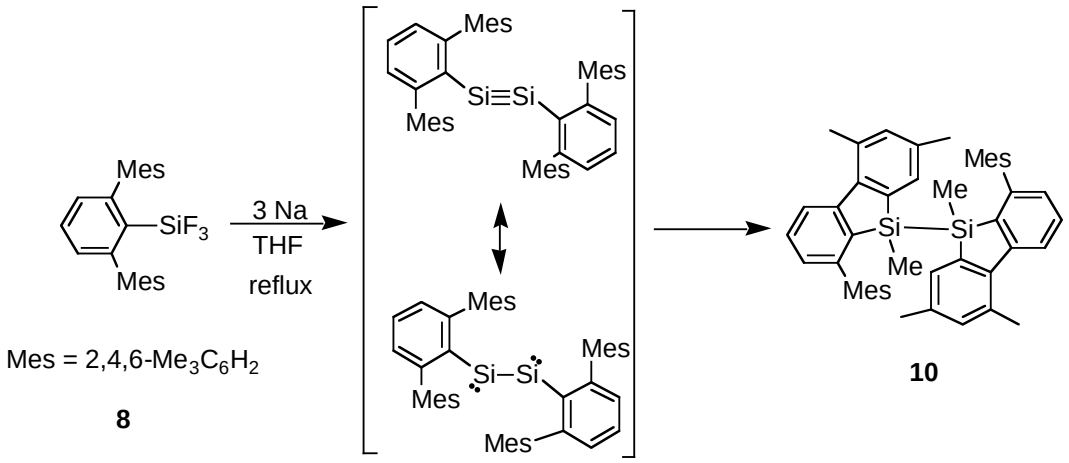

8 **9** **10**

The synthesis of the silicon analogue of an alkyne having a terphenyl ligand has been attempted by West and co-workers.[22] Thus, the reductive coupling of 2,6-dimesityl-phenyltrifluorosilane **8** with three equivalents of sodium in THF led to a product with the formal constitution $(Mes_2C_6H_3Si)_2$. However, the product is not a disilyne, but the bis(silafluorenyl) **10**. The disilyne **9** is postulated as an intermediate in this reaction (Scheme 1-2).

The closest work to a stable disilyne was reported by Wiberg *et al*. in 2002.[23] Thus, as shown in Scheme 1-3, the reaction of the disilene $(^tBu_3Si)_2MeSi(Cl)Si=Si(Cl)SiMe(Si^tBu_3)_2$ (**11**) with lithium naphthalenide in THF forms a reaction mixture containing a chlorine free species, which gives a low field ^{29}Si NMR signal at 91.5 ppm, which lies in the region that is reasonable for a triply-bonded silicon atom and is consistent enough with the calculated value for $(^tBu_3Si)_2MeSiSi{\equiv}SiSiMe(Si^tBu_3)_2$ (**12**) (δ Si≡Si = 111.2 ppm).[24] The disilyne **12** is not stable enough in solution at room temperature to be isolated and full characterization had not been reported until now. However, very recently the trapping reactions of **12** with ethylene and 1,3-butadiene to give the corresponding cyclic disilenes have been reported (*vide infra*).[25]

Scheme 1-3.

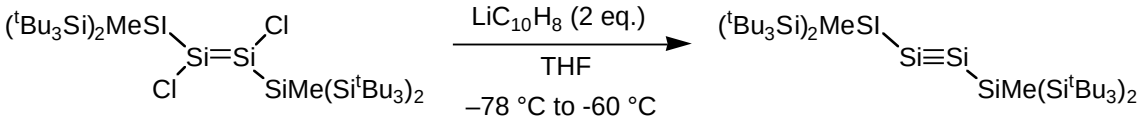

11 **12**

Although the theoretical analysis predicted the experimental accessibility of disilynes with a silicon-silicon triple bond,[24,26] all attempts to isolate such postulated molecules prior to our report had been unsuccessful. The difficulty in synthesizing disilynes is in part due to their high reactivitiy, especially toward dimerization and isomerization.[22,25,27,28]

Theoretical calculations not only on the parent H_2Si_2, but also on R_2Si_2 with various substituents R have been reported so far.[21] Among them, the calculation by Nagase *et al*. reported some very important predictions:

1: The introduction of the electropositive silyl group on the triply-bonded Si atom, especially a triorganosilyl group, instead of hydrogen or organic groups, such as methyl, extensively reduces the energy difference between the *trans*-bent and linear forms with an increase in the bend angle in the *trans*-bent structure (the geometry of the *trans*-bent structure becoming much closer to

linear) (Tables 1-1 and 1-2).[29]

2: The disilavinylidene structure, which is the most stable isomer for R_2Si_2 except for the case of R = H, would be relatively destabilized by the introduction of more bulky substituents on the silicon atoms. Thus, it is highly likely that the introduction of $^tBu_3Si$ or Dep_3Si groups, or their derivatives, would reverse the relative stability between *trans*-bent disilyne and disilavinylidene, the *trans*-bent structure being favored over disilavinylidene.

Based on both the theoretical prediction and experimental experience, previously, Dsi_2MeSi group (Dsi = $CH(SiMe_3)_2$) was designed as steric protection group by Sekiguchi group. The reductive debromination of tetrabromide precursor **13** having two Dsi_2MeSi groups by using various reducing agents, such as alkali metals (Li, Na, and K), lithium naphthalenide, potassium graphite, were investigated, and finally revealed the formation of tetrasilatetrahedrane **14** by the reaction with $^tBu_3SiNa$ in 46% yield (Scheme 1-4).[28] This clearly indicates that the Dsi_2MeSi group is not large enough to prevent the dimerization of the Si≡Si triple bond species.

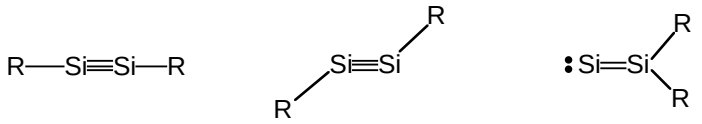

A B C

Table 1-1. Relative Energies (kcal/mol) of the Linear (A), Trans-Bent (B), and 1,2-R-Shifted (C) Structures of RSi≡SiR

R	A	B	C
H	0.0	–20.3(–22.1)	–28.2(–30.7)
CH_3	0.0	–18.4(–20.4)	–25.3(–28.2)
SiH_3	0.0	–10.1(–12.1)	–15.7(–17.7)
SiF_3	0.0	–7.0(–15.8)	–30.1(–25.6)
$SiMe_3$	0.0	–10.4(–8.5)	–10.5(–11.4)
SPh_3	0.0	–7.2	–17.3
$Si(SiH_3)_3$	0.0	–10.4	–16.6
Si^tBu_3	0.0	–4.0	5.7
$Si(2,6\text{-}Et_2C_6H_3)_3$	0.0	–5.5	6.5

At B3LYP/3-21G* Level (B3LYP/6-31G(d) level in parentheses).

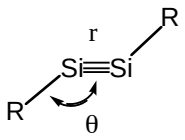

Table 1-2. Calculated Structural Parameters of *trans*-Bent Disilyne

R	r (Si≡Si/Å)	θ (Si≡Si-R/deg)
H	2.093(2.111)	124.9(124.4)
CH_3	2.104(2.123)	.
SiH_3	2.082(2.100)	.
SiF_3	2.069(2.094)	.
$SiMe_3$	2.075(2.095)	.
SPh_3	2.078	.
$Si(SiH_3)_3$	2.092	.
Si^tBu_3	2.068	.
$Si(2,6\text{-}Et_2C_6H_3)_3$	2.072	.

At B3LYP/3-21G* Level (B3LYP/6-31G(d) level in parentheses).

Scheme 1-4.

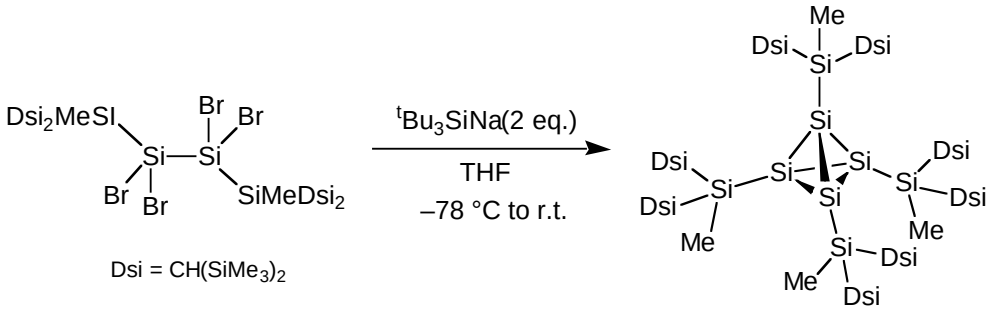

Dsi = $CH(SiMe_3)_2$

13 **14**

Development of Novel Substituents

Two bulky trialkyl groups ($SiDsi_3$ and Si^iPrDsi_2 (Dsi = $CH(SiMe_3)_2$)), that are apparently bigger than Dsi_2MeSi group, were designed as novel steric protecting group. The preparation of Dsi_3SiH **17** by the reaction of Dsi_2SiHBr **16** with Dsi-K, along with the subsequent transformation to Dsi_3SiBr **18**, was finally achieved (Scheme 1-5). However, preparation of the alkali metal derivative of Dsi_3Si-M (M = Li, Na, and K) **19** as a key reagent for the introduction of the Dsi_3Si group to the silicon atom was unsuccessful since Dsi_3Si-M **19** was not thermally stable and 1,2-shift of a Me_3Si group occurred to afford $[Dsi_2(Me_3Si)Si](Me_3Si)HC$-M **20** in which carboanion was stabilized by hyperconjugation (α-effect) of two silyl group (Scheme 1-6).

Scheme 1-5.

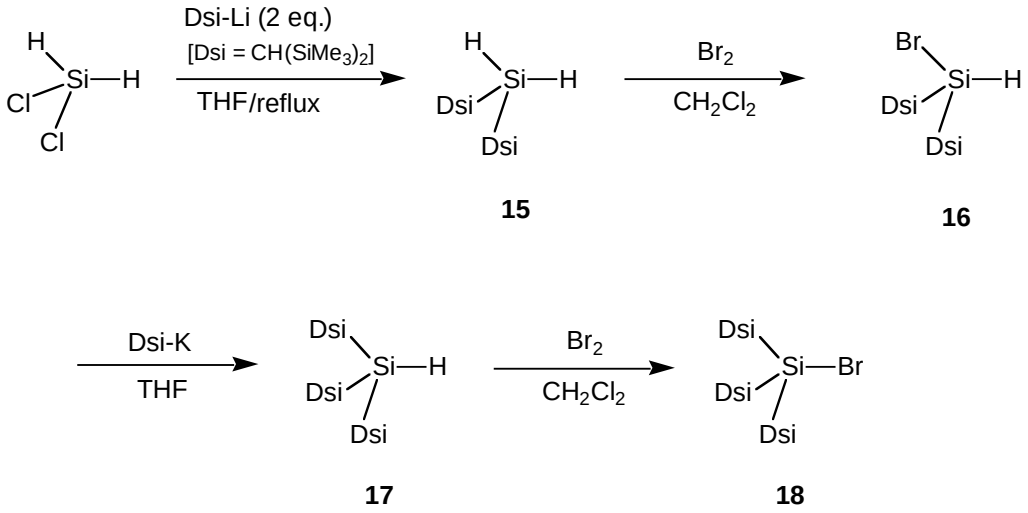

Scheme 1-6.

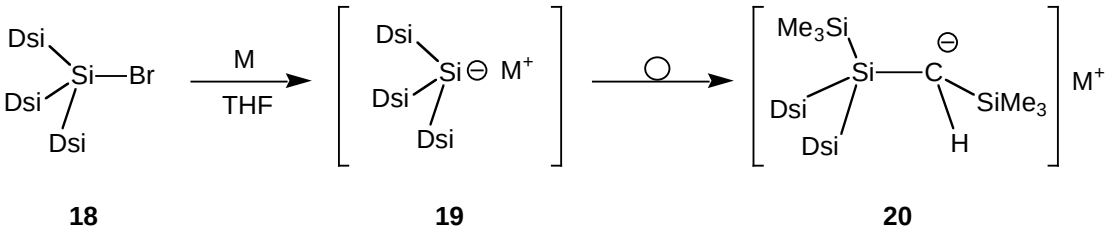

A second candidate $Dsi_2{}^iPrSi$ group as a protecting group was prepared as the corresponding hydrosilane by the reaction of $^iPrSiCl_2H$ **21** with two equivalents of Dsi-Li. The following halogenation, metallation, and coupling reaction with H_2SiCl_2 afforded chlorodihydrosilane bearing one bulky $Dsi_2{}^iPrSi$ group $Dsi_2{}^iPrSi\text{-}SiH_2Cl$, **25**. Reductive coupling of **25** with molten sodium in heptane gave the tetrahydrodisilane derivative **26**, and the tetrabromide precursor **27** was easily obtained by bromination with four equivalents of bromine (Scheme 1-7).

Scheme 1-7.

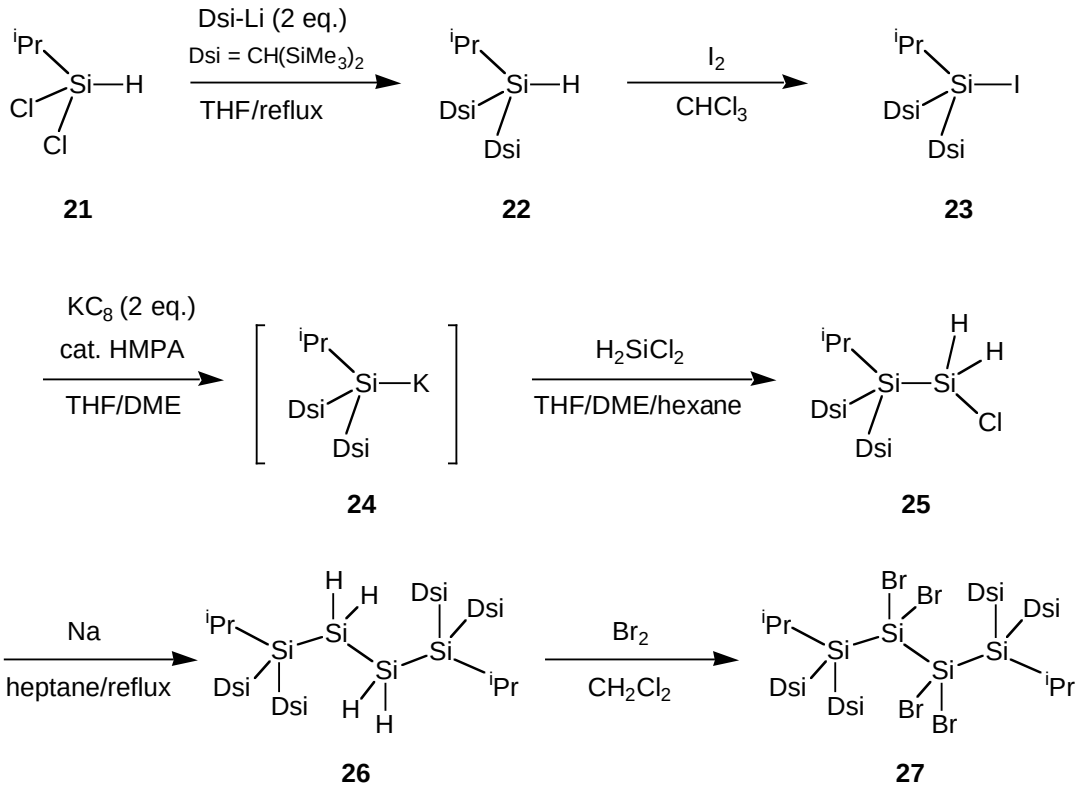

Results and Discussion

Synthesis of Disilyne 28

Disilyne **28** was prepared by reduction of a tetrabrominated precursor **27**. Thus, the reaction of **28** with four equivalents of potassium graphite (KC_8) in THF produces a dark green mixture, from which disilyne **28** can be isolated as extremely air and moisture-sensitive emerald green crystals in 73% isolated yield (Scheme 1-8, Figure 1-3a).[30]

Scheme 1-8

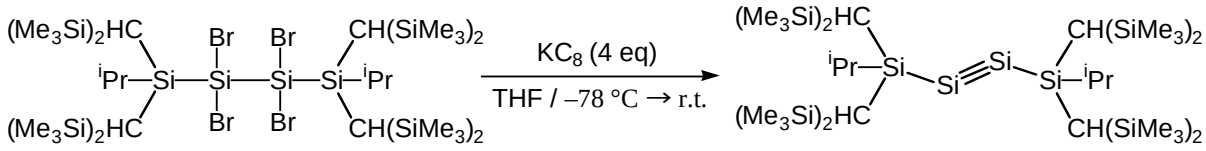

27 **28** (73%)

Despite the large steric congestion, the debromination reaction proceeds rapidly and cleanly. The disilyne **28** was isolated by recrystallization from pentane at –30 °C; it has a decomposition point of 127 °C (Figure 1-3a). No evidence for the isomerization of **28** to RRSi=Si: or dissociation into the two RSi: fragments (R = $Si^iPr[(CH(SiMe_3)]_2$) was observed, indicating that the two central Si atoms are strongly bonded. The disilyne **28** was characterized spectroscopically; the most informative data came from ^{29}Si NMR studies (Figure 1-3b). Four equal-intensity resonance signals with the chemical shifts δ = –0.3, 0.0, 20.7, and 89.9 ppm were observed in the ^{29}Si NMR spectrum, assigned as follows: The peak at 89.9 ppm corresponds to a triply bonded Si atom, the peak at 20.7 ppm corresponds to Si atoms bonded to the Si≡Si group, and peaks at –0.3 and 0.0 ppm correspond to the four $CH(SiMe_3)_2$ groups. The resonance of the sp-hybridized Si atoms is shifted upfield compared with that of silyl-substituted disilenes (δ = 142.1 to 154.5 ppm), as was observed in the case of ^{13}C NMR chemical shifts of silyl-substituted of alkenes (δ = 188 to 197 ppm)[31] and alkynes (δ = 112 to 114 ppm).[32] The mass spectrum shows a clear parent ion peak at m/z = 834, and reasonable fragmentation peaks for disilyne.

(a)

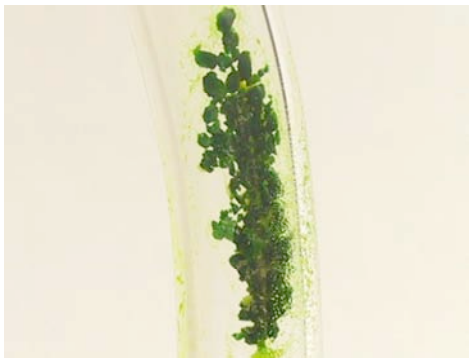

(b)

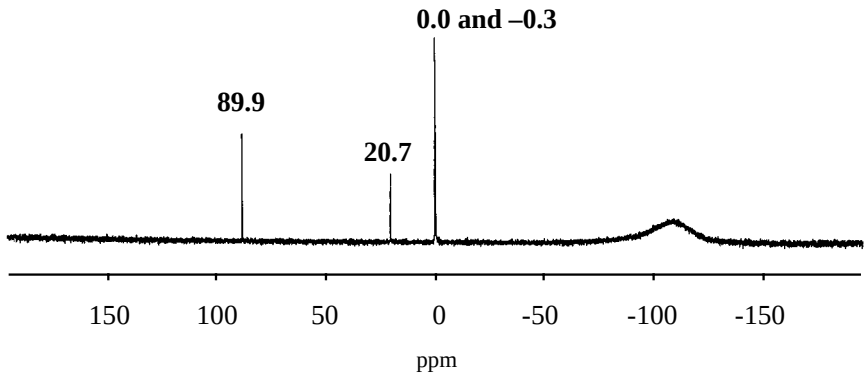

Figure 1-3. (a) Picture of disilyne **28** (b) ^{29}Si NMR(C_6D_6, δ) spectrum of disilyne **28**.

Solid-State ^{29}Si NMR Study of Disilyne 28

The solid-state ^{29}Si NMR measurements were carried out[33] using the CP/MAS technique.[34] Experimental (**28**) and calculated (**29**), (**30**)[35] data are given in Figure 1-4 and Table 1-3. The tensor directions are shown in Scheme 1-9. The observed isotropic δ (^{29}Si1) of **28** in the solid state is 78.4 ppm, shifted by 10 ppm to a higher field relative to that in benzene solution (89.9 ppm[30]). This difference may result from a small conformational change of the substituents in solution relative to that in the solid state.[36,37] The measured Chemical Shift Anisotropy (CSA) of Si^1 in **28** of −643 ppm (calculated: −740 to −764 ppm, Table 1-3[36]) is considerably larger than in disilenes (e.g., −364 ppm for $(^i\text{Pr}_3\text{Si})_2\text{Si}{=}\text{Si}(\text{Si}^i\text{Pr}_3)_2$[38]). The measured δ_{11} and δ_{22} (Scheme 1-9b)[39] are 364.6 and 221.2 ppm, respectively, considerably deshielded relative to δ_{33} of −350.4 ppm. The measured CSTs of **28** (which are generally in reasonable agreement with the calculated values[36]) provide strong evidence for its Si≡Si triple bond character.

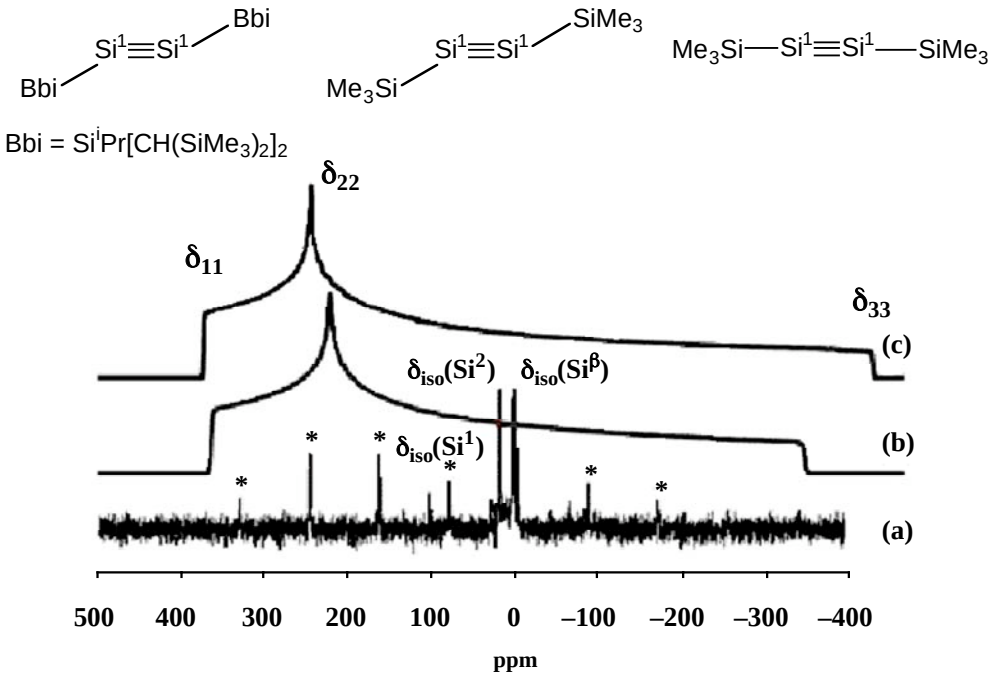

Figure 1-4. (a) CP/MAS ^{29}Si NMR spectrum of disilyne **28**; (b) and (c) show simulation of static ^{29}Si NMR spectrum of disilyne **28** using the experimental data (b) and (c) the calculated (C2-symmetry) CST components.

Scheme 1-9. Calculated orientation of the principal CST components. (a) linear REER; (b) in bent RSiSiR.

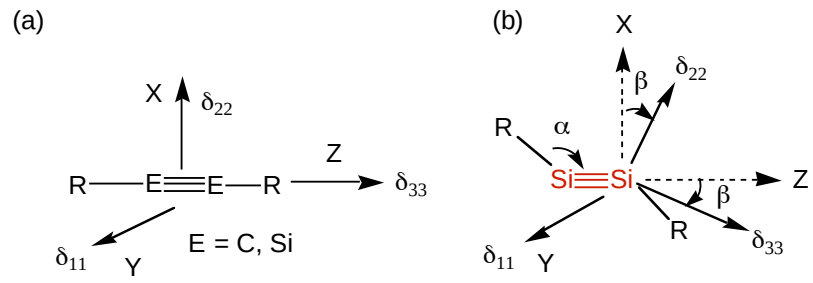

Table 1-3. Measured solid-state ^{29}Si NMR parameters of disilyne **28** and calculated values for **29**-**30**

		^{29}Si[1] values / ppm				
		δ_{11} / σ_{11}	δ_{22} / σ_{22}	δ_{33} / σ_{33}	δ_{iso} / σ_{iso}[a]	CSA[b]
28	**δ exp.**[c]	**364.6**	**221.2**	**–350.4**	**78.4**[d] **(89.9)**[e]	**–643.3**
	calculated[f-h]					
	δ total (C_2)[i]	373.1	224.4	–431.9	61.9	–740.6
	δ total (C_i)[i]	381.6	249.5	–435.2	65.3	–750.7
	σ^p (paramagnetic)	–964.9	–837.4	–141.7	–648.0	759.5
29 bent(C_i)	δ total[i]	442.4	285.2	–417.2	85.5	–835.1
	σ^p (paramagnetic)	–999.1	–834.6	87.9	–643.6	833.5
30 linear(D_{3d})	δ total[i]	162.5	162.5	–518.5	64.5	–681.0
	σ^p (paramagnetic)	–719.4	–719.4	–42.7	–493.9	676.7

[a] $\delta_{iso} = (\delta_{11} + \delta_{22} + \delta_{33})/3$; [b] Ref. 43; [c] The estimated an error is ca +15% ref. 36; [d] Exp.: δ_{iso} (^{29}Si^2) = 18 ppm, δ_{iso} (^{29}Si$^\beta$) = 0.4, 0.3, -0.4 and -1.0 ppm; [e] In d_6-benzene solution ref. 30; [f] δ (^{29}Si) = σ ($^{29}Si_{TMS}$) – σ (^{29}Si); TMS = $SiMe_4$, calculated σ ($^{29}Si_{TMS}$) = 331 ppm; [g] Ref. 35e; [h] Geometries are from Ref. 37; [i] δ_{ii} (total) = δ ($^{29}Si_{TMS}$) – [σ_{ii} (paramagnetic) + σ_{ii} (diamagnetic)]; [j] Ci

To understand this statement, let us first analyze the CSTs in model systems **30** (linear) and **29** (*trans*-bent). The measured CSTs of **28** exhibit a very similar behavior to that calculated for **29** (Table 1-3). In linear **30**, σ_{11} (δ_{11}) and σ_{22} (δ_{22}) are identical, and are oriented perpendicularly to the RSiSiR molecular axis (Z) i.e., along the X and Y axes (Scheme 1-9a). σ_{33} (δ_{33}) points along the Z axis and it is shifted to a higher field (Table 1-3). ^{13}C NMR of HC≡CH

σ (0.0) π_{in} (1.3) π_{out} (2.0) π^*_{in} (4.5) π^*_{out} (5.6) σ^* (7.1)

Figure 1-5. Frontier molecular orbitals of trans-bent $Me_3SiSi{\equiv}SiSIMe_3$ (in parentheses their relative energies in eV, at B3LYP/6-31G(d,p)).

exhibits the same tensor pattern i.e., $\delta_{11} = \delta_{22} = 150$ ppm, $\delta_{33} = -90$ ppm.[40] The paramagnetic contribution (σ^p)[41a] to the CST of Si^1 in **30** is highly anisotropic (CSA^p = 677 ppm) with high degenerate deshielding contributions along X and Y ($\sigma^p_{11} = \sigma^p_{22} = -719$ ppm) and a very small contribution along Z ($\sigma^p_{33} = -43$ ppm) (Table 1-3). σ^p_{11} and σ^p_{22} in linear disilynes (and acetylenes[40]) are attributed primarily[37,42] to the coupling, induced by the applied magnetic field, between the Si-Si σ orbital and the two degenerate π* orbitals, which in linear structures are oriented in perpendicular planes. Upon bending of **30**→**29**, the degeneracy of the π- and π* orbitals is lifted, forming two π-orbitals, π_{in} and π_{out} (and $\pi*_{in}$, $\pi*_{out}$) (Figure 1-5), leading consequently to different σ^p_{11} and σ^p_{22} components (Table 1-3), which are attributed primarily to the Si-Si σ-π^*_{in} and σ-π^*_{out} orbital coupling, respectively.[37,42] σ^p is inversely proportional to the energy difference between the interacting orbitals (ΔE),[41c] the smaller is ΔE the larger is the shift of σ^p to lower field. Upon bending, $\Delta E(\sigma\text{-}\pi*_{in})$ and $\Delta E(\sigma\text{-}\pi*_{out})$ decrease from 6.1 eV in **29** to 4.5 eV and 5.6 eV, respectively, in **28** (Figure 1-5), causing a significant down-field shift of σ^p_{11} and σ^p_{22} and consequently of δ_{11} and δ_{22} (Table 1-3). δ_{11}, oriented perpendicularly to the RSiSiR XZ molecular plane has the largest paramagnetic contribution (most down-field shifted). σ^p_{33} (−88 ppm) and δ_{33} (−471 ppm) remain highly shielded, as in **30** and in acetylene.[40b] In conclusion, the measured and calculated orientations and values of the CST components of bent disilyne **28** strongly support the description of the Si≡Si bond as a triple bond composed of a σ-*bond and two non-degenerate* π*-bonds.*

Molecular Structure of Disilyne

An emerald green single crystal of **28** suitable for X-ray crystallographic analysis was obtained by recrystallization from pentane. Figure 1-6 shows the molecular structure of disilyne **28**. The four Si atoms (Si2, Si1, Si1', and Si2') are perfectly coplanar and the bulky $Si^{i}Pr[(CH(SiMe_3)]_2$ groups protect the central Si≡Si triple bond. The most significant result is the Si≡Si triple-bond length of 2.0622(9) Å. This value is 3.8% shorter than typical Si=Si double-bond length (2.14 Å) and 13.5% shorter than the average Si-Si single-bond length of 2.34 Å[4]. This shortening is half the magnitude of that in the carbon counterparts. Moreover, alkynes have a linear geometry around the C≡C triple bond, whereas disilynes have been predicted to have a highly pronounced trans-bent geometry around the Si≡Si triple bond.[44,26a] The structure confirms this prediction: the substituents at the Si≡Si bond are not arranged in a linear fashion, but are trans-bent with a bend angle of 137.44(4)°, as determined by the Si2-Si1-Si1' angle. This bond angle is 12.5° smaller than that calculated for HSi≡SiH (124.9°). According to theoretical investigations, substitution by electropositive silyl groups leads to a less trans-bent disilyne structure.[29] The structure of **28** presented here is close to that predicted by a recent density functional (DFT) calculation on $(^{t}Bu_3Si)_2MeSiSi{\equiv}SiSiMe(Si^{t}Bu_3)_2$.[24] The space-filling model of **28** shown in Figure 1-7 highlights the steric protection of the Si≡Si group by isopropyl and bis(trimethylsilyl)methyl substituents. Upon replacement of the isopropyl groups in precursor with methyls, the reaction to produce the disilyne yields a dimerization product tetrasilatetrahedorane instead.[28] A DFT calculation on disilyne **28** at the B3LYP/6-31G(d) level of theory well reproduces the experimental geometry and the structural parameters (calculated value: 2.093 Å for the Si≡Si bond length, 136.1° for the trans-bending angle).

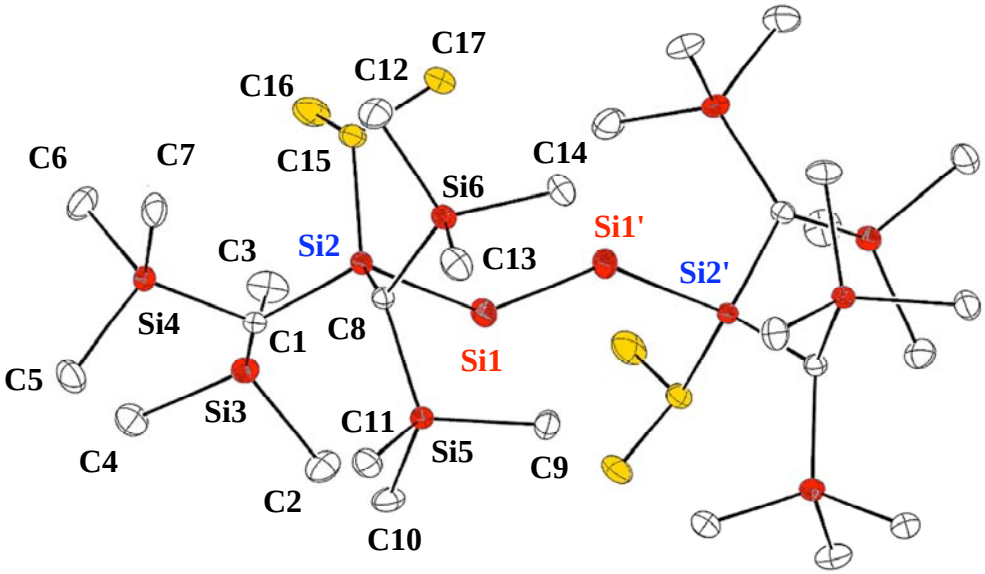

Figure 1-6. ORTEP drawing of disilyne **28**.

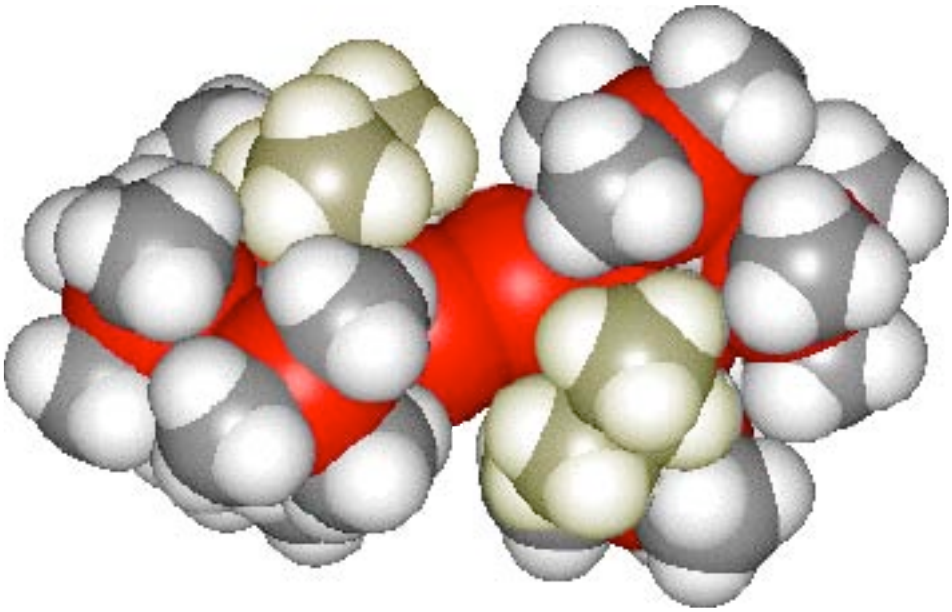

Figure 1-7. Space filling model of disilyne **28**.

The stable homonuclear alkyne analogues of all heavier group 14 elements have now been synthesized. The structural comparisons of RE≡ER (E = Si, Ge, S, Pb) are summarized in Table 1-4. The strong *trans*-bending observed in these compounds shows that the bond order is less than three and that the non-bonding lone pair character increases as group 14 is descended. The bending is thought to be the result of the mixing of an in-plane π-orbital with a σ* orbital whose energies are close enough to cause the interaction of these orbitals in the heavier elements (Figure 1-8). The σ orbital of the C-C bond cannot interact with an in-plane π -orbital because of the large energy difference, whereas the Si-Si σ* orbital can interact with the in-plane π orbital to produce the *trans*-bent structure of R*Si≡SiR* (R* = $Si^{i}Pr[CH(SiMe_3)_2]_2$), resulting in the bond order of 2.618. However, Ar*PbPbAr* (Ar* = C_6H_2-2,4,6-$^{i}Pr_3$) has Pb-Pb bonding that is essentially a single bond and there is a lone pair at each Pb atom.[14a] The Ge and Sn alkyne analogues lie between those of Si and Pb, with bond orders of 2.1.[14a]

Table 1-4. Comparative Data of Heavier Analogues of the Alkynes E_2R_2 (E = Si, Ge, Sn, Pb)

REER	R–Si≡Si–R [a]	Bbt–Ge≡Ge–Bbt [b]	Ar'–Ge=Ge–Ar' [c]	Ar'–Sn=Sn–Ar' [c]	Ar*–Pb–Pb–Ar* [d]
Color	Emerald Green [e]	Red [f]	Orange Red [g]	Purple [h]	Dark Green [i]
		A [j] B [j]			
d_{E-E}/Å	2.0622(9)	2.2060(8) 2.2060(8)	2.2850(6)	2.6675(4)	3.1881(10)
θ_{E-E-R}/deg	137.44(4)	126.19(13) 123.60(13) 136.18(14) 138.66(14)	126.67(8)	125.24(7)	94.26(4)

[a] R = $Si^{i}Pr[CH(SiMe_3)_2]_2$; [b] Bbt = C_6H_2-2,6-$[CH(SiMe_3)_2]_2$-4-$C(SiMe_3)_3$; [c] Ar' = C_6H_3-2,6-$[C_6H_3$-2,6-$^{i}Pr_2]_2$; [d] Ar* = C_6H_3-2,6-$[C_6H_2$-2,4,6-$^{i}Pr_3]_2$; [e] Ref.30; [f] Ref.19; [g] Ref.18; [h] Ref.17; [i] Ref.16; [j] two geometries in which configuration of Bbt group is different, were reported.

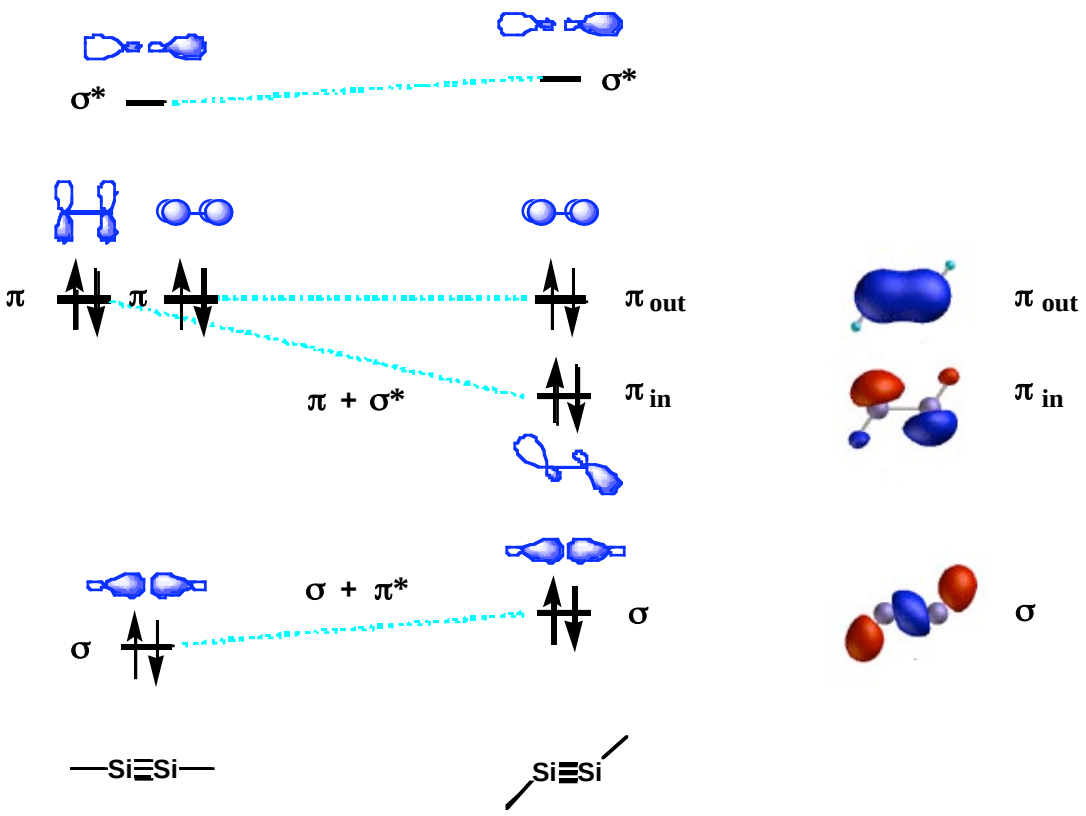

Figure 1-8. Schematic MO diagram of linear and *trans*-bent disilynes.

π-Molecular Orbitals and UV-Vis Spectrum of Disilyne

The molecular orbitals (MOs) of disilyne **28** calculated at the HF/6-311G(d)//B3LYP/6-31G(d) level presented in Figure 1-9 show two nondegenerate highest occupied π MOs (HOMO-1 and HOMO) and two lowest unoccupied antibonding π* MOs (LUMO and LUMO+1). The out-of plane HOMO and LUMO+1 are represented by the pure (p_z-p_z) π MOs, whereas the in-plane HOMO-1 and LUMO are represented mainly by (p_y-p_y) π MOs with a slight contribution from the antibonding σ* (Si-Si) orbital of the central bond. In accordance with the triple-bond structure, natural bond orbital analysis of **28** shows electron occupation of the two π (Si≡Si) orbitals (1.934 and 1.897 electron), indicating their bonding character. The bond order (Wiberg bond index) of Si1≡Si1' is 2.618, which agrees with the real Si≡Si triple bond. The presence of the two nondegenerate π and two π* MOs in **28** is reflected in the ultraviolet-visible absorption spectrum of **28**, as shown in Figure 1-10. The UV-Vis spectrum of **28** in hexane at room temperature shows two weak absorption bands at 690 and 483 nm in the visible region and two relatively strong absorption bands at 328 and 259 nm in the ultraviolet region (Figure 1-10). A time-dependent (TD) DFT calculation on **28** at the B3LYP/6-31G(d) level revealed the three π–π∗ transitions at 734.6 nm (HOMO to LUMO, *f* (oscillator strength) = 0.0020), 502.9 nm (HOMO–1 to LUMO/HOMO to LUMO+1, *f* = 0.0086), and 402.0 nm (HOMO–1 to LUMO+1, *f* = 0.0016). On the basis of the TD-DFT calculation, weak absorption peaks at 690 and 483 nm in the visible region could be assigned to HOMO to LUMO and HOMO–1 to LUMO/HOMO to LUMO+1, respectively. The very weak absorption bands at 690 nm is a result of forbidden transition, which is responsible for the emerald green color of **28**. The shortest wavelength π–π∗ transition of HOMO–1 to LUMO+1 is expected to be very weak, and may be overlapped by the tail of the strong absorption band at 328 nm involving the σ and σ∗–orbitals of the tetrasilane skeleton.

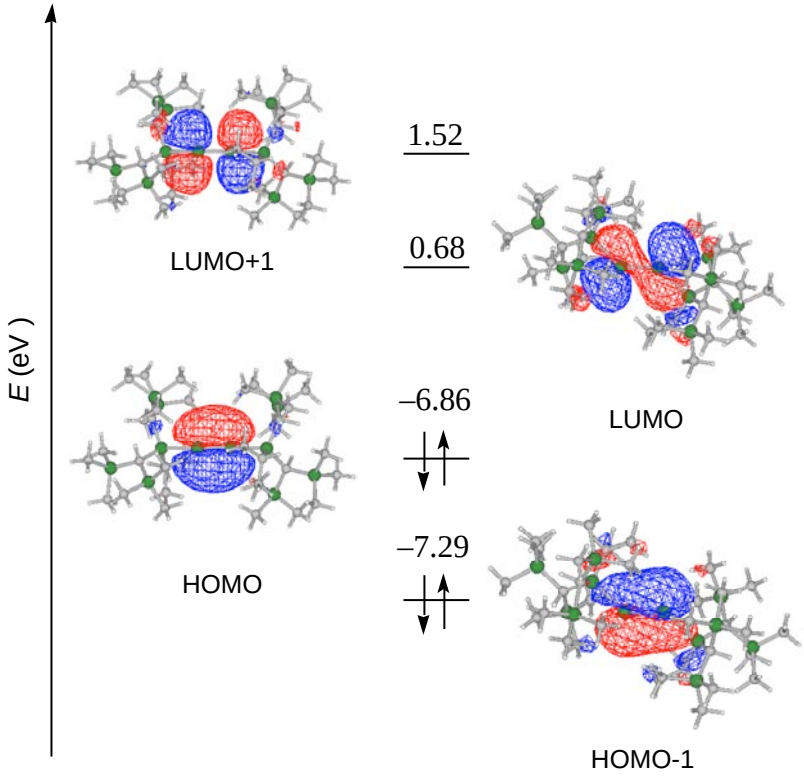

Figure 1-9. Molecular Orbitals of disilyne **28** calculated at the HF/6-311G(d)//B3LYP/6-31G(d) level.

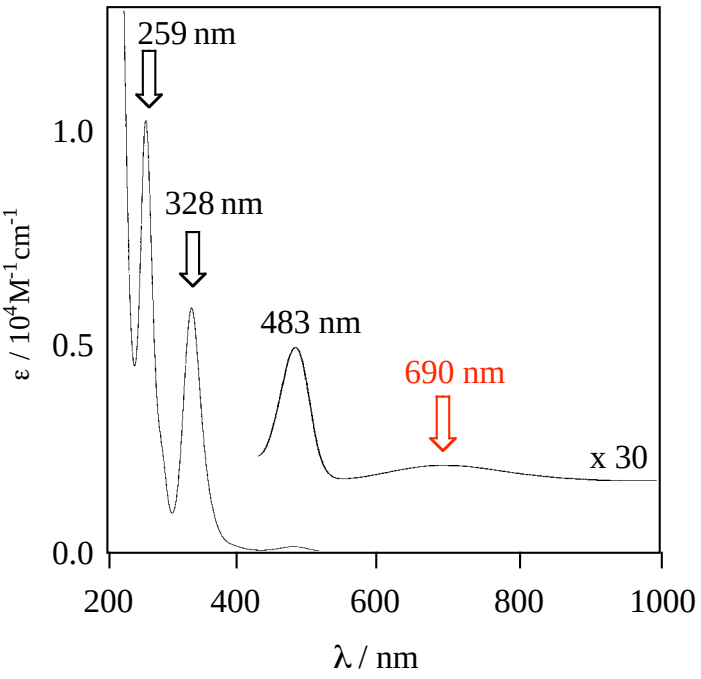

Figure 1-10. UV-Vis spectrum of disilyne **28** in hexane at room temperature.

Raman Spectrum of Disilyne

The raman spectrum of disilyne was measured (Figure 1-11-a)[45] and two characteristic signals appeared at 347 and 654 cm^{-1}. These signals well agreed with a theoretical calculation result. The vibration mode of model compound $Me_3SiSi{\equiv}SiSiMe_3$, calculated at the B3LYP/6-31+G(d, p)//B3LYP/6-31G(d) level (Figure 1-11-b), showed two signals 350 and 651 cm^{-1}. These are assigned to Si–Si≡Si bending vibration (Figure 1-11-c) and Si≡Si stretching vibration (Figure 1-11-d), respectively. The Si≡Si stretching vibration signal of 654 cm^{-1} is upper field shifted than Si=Si stretching vibration signal (593 cm^{-1}) of Mes-substituted disilene, which indicates the strong Si≡Si triple bond character of disilyne **28**. Indeed, in carbon's case, C≡C stretching vibration signals of acetylene appear in the range of 2100 to 2260 cm^{-1}, which are upper field shifted than C=C stretching vibration signals (1640 to 1670 cm^{-1}).

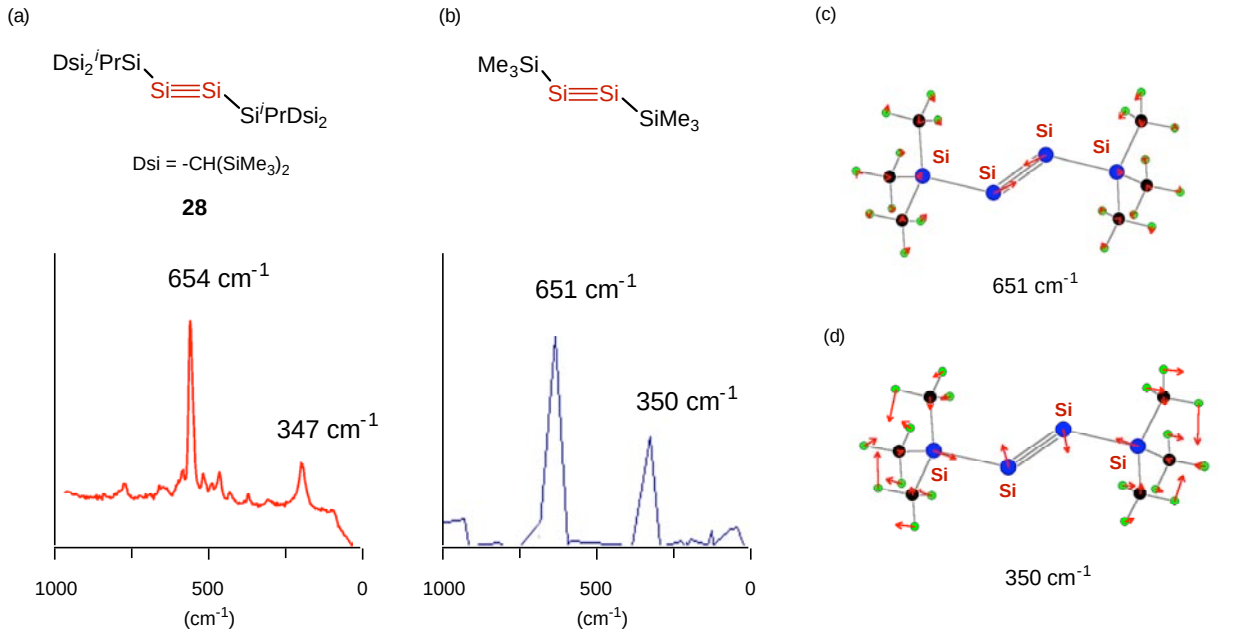

Figure 1-11. (a) Raman spectrum of disilyne **28**; (b) Raman spectrum simulation of $Me_3SiSi{\equiv}SiSiMe_3$ calculated at the B3LYP/6-31+G(d,p)//B3LYP/6-31G(d) level. (c) Si–Si≡Si bending vibration (d) Si≡Si stretching vibration.

Conclusion

The first isolable disilyne **28** was synthesized by the very simple reaction of tetrabromide precursor **27** with potassium graphite in THF. Disilyne was isolated as emerald-green crystals, which are thermally stable up to 127 °C. According to X-ray diffraction study, molecular structures of disilyne adopt *trans*-bent and planar structure with a bond angle of 137.44(4)°. The Si≡Si triple-bond length is 2.0622(9) Å, which is the shortest silicon-silicon bond length for all known silicon compounds. The frontier molecular orbitals show two sets of π-orbitals and the splitting of degenerate levels is found between these two π orbitals. It is due to the contribution from the antibonding σ∗−orbital of the central Si-Si bond. ^{29}Si NMR showed the signal of sp-silicon atom at 89.9 ppm and Raman spectrum of disilyne indicate strong bonding between the central silicon atoms. DFT calculation well reproduces the experimental geometry. Particularly, the bond order of 2.6 well agrees with the real Si≡Si triple bond.

Experimental Section

Synthesis of bis[bis(trimethylsilyl)methyl]bromosilane (16)

To a dichloromethane solution (100 ml) of bis[bis(trimethylsilyl)methyl]silane (14.0 g, 40.0 mmol), bromine (6.73 g, 42.0 mmol) was added at 0 °C in the dark. The reaction mixture was allowed to warm to room temperature with stirring. After evaporation of solvent, the residue was distillated at reduced pressure by using Kugelrohr short-path distillation apparatus to give bis[bis(trimethylsilyl)methyl] bromosilane at 84% yield.

bis[bis(trimethylsilyl)methyl] bromosilane: a colorless crystal; bp 88 °C/ 0.5 Torr;; ^{1}H NMR (C_6D_6, δ) 0.12 (d, J = 3.6 Hz, 2 H), 0.19 (s, 18 H), 0.29 (s, 18 H), 5.24 (t, J = 3.6 Hz, 1 H); ^{13}C NMR (C_6D_6, δ) 3.5, 3.6, 6.8; ^{29}Si NMR (C_6D_6, δ) 0.0, 1.1, 1.6.

Synthesis of tris[bis(trimethylsilyl)methyl]silane (17)

A mixture of bis[bis(trimethylsilyl)methyl]bromosilane (1.43 g, 3.3 mmol) and bis(trimethylsilyl)methylpotassium (1.0 mg, 5.0 mmol) in THF (7.0 ml) was stirred under room temperature overnight. After the replacement of THF solvent by hexane (10 ml), the reaction mixture was filtered for the removing of the resulting potassium salt. The residue was washed by hexane and to evaporate the hexane gave tris[bis(trimethylsilyl)methyl]silane at 49% yield. tris[bis(trimethylsilyl)methyl]silane: a colorless crystals; ^{1}H NMR (C_6D_6, δ) –0.09 (d, *J* = 2.3 Hz, 3 H), 0.27 (s, 27 H), 0.29 (s, 27 H), 4.78 (q, *J* = 2.3 Hz, 1 H); ^{13}C NMR (C_6D_6, δ) 4.3, 5.2, 6.1; ^{29}Si NMR (C_7D_8, δ) –17.5, –0.2, 1.6.

Synthesis of bis[bis(trimethylsilyl)methyl]isopropylsilane (22)

A mixture of bis(trimethylsilyl)methylchloride (16.4 g, 84.0 mmol) and lithium dispersion (2.1 g, 0.30 mol) in Et_2O (100 ml) was stirred under reflux condition for 3 days, and

bis(trimethylsilyl)methyllithium was prepared. After the solution was allowed to cool to room temperature with stirring, the solvent was replaced by hexane (100 ml), and then the reaction mixture was filtered for the removing of the resulting lithium salt and excess lithium. Again, the solvent was replaced by THF (100 ml), dichloroisoprorylsilane (6.0 g, 42 mmol) was added to the THF solution at room temperature and the reaction mixture was stirred under reflux condition overnight. After filtration and evaporation of solvent, the residue was distillated at reduced pressure by using Kugelrohr short-path distillation apparatus to give bis[bis(trimethylsilyl)methyl]isopropylsilane at 63% yield. bis[bis(trimethylsilyl)methyl]-isopropylsilane: a colorless oil; bp 70-75 °C/ 0.4 Torr; ^{1}H NMR (C_6D_6, δ) –0.68 (d, *J* = 1.3 Hz, 2 H), 0.18 (s, 36 H), 1.05 (d, *J* = 5.0 Hz, 6 H), 1.06 (dsept, *J* = 3.0 and 5.0 Hz, 1 H), 4.07 (dt, *J* = 1.3 and 3.0 Hz, 1 H); ^{13}C NMR (C_6D_6, δ) 3.3, 3.4, 4.2, 14.0, 20.4 ; ^{29}Si NMR (C_6D_6, δ) 0.2, 0.6, 0.7 ; MS (EI, 70 eV): m/e (%) 375 (M^+ – H), 347 (M^+ – ^{i}Pr).

Synthesis of iodobis[bis(trimethylsilyl)methyl]isopropylsilane (23)

A mixture of chrolohorm solution (4.5 ml) of bis[bis(trimethylsilyl)methyl]-isopropylsilane **22** (1.00 g, 2.6 mmol) and iodine (0.64 g, 2.6 mmol) was stirred at 0 °C in the dark for 2 hours. After evaporation of solvent, the residue was distillated at reduced pressure by using Kugelrohr short-path distillation apparatus to give iodo[bis(trimethylsilyl)methyl]-isopropylsilane at 75% yield. iodo[bis(trimethylsilyl)methyl]isopropylsilane: a colorless crystal; bp 130-135 °C/ 0.4 Torr; ^{1}H NMR (C_6D_6, δ) 0.23 (s, 18 H), 0.35 (s, 18 H), 0.39 (s, 2 H), 1.12 (d, *J* = 7.0 Hz, 6 H), 1.24 (sep, *J* = 7.0 Hz, 1 H) ; ^{13}C NMR (C_6D_6, δ) 4.9, 5.1, 9.7, 19.4, 21.5 ; ^{29}Si NMR (C_6D_6, δ) –1.0, 1.2, 21.7 ; MS (EI, 70 eV): m/e (%) 501 (M^+ – Me), 473 (M^+ – ^{i}Pr), 389 (M^+ – I).

Synethesis of 2,2-bis[bis(trimethylsilyl)methyl]-2-isopropyl-1-chlorodisilane (25)

To a mixture of iodo[bis(trimethylsilyl)methyl]isopropylsilane (1.00 g, 1.93 mmol) and KC_8 (650 mg, 4.81 mmol), dry oxygen-free THF (6.0 ml) and DME (6.0 ml) was added by vacuum transfer, and then the reaction mixture was stirred at –45 °C for 2.5 hours. After dichlorosilane (1.0 g, 9.0 mmol) was added to reaction mixture by vacuum transfer, the reaction mixture was allowed to warm to room temperature with stirring. The solvent was replaced by hexane, and then the reaction mixture was filtered for the removing of the resulting potassium salt and graphite. After evaporation of solvent, the residue was distillated at reduced pressure by using Kugelrohr short-path distillation apparatus to give 2,2-bis[bis(trimethylsilyl)methyl]-2-isopropyl-1-chlorodisilane at 58% yield. 2,2-bis[bis(trimethylsilyl)methyl]-2-isopropyl-1-chlorodisilane: a colorless crystal; bp 100-110 °C/ 0.1 Torr; ^{1}H NMR (C_6D_6, δ) –0.12 (s, 2 H), 0.23 (s, 18 H), 0.25 (s, 18 H), 1.24 (d, *J* = 7.2 Hz, 6 H), 1.44 (sep, *J* = 7.2 Hz, 1H), 5.07 (s, 2 H) ; ^{13}C NMR (C_6D_6, δ) 5.0, 5.1, 5.7, 17.2, 21.0 ; ^{29}Si NMR (C_6D_6, δ) –25.4, 0.0, 0.2, 0.5 ; MS (EI, 70 eV): m/e (%) 439 (M^+ – Me), 411 (M^+ – ^{i}Pr), 389 (M^+ – SiH_2Cl).

Synthesis of 1,1,4,4-tetrakis[bis(trimethylsilyl)methyl]-1,4-diisopropyltetrasilane (26)

To a mixture of 2,2-bis[bis(trimethylsilyl)methyl]-2-isopropyl-1-chlorodisilane (400 mg, 0.88 mmol) and a one piece of sodium (130 mg, 5.65 mmol), dry oxygen-free heptane (2.0 ml) was added by vacuum transfer, and then the reaction mixture was stirred under reflex condition for overnight. After filtration for the removing of the resulting sodium salt and excess sodium, the solvent was replaced by EtOH (5.0 ml) and recrystallized at 0 °C to give 1,1,4,4-tetrakis[bis(trimethylsilyl)methyl]-1,4-diisopropyltetrasilane at 70% yield. 1,1,4,4-tetrakis[bis(trimethylsilyl)methyl]-1,4-diisopropyltetrasilane: a colorless crystal; mp 182-185 °C;

^{1}H NMR (C_6D_6, δ) 0.00 (s, 4 H), 0.30 (s, 36 H), 0.37 (s, 36 H), 1.30 (d, *J* = 7.1 Hz, 12 H), 1.51 (sept, *J* = 7.1 Hz, 2H), 3.68 (s, 4 H) ; ^{13}C NMR (C_6D_6, δ) 5.2, 5.4, 7.3, 17.9, 21.8 ; ^{29}Si NMR (C_6D_6, δ) –94.3, –0.2, 0.2, 6.5 ; MS (EI, 70 eV): m/e (%) 823 (M^+ – Me), 795 (M^+ – ^{i}Pr), 419 (M^+ – $SiH_2Si[CH(SiMe_3)_2]_2{}^{i}Pr$).

Synthesis of 2,2,3,3-tetrabromo-1,1,4,4-tetrakis[bis(trimethylsilyl)methyl]-1,4-diisopropyl-tetrasilane (27)

To a dichloromethane solution (5.0 ml) of 1,1,4,4-tetrakis[bis(trimethylsilyl)methyl]-1,4-diisopropyltetrasilane (200 mg, 0.24 mmol), bromine (152 mg, 0.95 mmol) was added at -78 °C in the dark. And then the reaction mixture was allowed to warm from at -78 °C to room temperature with stirring. After evaporation of solvent, the pentane (3.0 ml) was added and the solution was recrystallized at room temperature to give 2,2,3,3-tetrabromo-1,1,4,4-tetrakis[bis(trimethylsilyl)methyl]-1,4-diisopropyltetrasilane at 59% yield. 2,2,3,3-tetrabromo-1,1,4,4-tetrakis[bis(trimethylsilyl)methyl]-1,4-diisopropyltetrasilane:
a colorless crystal; mp 193-194 °C; ^{1}H NMR (C_6D_6, δ) 0.23 (s, 2 H), 0.32 (s, 18 H), 0.34 (s, 2 H), 0.45 (s, 18 H), 0.46 (s, 18 H), 0.49 (s, 18 H), 1.21 (d, *J* = 7.0 Hz, 6 H), 1.42 (d, *J* = 7.0 Hz, 6 H), 2.16 (sept, *J* = 7.0 Hz, 2H); ^{13}C NMR (C_6D_6, δ) 2.9, 5.8, 6.0, 6.1, 6.3, 7.0, 17.7, 19.3, 20.6 ; ^{29}Si NMR (C_6D_6, δ) –1.3, –0.9, 0.0, 0.4, 1.4, 29.8.

Synthesis of 1,1,4,4-tetrakis[bis(trimethylsilyl)methyl]-1,4-diisopropyl-2-tetrasilyne (28)

To a mixture of 2,2,3,3-tetrabromo-1,1,4,4-tetrakis[bis(trimethylsilyl)methyl]-1,4-diisopropyl-tetrasilane (50 mg, 0.043 mmol) and KC_8 (25 mg, 0.182 mmol), dry oxygen-free THF (1.0 ml) was added by vacuum transfer, and then the reaction mixture was allowed to warm from at –78 °C to room temperature with stirring overnight. The solvent was replaced by hexane, and

then the reaction mixture was filtered for the removing of the resulting potassium salt and graphite. After evaporation of solvent, the pentane (1.0 ml) was added and the solution was recrystallized at –30 °C to give 1,1,4,4-tetrakis[bis(trimethylsilyl)methyl]-1,4-diisopropyl-2-tetrasilayne at 47% yield. 1,1,4,4-tetrakis[bis(trimethylsilyl)methyl]-1,4-diisopropyl-2-tetrasilayne; mp 127-129 °C (dec); ^{1}H NMR (C_6D_6, δ) –0.01 (s, 4 H), 0.39 (s, 36 H), 0.57 (s, 36 H), 1.44 (d, *J* = 6.0 Hz, 12 H), 1.49 (sept, *J* = 6.0 Hz, 2H); ^{13}C NMR (C_6D_6, δ) 5.1, 5.7, 8.9, 17.8, 22.3; ^{29}Si NMR (C_6D_6, δ) –0.3, 0.0, 20.7, 89.9; MS (EI, 70 eV): m/e (%) 834 (M^+, 10), 819 (M^+ – Me), 791 (M^+ – ^{i}Pr) ; HRMS: *m/z* calcd for $C_{34}H_{90}Si_{12}$ 834.4274, found 834.4275, UV-Vis λmax / nm (hexane, ε) 690 (14), 483 (120), 328 (5800), 259 (10300).

X-ray Crystal Structure Determination of 28

The single crystals of **28** for X-ray analysis were obtained by the recrystallization from pentane. The X-ray crystallographic experiments were performed on a MacScience DIP2030 image plate diffractometer equipped with graphite-monochromatized Mo-Kα radiation (λ = 0.71070 Å). Details of crystal data and structure refinement are summarized in Table a-(**28**). The final atomic parameters, the bond lengths and the bond angles of **28** are listed in Table b-(**28**) and c-(**28**), respectively.

Appendix

Table a-(**28**). Crystal Data and Structure Refinement for Compound **28**.

Identification code	$Dsi_2{}^{i}PrSiSiSiSi^{i}PrDsi_2$
Empirical formula	$C_{34}H_{90}Si_{12}$
Formula weight	836.14
Temperature	120.0(1) K
Wavelength	0.71070 Å
Crystal system, space group	Monoclinic, C 2/c
Unit cell dimensions	a = 30.9620(11)Å alpha = 90 deg.
	b = 10.9060(2) Å beta = 118.995(2) deg.
	c = 18.1170(7) Å gamma = 90 deg.
Volume	5350.8(3) $Å^3$
Z, Calculated density	4, 1.038 Mg/m^3
Absorption coefficient	0.312 mm^{-1}
F(000)	1848
Crystal size	0.3 x 0.15 x 0.15 mm
Theta range for data collection	2.18 to 28.01 deg.
Limiting indices	0<=h<=40, 0<=k<=14, -23<=l<=20
Reflections collected / unique	26993 / 6412 [R(int) = 0.0290]
Completeness to theta = 28.01	99.1 %
Absorption correction	None
Refinement method	Full-matrix least-squares on F^2
Data / restraints / parameters	6412 / 0 / 209
Goodness-of-fit on F^2	1.036
Final R indices [I>2sigma(I)]	R1 = 0.0373, wR2 = 0.1046
R indices (all data)	R1 = 0.0445, wR2 = 0.1096
Extinction coefficient	0.0044(3)
Largest diff. peak and hole	0.451 and -0.473 $e.Å^{-3}$

Table b-(**28**). Atomic coordinates (x 10^4) and equivalent isotropic displacement parameters ($Å^2$ x 10^3) for compound.

U(eq) is defined as one third of the trace of the orthogonalized U_{ij} tensor.

	x	y	z	U(eq)
Si(1)	249(1)	3294(1)	7276(1)	35(1)
Si(2)	1118(1)	3301(1)	7846(1)	20(1)
Si(3)	841(1)	1342(1)	6279(1)	27(1)
Si(4)	1958(1)	2138(1)	7475(1)	24(1)
Si(5)	962(1)	5984(1)	6986(1)	22(1)
Si(6)	1524(1)	5842(1)	8962(1)	25(1)
C(1)	1280(1)	2516(1)	7067(1)	21(1)
C(2)	254(1)	2065(2)	5458(1)	39(1)
C(3)	661(1)	63(2)	6758(1)	44(1)
C(4)	1096(1)	624(2)	5626(1)	42(1)
C(5)	2113(1)	2496(2)	6617(1)	41(1)
C(6)	2118(1)	495(2)	7797(1)	43(1)
C(7)	2405(1)	3075(2)	8404(1)	37(1)
C(8)	1334(1)	4965(1)	7944(1)	21(1)
C(9)	475(1)	6854(2)	7093(1)	31(1)
C(10)	628(1)	5173(2)	5951(1)	35(1)
C(11)	1394(1)	7038(2)	6840(1)	34(1)
C(12)	2087(1)	5126(2)	9852(1)	38(1)
C(13)	1734(1)	7454(2)	8936(1)	35(1)
C(14)	1008(1)	6013(2)	9223(1)	34(1)
C(15)	1385(1)	2422(2)	8892(1)	27(1)
C(16)	1318(1)	1032(2)	8772(1)	43(1)
C(17)	1200(1)	2808(2)	9506(1)	35(1)

Table c-(**28**). Bond lengths [Å] and angles [deg] for compound **28**.

Si(1)-Si(1)#1	2.0622(9)	Si(1)#1-Si(1)-Si(2)	137.44(4)
Si(1)-Si(2)	2.3698(6)	C(1)-Si(2)-C(8)	106.83(6)
Si(2)-C(1)	1.9119(15)	C(1)-Si(2)-C(15)	111.30(7)
Si(2)-C(8)	1.9120(15)	C(8)-Si(2)-C(15)	114.77(7)
Si(2)-C(15)	1.9180(16)	C(1)-Si(2)-Si(1)	108.97(5)
Si(3)-C(3)	1.8657(19)	C(8)-Si(2)-Si(1)	108.38(5)
Si(3)-C(2)	1.8759(19)	C(15)-Si(2)-Si(1)	106.47(5)
Si(3)-C(4)	1.8815(19)	C(3)-Si(3)-C(2)	106.78(10)
Si(3)-C(1)	1.9083(15)	C(3)-Si(3)-C(4)	106.97(10)
Si(4)-C(6)	1.8755(19)	C(2)-Si(3)-C(4)	102.54(9)
Si(4)-C(5)	1.8764(19)	C(3)-Si(3)-C(1)	114.75(8)
Si(4)-C(7)	1.8794(19)	C(2)-Si(3)-C(1)	112.12(7)
Si(4)-C(1)	1.9035(15)	C(4)-Si(3)-C(1)	112.76(8)
Si(5)-C(10)	1.8662(17)	C(6)-Si(4)-C(5)	108.72(10)
Si(5)-C(9)	1.8696(17)	C(6)-Si(4)-C(7)	105.78(9)
Si(5)-C(11)	1.8783(18)	C(5)-Si(4)-C(7)	104.87(9)
Si(5)-C(8)	1.9070(15)	C(6)-Si(4)-C(1)	113.78(8)
Si(6)-C(12)	1.8767(19)	C(5)-Si(4)-C(1)	108.10(8)
Si(6)-C(14)	1.8812(18)	C(7)-Si(4)-C(1)	115.10(7)
Si(6)-C(13)	1.8835(19)	C(10)-Si(5)-C(9)	105.32(8)
Si(6)-C(8)	1.8999(15)	C(10)-Si(5)-C(11)	103.52(9)
C(15)-C(16)	1.531(2)	C(9)-Si(5)-C(11)	111.69(8)
C(15)-C(17)	1.537(2)	C(10)-Si(5)-C(8)	115.72(7)

C(9)-Si(5)-C(8)	111.29(7)
C(11)-Si(5)-C(8)	109.07(7)
C(12)-Si(6)-C(14)	111.93(9)
C(12)-Si(6)-C(13)	102.83(9)
C(14)-Si(6)-C(13)	104.97(8)
C(12)-Si(6)-C(8)	110.28(7)
C(14)-Si(6)-C(8)	113.11(7)
C(13)-Si(6)-C(8)	113.18(7)
Si(4)-C(1)-Si(3)	113.36(7)
Si(4)-C(1)-Si(2)	116.41(8)
Si(3)-C(1)-Si(2)	120.43(8)
Si(6)-C(8)-Si(5)	110.91(7)
Si(6)-C(8)-Si(2)	119.85(8)
Si(5)-C(8)-Si(2)	116.01(7)
C(16)-C(15)-C(17)	107.55(14)
C(16)-C(15)-Si(2)	112.99(12)
C(17)-C(15)-Si(2)	116.40(12)

Symmetry transformations used to generate equivalent atoms: #1 -x,y,-z+3/2

Reference

1. West, R. *Angew. Chem. Int. Ed. Engl.* **1978**, *26*, 1201.
2. Raabe, G.; Michl, J. in *The Chemistry of Organic Silicon Compounds*, Patai, S.; Rappoport, Z. Eds. (Wiley, New York, 1989), part 2, chap. 17.
3. Power, P. P. *Chem. Rev.* **1999**, *99*, 3463.
4. Weidenbruch, M. *The Chemistry of Organic Silicon Compounds*, Rappoport, Z.; Apeloig, Y. Eds. (Wiley, Chichester, UK, 2001), vol. 3, chap. 5.
5. Wiberg, E. *Lehrbuch der Anorganischen Chemie*, Holleman, A. F.; Wiberg, E. Eds. (W. de Gruyter, Berlin, Germany, eds. 22 and 23, 1943).
6. Goubeau, J. *Angew. Chem.* **1957**, *69*, 77.
7. Jutzi, P. *Angew. Chem. Int. Ed. Engl.* **1957**, *14*, 232.
8. Davidson, P. J.; Lappert, M. F. *J. Chem. Soc., Chem. Commun.* **1973**, 317.
9. West, R.; Fink, M. J.; Michl, J. *Science* **1981**, *214*, 1343.
10. Brook, A. G.; Abdesaken, F.; Gutekunst, B.; Gutekunst, G. Kallury, R. K. *J. Chem. Soc., Chem. Commun.* **1981**, 191.
11. Reviews on double bond chemistry of heavier group 14 elements: a) West, R. *Pure Appl. Chem.* **1984**, *56*, 163. b) Raabe, G.; Michl, J. *Chem. Rev.* **1985**, *85*, 5. c) West, R. *Angew. Chem., Int. Ed. Engl.* **1987**, *26*, 1201. d) Raabe, G; Michl, J. *The Chemistry of Organic Silicon Compounds*, ed by Patai, S.; Rappoport, Z. Wiley, New York (1989), part 2, chap. 17. e) Tsumuraya, T.; Batcheller, S. A.; Masamune, S. *Angew. Chem., Int. Ed. Engl.* **1991**, *30*, 902. f) Grev, R. S. *Adv. Organomet. Chem.* **1991**, *39*, 231. g) Weidenbruch, M. *Coord. Chem. Rev.* **1994**, *130*, 275. h) Okazaki, R.; West, R. *Adv. Organomet. Chem.* **1996**, *39*, 231. i) Power, P. P. *J. Chem. Soc., Dalton Trans*. **1998**, 2939. j) Weidenbruch, M. *Eur. J. Inorg. Chem*. **1999**, 373. k) Kira, M.; Iwamoto, T. *J. Organomet. Chem.* **2000**, *611*, 236. l) Weidenbruch, M. *Chemistry of Organic Silicon Compounds*, ed Rappoport, Z.; Apeloig, Y. Wiley, Chichester, UK (2001), vol. 3, chap. 5. m) West, R. *Polyhedron* **2002**, **21**, 467. n) Sekiguchi, A.; Lee, V. Ya.; *Chem. Rev.* **2003**, *103*, 1429. o) Weidenbruch, M. *Organometallics* **2003**, *22*, 4348. p) Lee, V. Ya.; Sekiguchi, A. *Organometalics* **2004**, **23**, 2822 .
12. For the transient dimethyldisilyne: a) Sekiguchi, A.; Zigler, S. S.; West, R.; Michl, J. *J. Am. Chem. Soc.* **1986**, *108*, 4241. b) Sekiguchi, A.; Zigler, S. S.; Haller, K. J.; West, R. *Recl. Trav. Chim. Pays-Bas*. **1988**, *107*, 197. c) Sekiguchi, A.; Gilette, G. R.; West, R. *Organometallics*

1988, **7**, 1226.

13. For the transient sila-, germa-, and stannaalkynes: a) Karni, M.; Apeloig, Y.; Schröder, D.; Zummack, W.; Rabezzana, R.; Schwarz, H. *Angew. Chem., Int. Ed.* **1999**, *38*, 332. b) Bibal, C.; Maziéres, S.; Gornitzka, H.; Couret, C. *Angew. Chem., Int. Ed.* **2001**, *40*, 952. c) Setaka, W.; Hirai, K.; Tomioka, H.; Sakamoto, K.; Kira, M. *J. Am. Chem. Soc.* **2004**, *126*, 2696.
14. Recent reviews on triple bond chemistry of heavier group 14 elements: a) Power, P. P. *Chem. Rev.* **1999**, *99*, 3463. b) Robinson, G. H. *Acc. Chem. Res.* **1999**, *32*, 773. c) Jutzi, P. *Angew. Chem., Int. Ed.* **2000**, *39*, 3797. d) Weidenbruch, M. *J. Organomet. Chem.* **2002**, *646*, 39. e) Power, P. P. *Chem. Commun.* **2003**, 2091. f) Weidenbruch, M. *Angew. Chem., Int. Ed. Engl.* **2004**, *43*, 2. g) Power, P. P. *Appl. Organomet. Chem.* **2005**, *19*, 488.
15. The topic of complexes with a triple bond between a transition metal and a heavier group 14 element was briefly described in the recent review on the chemistry of heavier analogues of alkynes. See ref. 14.
16. Pu, L.; Twamley, B.; Power, P. P. *J. Am. Chem. Soc.* **2000**, *122*, 3524.
17. Stender, M.; Phillips, A. D.; Wright, R. J.; Power, P. P. *Angew. Chem., Int. Ed. Engl.* **2002**, *41*, 1785.
18. Phillips, A. D.; Wright, R. J.; Olmstead, M. M.; Power, P. P. *J. Am. Chem. Soc.* **2002**, *124*, 5930.
19. Sugiyama, Y.; Sasamori, T.; Hosoi, Y.; Furukawa. Y.; Takagi, N.; Nagase, S.; Tokitoh, N. *J. Am. Chem. Soc.* **2006**, *128*, 1023.
20. Lein, M.; Krapp, A.; Frenking, G. *J. Am. Chem. Soc.* **2005**, *127*, 6290.
21. Bridgeman, A. J.; Ireland, L. R. *Polyhedron* **2001**, *20*, 2841.
22. Pietschnig, R.; West, R. Powell, D. R. *Oragnometallics* **2000**, *19*, 2724.
23. Wiberg, N.; Niedermayer, W.; Fischer, G.; Nöth, H.; Suter, M. *Eur. J. Inorg. Chem.* **2002**, 1066.
24. Takagi, N.; Nagase, S. *Eur. J. Inorg. Chem.* **2002**, 2775.
25. Wiberg, N.; Vasisht, S. K.; Fischer, G.; Mayer, P. *Z. Anorg. Allg. Chem.* **2004**, *630*, 1823.
26. a) Nagase, S.; Kobayashi, K.; Takagi, N. *J. Organomet. Chem.* **2000**, *611*, 264. b) Kobayashi, K.; Takagi, N.; Nagase, S. *Oraganometallics* **2001**, *20*, 234. c) Takagi, N.; Nagase, S. *Chem. Lett.* **2001**, 966.
27. Wiberg, N.; Finger, C. M. M.; Polborn, K. *Angew. Chem., Int. Ed. Engl.* **1993**, *32*, 1054.
28. Ichinohe, M.; Toyoshima, M.; Kinjo, R.; Sekiguchi, A. *J. Am. Chem. Soc.* **2003**, *125*, 13328.

29. K. Kobayashi and S. Nagase, *Organometallics*, **1997**, *16*, 2489.
30. (a) Sekiguchi, A.; Kinjo, R.; Ichinohe, M. *Science* **2004**, *305*, 1755; (b) Sekiguchi, A.; Ichinohe, M.; Kinjo, R. *Bull. Chem. Soc. Jpn* **2006**, *79*, 825.
31. Kira, M.; Maruyama, T.; Kabuto, C.; Ebata, K.; Sakurai, H. *Angew. Chem., Int. Ed. Engl.* **1994**, *33*, 1489.
32. Sakurai, H.; Tobita, H.; Nakadaira, Y. *Chem. Lett.* **1982**, 1251.
33. (a) 37 mg of **28** were placed under vacuum in an air-tight 7.5-mm ZrO_2 rotor. Measurements were made at r.t. on a Chemmagnetics Unity 300 MHz (proton) NMR spectrometer operating at a sample frequency of 59.606 MHz (for ^{29}Si), with a Doty Scientific Inc. probe. Spinning speed was 5-5.33 kHz, the CP mixing time was 5.0 ms followed by a 3s delay; the pulse width was 12 ms. The spectra were referenced to external $(Me_3Si)_4Si$ for ^{29}Si. Analysis of the sidebands was done using Bruker Xwin-NMR Version 3.5 patch level 6, and followed by Herzfeld-Berger method[33b] to obtain the CST; (b) Herzfeld, J.; Berger, A. E. *J. Chem. Phys.* **1980**, *73*, 6021.
34. Taylor, R. E. *Concepts in Magnetic Resonance*, Part A, **2004**, *22A*(1), 37. John Wiley & Sons, Inc.
35. (a) Using Gaussian 98 (Revision A.11) and Gaussian 03 (Revision B.05), Gaussian, Inc., Pittsburgh PA, the full list of authors is given in the Supporting information. (b) Boese, A. D.; Handy, N. C. *J. Chem. Phys.* **2001**, *114*, 5497. (c) Koch. W.; Holthausen, M. C. *A Chemist's Guide to Density Functional Theory*, Wiley-VCH: Weinheim, 2000. (d) For basis sets and references see: http://www.emsl.pnl.gov/forms/basisform.html. (e) At HCTH40714b/6-311G(3d)[Si]:6-31G(d)[C,H]//B3LYP15c/6-311G(d)[Si]:6-31G(d)[C,H]14d,f for **28** and at HCTH407/6-311G(3d)//B3LYP/6-31G(d,p) for **29** and **30**. (f) The notation: "method/base a [A]:base b [B]" indicates that bases a and b are used for atoms A and B, respectively.
36. The largest difference between experiment and theory of ca. 85 ppm is found for δ_{33} (Table 1-3). This discrepancy may result from a large noise/signal ratio that obscures several side-bands in the high field and may lead to an error of ca. 15%.
37. Karni, M.; Apeloig, Y.; Takagi, N.; Nagase, S. *Organometallics* **2005**, *24*, 6319.
38. West, R.; Cavalieri, J. D.; Buffy, J. J.; Fry, C.; Zlim, K. W.; Duchamp, J. C.; Kira, M.; Iwamoto, T.; Müler, T.; Apeloig, Y. *J. Am. Chem. Soc.* **1997**, *119*, 4927.
39. The calculated δ_{22} and $\delta_{33}$are rotated about the Y axis by β = 17° and 20° for **28** and **29**,

respectively.

40. (a) Zilm, K. W.; Conlin, R. T.; Grant, D. M.; Michl, J. *J. Am. Chem. Soc*. **1980**, *102*, 6672. (b) Beeler, A. J.; Orendt, A. M.; Grant, D. M.; Cutts, P. W.; Michl, J.; Zilm, K. W.; Downing, J. W.; Facelli, J. C.; Schindlet, M. S.; Kutzelnigg, W. *J. Am. Chem. Soc*. **1984**, *106*, 7673.
41. (a) The total chemical shielding (and CSTs) are a sum of diamagnetic and paramagnetic contributions.[41b] The behavior of the CSTs and the CSA are primarily determined by the paramagnetic contribution σp. (b) *Molecular Quantum Mechanics*, Atkins, P. W.; Friedman, R. S. Eds., 3rd Ed. Oxford University Press, 1997. (c) Ramsey, N. F. *Phys. Rev.* **1950**, *78*, 699.
42. Auer, D.; Kaupp, M.; Strohmann, C. *Organometallics* **2005**, *24*, 6331.
43. CSA = $\sigma_{33} - (\sigma_{22} + \sigma_{11})/2$ (or $\delta_{33} - (\delta_{11} + \delta_{22})/2$); σ_{33} or δ_{33} represent the highest field tensor components.
44. Power, P. P. *Chem. Commun.* **2003**, 2091.

Chapter 2

Stereospecific [2+2] cycloaddition of Disilyne. Synthesis of *cis*- and *trans*-3,4-dimethyl-1,2-bis[bis(trimethylsilyl)methylisopropylsilyl]-1,2-disilacylobut-1-ene

Summary

The reactions of 1,1,4,4-tetrakis[bis(trimethylsilyl)methyl]-1,4-diisopropyl-2-tetrasilyne **28** with excess amounts of *cis*- or *trans*-2-butene in hexane produces *cis*-3,4-dimethyl-1,2-bis[bis(trimethylsilyl)methylisopropylsilyl]-1,2-disilacylobut-1-ene or *trans*-3,4-dimethyl-1,2-bis[bis(trimethylsilyl)methylisopropylsilyl]-1,2-disilacylobut-1-ene, respectively. The cycloaddition of 2-butene to 1,1,4,4-tetrakis[bis(trimethylsilyl)methyl]-1,4-diisopropyl-2-tetrasilyne **28** was found to be completely stereospesific. The reaction of 1,1,4,4-tetrakis[bis(trimethylsilyl)methyl]-1,4-diisopropyl-2-tetrasilyne **28** with *cis*-2-butene is faster than addition of *trans*-2-butene. The molecular structure of the [2+2] cycloaddition product, *trans*-3,4-dimethyl-1,2-bis[bis(trimethylsilyl)methylisopropylsilyl]-1,2-disilacylobut-1-ene was determined by X-ray crystallography. The reaction mechanism of [2+2] cycloadditions is discussed on the basis of theoretical calculation.

Introduction

Recently, numerous multiple bond species including heavier group 14 elements have been isolated and characterized.[1] Especially, a considerable interest has been focussed on the nature of alkene analogues of silicon[2] due to their unusual structures and bonding since the isolation of stable crystalline disilene derivatives by West, Masamune and co-workers.[3] In many cases, π bond of disilene has displayed an increased reactivity toward many reagents relative to alkenes because of relatively weak silicon-silicon π bond and its biradical character.[4] For example, π bond of disilene is known to undergo efficient [2+2] cycloaddition with alkene or acetylene to give disilacyclobutane or disilacyclobutene, respectively, though [2+2] cycloaddition is thermally forbidden (Scheme 2-1a-f).[5]

Scheme 2-1.

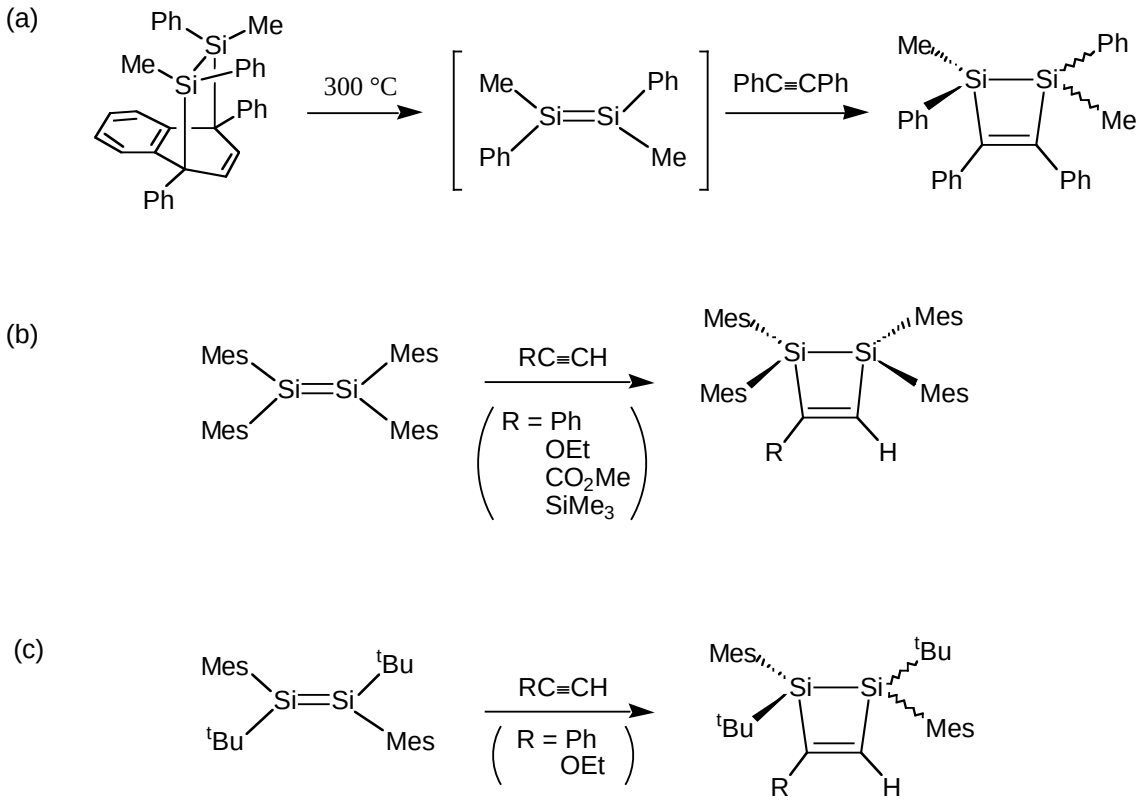

(d)

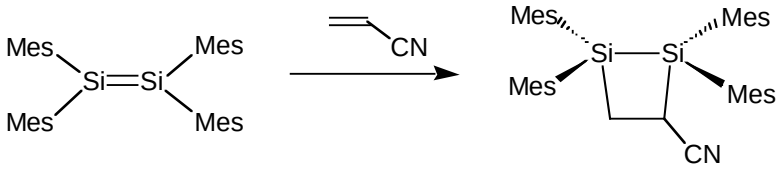

(e)

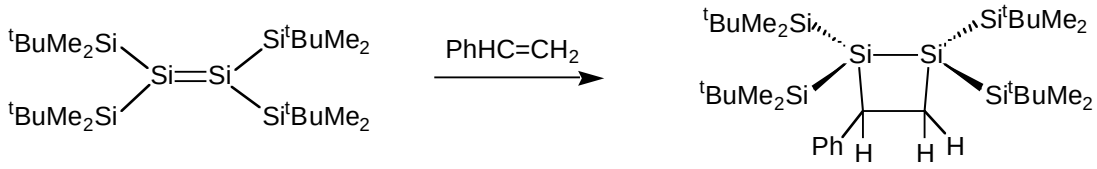

(f)

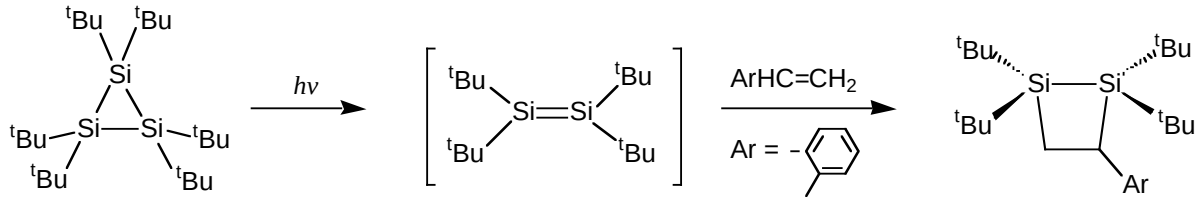

On the other hand, much remained uncovered in the chemistry of disilyne with two different kinds of π bond.[6] Comparison of the chemical behavior of disilyne with that of alkynes is of special interest. In spite of the presence of spatially-demanding substituents, which are necessary to protect the silicon-silicon triple bond, the relatively stable disilynes have been frequently proved to be more reactive than simple alkynes. For example, Wiberg's disilyne **12** undergoes smooth [2+2] cycloaddition reaction with C=C double–bond of ethylene, though the reaction mechanism has not been revealed (Scheme 2-2).[6n] Then, to examine the nature of the π bond of silicon-silicon triple bond in detail, the reaction of disilyne[7] and alkene was examined. In this chapter, the stereospecific [2+2] cycloaddition of silicon-silicon triple bond with 2-butene, together with the reaction mechanisms and stereochemistry by theoretical calculation are presented.

Scheme 2-2.

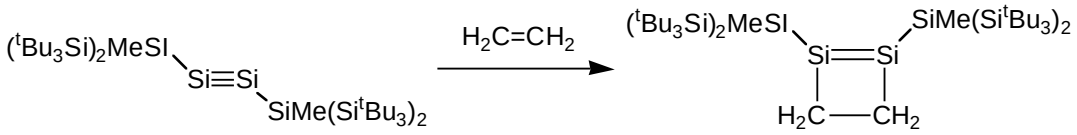

12 **31**

Reaction of Disilyne and 2-butene

When the hexane solution of disilyne **28** was treated with excess of *cis*-2-butene at room temperature, the cis-3,4-dimethyl-1,2-disilacyclobutene **32a** was obtained as a sole product (Scheme 2-3). This reaction cleanly completed in 30 minutes. **32a** was isolated as yellow crystals (89%) thermally stable in the absence of air. On the other hand, the reaction of disilyne with *trans*-2-butene under the same condition afforded *trans*-3,4-dimethyl-1,2-disilacyclobutene **32b** as yellow crystals (85%) thermally stable in the absence of air. In contrast to the reaction with *cis*-2-butene, it took 1 day to complete this reaction. Interestingly, it was found that these reactions proceeded stereospesifically, as expected for the concerted [2+2] cycloaddition reaction. Although excess of 2-butenes were used in both reactions, subsequent cycloaddition reaction was not observed. The constitutions of both products were substantiated by ^{1}H, ^{13}C and ^{29}Si NMR data and confirmed, in case of **32b**, by X-ray structure analysis. In the ^{29}Si NMR spectrum, low-field shifted signals (156.0 and 152.1 ppm for **32a** and **32b**, respectively) characteristic of sp^2–silicon atoms were observed. Each signal for 1,2-disilacyclobutene skeletons appeared at 39.0 ppm for **32a** and 46.8 ppm for **32b** in ^{13}C NMR.

Scheme 2-3.

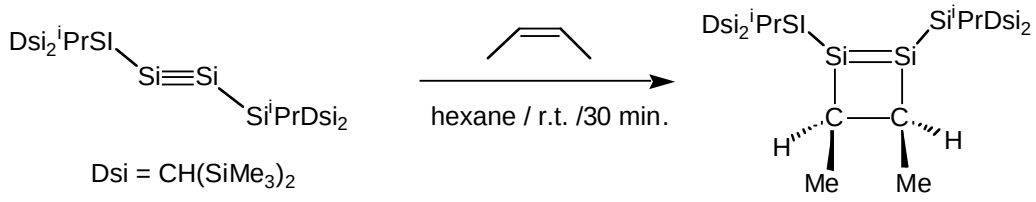

28 **32a**

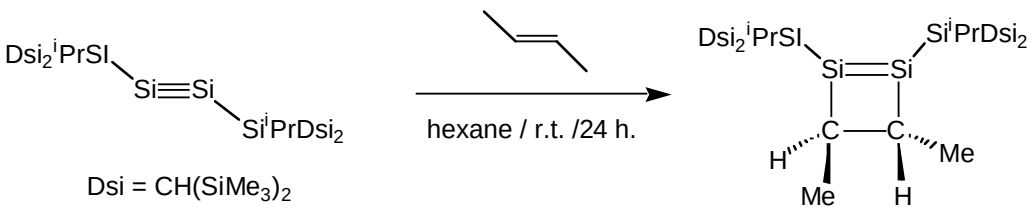

28 **32b**

Molecular Structure of 1,2disilacyclobutene 32b

Compound **32b** contains a planar four-membered ring, and sum of the interior bond angles of four-membered ring is 359.99° (Figure 2-1). The geometries around the silicon-silicon double bond is a little trans-bent (θ = 10.88° around Si1 and 13.79° around Si2; bend angle θ is defined as an angle between the Si3–Si1–C4 plane and Si1–Si2 bond). The twist angle γ determined by the angle between two the Si(sp^3)–Si(sp^2)–C(sp^3) planes is 5.18°. The length of Si1–Si2 bond is 2.1632 Å, which is 4.9% longer than silicon-silicon triple bond length of precursor, disilyne (2.0622 Å). The lengths of Si1–C4 (1.933(3)) and Si2–C3 (1.949(3)) bonds were found to be longer than typical Si–C single bond (1.89 Å). Furthermore, the C3–C4 bond length is 1.579(4) Å, which is also longer than typical C–C single bond (1.54 Å).

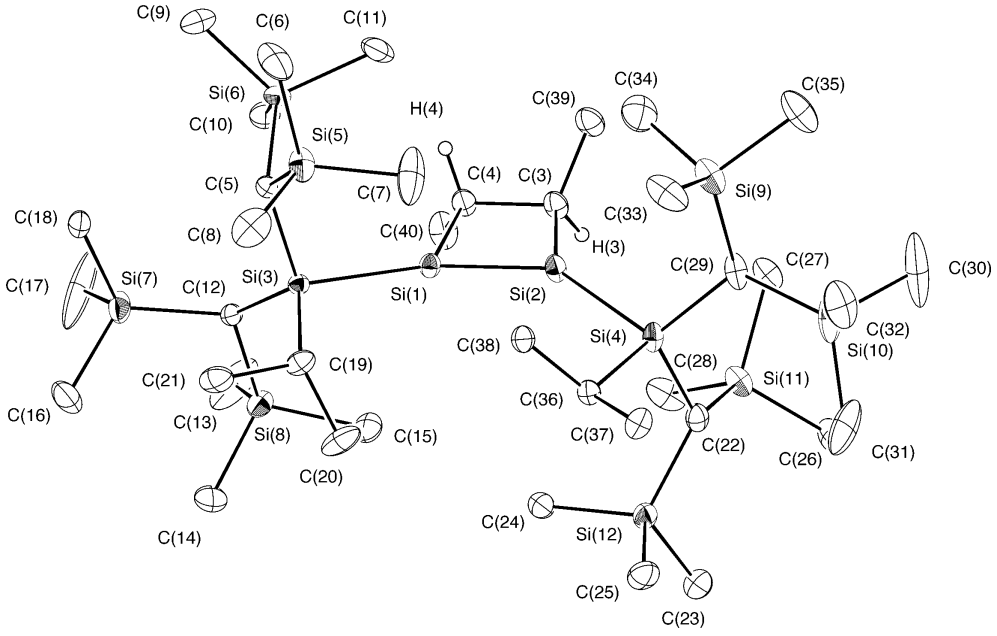

Figure 2-1. ORTEP drawing of 1,2-disilacyclobutene **32b**.

Theoretical Study: Formation Mechanism of 1,2-disilacyclobutenes

In general, [2+2] cycloaddition is thermally forbidden. Nevertheless, [2+2] cycloaddition reactions of disilyne and 2-butene proceeded cleanly at room temperature. Then, the reaction mechanism was examined by theoretical calculations. Figure 2-2 shows the reaction mechanisms of disilyne **28** with 2-butenes, together with the energies of both transition states and intermediates found by theoretical calculation of B3LYP/6-31G(d) level.[8] As shown in Figure 2-2, the [1+2] interaction between LUMO (in plane) of disilyne and HOMO of 2-butene is the first step in both reactions to generate the silylene-substituted silacyclopropane intermediate (**Int1**). Another [1+2] interaction between HOMO (out plane) of disilyne and LUMO of 2-butene is unfavorable because of the bigger steric repulsion between 2-butene and bis[bis(trimethylsilyl)methyl]isopropylsilyl group of disilyne. Since reaction time depends on the activation barrier on the first step which is the rate–determining stage, it was found that the reaction with *trans*-2-butene (E_a = +23.3 kcal/mol) takes a longer time than that with *cis*-2-butene (E_a = +18.5 kcal/mol). The difference of activation barriers is attributed to the degree of steric repulsion between Me group of 2-butene and bis[bis(trimethylsilyl)methyl]isopropylsilyl group of disilyne. Next, the intramolecular insertion of the silylene into the neighboring Si–C bond follows the rotation about the Si1–Si2 bond with the retention of stereo configuration to give 1,2-disilacyclobutene. Steric protection around silicon-silicon double bond of 1,2-disilacyclobutenes by two bulky substituents prevents the following [2+2] cycloaddtion with another 2-butene.

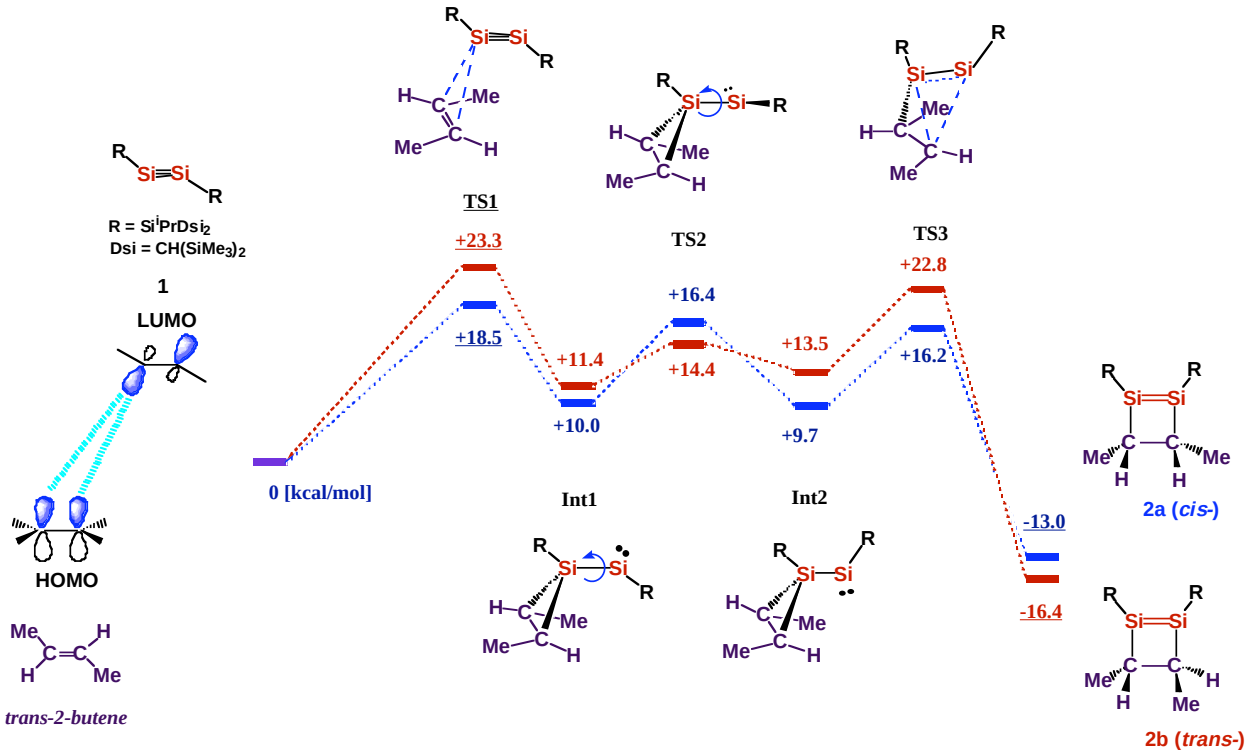

Figure 2-2. Calculated energies of transition state and intermediates (kcal/mol, B3LYP/6-31G).

Conclusion

The stereospecific synthesis of 1,2-disilacyclobutenes **32a** and **32b**, by the [2+2] cycloaddition reactions of disilyne **28** with 2-butenes was performed. It appears that the reaction with *cis*-2-butene occurs faster than the reaction with *trans*-2-butene. The structure of *trans*-2,3-dimethyl-1,2-disilacyclobutene **32b** was unequivocally determined by X-ray crystallography. Furthermore, theoretical calculation results showed that these reactions begin from the [1+2] interaction between LUMO of disilyne and HOMO of 2-butene affording silylene-substituted silacyclopropane intermediate. Because the intramolecular insertion of the silylene into the neighboring Si–C bond follows the rotation about the Si–Si bond with the retention of stereo configuration, these reactions proceed stereospecifically.

Experimental Section

Synthesis of *cis*-3,4-dimethyl-1,2-bis[bis(trimethylsilyl)methylisopropylsilyl]-1,2-disilacylobut-1-ene (32a)

To dry oxygen-free hexane (1.0 ml) solution of 1,1,4,4-tetrakis[bis(trimethylsilyl)methyl]-1,4-diisopropyl-tetrasila-2-yne (72 mg, 0.086 mmol), *cis*-2-butene (1.5 ml at –30°C) was added by vacuum transfer, and then the reaction mixture was stirred at room temperature for 30 minutes. After evaporation of solvent and remaining *cis*-2-butene, the residue was recrystallized from hexane (0.5 ml) at –30 °C to give *cis*-3,4-dimethyl-1,2-bis[bis(trimethylsilyl)methylisopropylsilyl] -1,2-disilacylobut-1-ene as yellow crystals (68 mg, 89%); Mp 161 °C (dec); ^{1}H NMR (C_6D_6, δ) 0.15 (s, 2 H, C*H*($SiMe_3$)$_2$), 0.17 (s, 2 H, C*H*($SiMe_3$)$_2$), 0.33 (s, 18 H, Si*Me*$_3$), 0.36 (s, 18 H, Si*Me*$_3$), 0.40 (s, 18 H, Si*Me*$_3$), 0.45 (s, 18 H, Si*Me*$_3$), 1.32 (d, *J* = 7.2 Hz, 6 H, CH(C*H*$_3$)$_2$), 1.37 (d, *J* = 7.2 Hz, 6 H, CH(C*H*$_3$)$_2$), 1.50 (d, *J* = 7.1 Hz, 6 H, =SiCH(*CH*$_3$)), 1.54 (qq, *J* = 7.2 and 7.2 Hz, 2 H, C*H*(CH_3)$_2$), 3.06 (q, *J* = 7.1 Hz, 2 H, =SiC*H*(CH_3)); ^{13}C NMR (C_6D_6, d) 5.51 (Si*Me*$_3$), 5.53 (Si*Me*$_3$), 5.9 (Si*Me*$_3$), 6.1 (*C*H($SiMe_3$)$_2$), 6.26 (Si*Me*$_3$), 6.34 (*C*H($SiMe_3$)$_2$), 17.9 (*C*H(CH_3)$_2$), 19.9 (=SiCH(*C*H$_3$)$_2$), 22.0 (CH(*C*H$_3$)$_2$), 22.6 (CH(*C*H$_3$)$_2$), 39.9 (=Si*C*H(CH_3)$_2$); ^{29}Si NMR (C_6D_6, d) –0.6 (*Si*Me_3), –0.3 (*Si*Me_3), –0.2 (*Si*Me_3), 0.0 (*Si*Me_3), 5.8 (*Si*^{i}PrDsi$_2$), 156.0 (=*Si*Si^{i}PrDsi$_2$); HRMS: *m/z* calcd for $C_{34}H_{90}Si_{12}$ 890.4900, found 890.4907; UV-Vis (hexane) λ_{max} / nm (ε) 420 (6040), 234 (21880).

Synthesis of *trans*-3,4-dimethyl-1,2-bis[bis(trimethylsilyl)methylisopropylsilyl]-1,2-disilacylobut-1-ene (32a)

To dry oxygen-free hexane (1.0 ml) solution of 1,1,4,4-tetrakis[bis(trimethylsilyl)methyl]-1,4-diisopropyl-tetrasila-2-yne (72 mg, 0.086 mmol), *trans*-2-butene (2.0 ml at –30°C) was added by vacuum transfer, and then the reaction mixture was stirred at room temperature for 24 hours. After evaporation of solvent and remaining *trans*-2-butene, the residue was recrystallized from hexane (0.5 ml) at –30 °C to give *trans*-3,4-dimethyl-1,2-bis[bis(trimethylsilyl)methyl-isopropylsilyl]-1,2-disilacylobut-1-ene as yellow crystals (65 mg, 85%); Mp 164 °C (dec); ^{1}H NMR (C_6D_6, δ) 0.06 (s, 2 H, C*H*($SiMe_3$)$_2$), 0.21 (s, 2 H, C*H*($SiMe_3$)$_2$), 0.31 (s, 18 H, Si*Me*$_3$), 0.41 (s, 18 H, Si*Me*$_3$), 0.42 (s, 18 H, Si*Me*$_3$), 0.43 (s, 18 H, Si*Me*$_3$), 1.30 (d, *J* = 6.8 Hz, 6 H, CH(C*H*$_3$)$_2$), 1.44 (d, *J* = 6.8 Hz, 6 H, CH(C*H*$_3$)$_2$), 1.52 (qq, *J* = 6.8 and 6.8 Hz, 2 H, C*H*(CH_3)$_2$), 1.68 (d, *J* = 7.0 Hz, 6 H, =SiCH(C*H*$_3$)), 2.42 (q, *J* = 7.0 Hz, 2 H, =SiC*H*(CH_3)); ^{13}C NMR (C_6D_6, δ) 5.4 (Si*Me*$_3$), 5.5 (Si*Me*$_3$), 5.8 (*C*H($SiMe_3$)$_2$), 5.9 (Si*Me*$_3$), 6.1 (Si*Me*$_3$), 7.2 (*C*H($SiMe_3$)$_2$), 17.9 (*C*H(CH_3)$_2$), 21.9 (CH(*C*H$_3$)$_2$), 23.0 (CH(*C*H$_3$)$_2$), 23.5 (=SiCH(*C*H$_3$)), 46.8 (=Si*C*H(CH_3)); ^{29}Si NMR (C_6D_6, δ) –0.9 (*Si*Me_3), –0.5 (*Si*Me_3), –0.1 (*Si*Me_3), 0.2 (*Si*Me_3), 6.6 (*Si*^{i}PrDsi$_2$), 152.1 (=*Si*Si^{i}PrDsi$_2$); HRMS: *m/z* calcd for $C_{34}H_{90}Si_{12}$ 890.4900, found 890.4905; UV-Vis (hexane) λ_{max} / nm (ε) 422 (5320), 237 (15490).

X-ray Crystal Structure Determination of 32b

The single crystals of **32b** for X-ray analysis were obtained by the recrystallization from hexane. The X-ray crystallographic experiments were performed on a MacScience DIP2030 image plate diffractometer equipped with graphite-monochromatized Mo-Kα radiation (λ = 0.71070 Å). Details of crystal data and structure refinement are summarized in Table a-(**32b**). The final atomic parameters, the bond lengths and the bond angles of **32b** are listed in Table b-(**32b**) and c-(**32b**), respectively.

Appendix

Table a-(**32b**). Crystal Data and Structure Refinement for Compound **32b**.

Identification code	$(Dsi_2{}^{i}PrSi)_2Si_2C_2(Me_2)(H_2)$
Empirical formula	$C_{38}H_{98}Si_{12}$
Formula weight	892.24
Temperature	120.0(1) K
Wavelength	0.71070 Å
Crystal system, space group	Monoclinic, C c
Unit cell dimensions	a = 11.8790(3)Å alpha = 90 deg.
	b = 16.2050(6) Å beta = 90.886(2) deg.
	c = 29.3670(9) Å gamma = 90 deg.
Volume	5652.4(3) $Å^3$
Z, Calculated density	4, 1.048 Mg/m^3
Absorption coefficient	0.299 mm^{-1}
F(000)	1976
Crystal size	0.5 x 0.25 x 0.15 mm
Theta range for data collection	2.13 to 28.01 deg.
Limiting indices	0<=h<=15, 0<=k<=21, -38<=l<=38
Reflections collected / unique	29754 / 6682 [R(int) = 0.0400]
Completeness to theta = 28.01	97.8 %
Absorption correction	None
Refinement method	Full-matrix least-squares on F^2
Data / restraints / parameters	6687 / 11 / 463
Goodness-of-fit on F^2	1.021
Final R indices [I>2sigma(I)]	R1 = 0.0381, wR2 = 0.0965
R indices (all data)	R1 = 0.0412, wR2 = 0.0992
Extinction coefficient	0.0031(3)
Largest diff. peak and hole	0.446 and -0.430 $e.Å^{-3}$

Table b-(**32b**). Atomic coordinates (x 10^4) and equivalent isotropic displacement parameters ($Å^2$ x 10^3) for compound.

U(eq) is defined as one third of the trace of the orthogonalized U_{ij} tensor.

	x	y	z	U(eq)
Si(1)	7468(1)	1745(1)	7959(1)	26(1)
Si(2)	6644(1)	1757(1)	8611(1)	31(1)
Si(3)	7878(1)	1035(1)	7269(1)	22(1)
Si(4)	6101(1)	862(1)	9215(1)	30(1)
Si(5)	5312(1)	666(1)	6903(1)	44(1)
Si(6)	6363(1)	2416(1)	6759(1)	39(1)
Si(7)	9747(1)	1211(1)	6435(1)	45(1)
Si(8)	10602(1)	1330(1)	7445(1)	36(1)
Si(9)	3405(1)	1305(1)	9091(1)	46(1)
Si(10)	4248(1)	638(1)	10042(1)	62(1)
Si(11)	7605(1)	1978(1)	9896(1)	37(1)
Si(12)	8562(1)	244(1)	9626(1)	35(1)
C(3)	6938(3)	2935(2)	8552(1)	33(1)
C(4)	7524(3)	2920(2)	8073(1)	33(1)
C(5)	6675(2)	1278(2)	6849(1)	27(1)
C(6)	4167(3)	1069(4)	6512(2)	73(2)
C(7)	4736(4)	662(5)	7494(2)	89(2)
C(8)	5453(4)	-439(3)	6713(2)	62(1)
C(9)	5848(5)	2614(3)	6159(2)	68(1)
C(10)	7618(4)	3112(2)	6821(1)	47(1)
C(11)	5294(4)	2790(3)	7178(2)	55(1)
C(12)	9314(2)	1396(2)	7049(1)	26(1)
C(13)	11527(5)	2243(5)	7347(2)	96(3)
C(14)	11479(4)	375(4)	7367(2)	76(2)

C(15)	10315(3)	1375(3)	8069(1)	44(1)
C(16)	10511(7)	213(6)	6322(2)	130(4)
C(17)	10715(7)	2058(7)	6267(2)	155(5)
C(18)	8600(3)	1234(3)	5993(1)	41(1)
C(19)	7864(3)	-119(2)	7385(1)	34(1)
C(20)	8590(4)	-423(2)	7785(2)	56(1)
C(21)	8180(4)	-596(2)	6954(1)	47(1)
C(22)	7253(3)	903(2)	9677(1)	32(1)
C(23)	9596(3)	418(3)	10110(1)	46(1)
C(24)	9329(3)	429(2)	9083(1)	41(1)
C(25)	8259(4)	-895(2)	9671(1)	48(1)
C(26)	7863(4)	1938(3)	10532(2)	57(1)
C(27)	6444(3)	2760(2)	9815(1)	41(1)
C(28)	8871(3)	2419(2)	9606(2)	56(1)
C(29)	4690(3)	1142(2)	9480(1)	38(1)
C(30)	3806(8)	1487(4)	10437(2)	127(4)
C(31)	5341(5)	28(5)	10371(2)	91(2)
C(32)	3045(4)	-112(3)	9981(2)	70(2)
C(33)	2843(3)	337(3)	8822(2)	65(1)
C(34)	3682(4)	2050(4)	8624(2)	64(1)
C(35)	2228(4)	1804(3)	9413(2)	66(1)
C(36)	6246(6)	-208(3)	8938(2)	27(1)
C(37)	5646(11)	-875(8)	9212(4)	36(3)
C(38)	5790(5)	-194(4)	8448(2)	31(1)
C(39)	5931(3)	3518(2)	8546(1)	42(1)
C(40)	8664(4)	3345(2)	8090(1)	47(1)
C(86)	5730(5)	-133(3)	8886(2)	27(1)
C(87)	5309(10)	-847(7)	9178(4)	36(3)
C(88)	6634(5)	-432(4)	8559(2)	31(1)

Table c-(**32b**). Bond lengths [Å] and angles [deg] for compound **32b**.

Si(1)-Si(1)#1	2.0622(9)	Si(1)#1-Si(1)-Si(2)	137.44(4)	C(9)-Si(5)-C(8)	111.29(7)
Si(1)-Si(2)	2.3698(6)	C(1)-Si(2)-C(8)	106.83(6)	C(11)-Si(5)-C(8)	109.07(7)
Si(2)-C(1)	1.9119(15)	C(1)-Si(2)-C(15)	111.30(7)	C(12)-Si(6)-C(14)	111.93(9)
Si(2)-C(8)	1.9120(15)	C(8)-Si(2)-C(15)	114.77(7)	C(12)-Si(6)-C(13)	102.83(9)
Si(2)-C(15)	1.9180(16)	C(1)-Si(2)-Si(1)	108.97(5)	C(14)-Si(6)-C(13)	104.97(8)
Si(3)-C(3)	1.8657(19)	C(8)-Si(2)-Si(1)	108.38(5)	C(12)-Si(6)-C(8)	110.28(7)
Si(3)-C(2)	1.8759(19)	C(15)-Si(2)-Si(1)	106.47(5)	C(14)-Si(6)-C(8)	113.11(7)
Si(3)-C(4)	1.8815(19)	C(3)-Si(3)-C(2)	106.78(10)	C(13)-Si(6)-C(8)	113.18(7)
Si(3)-C(1)	1.9083(15)	C(3)-Si(3)-C(4)	106.97(10)	Si(4)-C(1)-Si(3)	113.36(7)
Si(4)-C(6)	1.8755(19)	C(2)-Si(3)-C(4)	102.54(9)	Si(4)-C(1)-Si(2)	116.41(8)
Si(4)-C(5)	1.8764(19)	C(3)-Si(3)-C(1)	114.75(8)	Si(3)-C(1)-Si(2)	120.43(8)
Si(4)-C(7)	1.8794(19)	C(2)-Si(3)-C(1)	112.12(7)	Si(6)-C(8)-Si(5)	110.91(7)
Si(4)-C(1)	1.9035(15)	C(4)-Si(3)-C(1)	112.76(8)	Si(6)-C(8)-Si(2)	119.85(8)
Si(5)-C(10)	1.8662(17)	C(6)-Si(4)-C(5)	108.72(10)	Si(5)-C(8)-Si(2)	116.01(7)
Si(5)-C(9)	1.8696(17)	C(6)-Si(4)-C(7)	105.78(9)	C(16)-C(15)-C(17)	107.55(14)
Si(5)-C(11)	1.8783(18)	C(5)-Si(4)-C(7)	104.87(9)	C(16)-C(15)-Si(2)	112.99(12)
Si(5)-C(8)	1.9070(15)	C(6)-Si(4)-C(1)	113.78(8)	C(17)-C(15)-Si(2)	116.40(12)
Si(6)-C(12)	1.8767(19)	C(5)-Si(4)-C(1)	108.10(8)		
Si(6)-C(14)	1.8812(18)	C(7)-Si(4)-C(1)	115.10(7)		
Si(6)-C(13)	1.8835(19)	C(10)-Si(5)-C(9)	105.32(8)		
Si(6)-C(8)	1.8999(15)	C(10)-Si(5)-C(11)	103.52(9)		
C(15)-C(16)	1.531(2)	C(9)-Si(5)-C(11)	111.69(8)		
C(15)-C(17)	1.537(2)	C(10)-Si(5)-C(8)	115.72(7)		

C(22)-Si(4)-C(86)	122.7(2)	C(15)-Si(8)-C(12)	115.96(14)	C(39)-C(3)-Si(2)	117.8(2)
C(36)-Si(4)-C(86)	19.1(2)	C(14)-Si(8)-C(12)	114.3(2)	C(4)-C(3)-Si(2)	98.40(19)
C(29)-Si(4)-Si(2)	113.98(13)	C(34)-Si(9)-C(33)	107.3(3)	C(40)-C(4)-C(3)	111.6(3)
C(22)-Si(4)-Si(2)	107.87(10)	C(34)-Si(9)-C(35)	103.5(2)	C(40)-C(4)-Si(1)	118.7(2)
C(36)-Si(4)-Si(2)	101.87(18)	C(33)-Si(9)-C(35)	108.0(2)	C(3)-C(4)-Si(1)	98.90(19)
C(86)-Si(4)-Si(2)	101.41(18)	C(34)-Si(9)-C(29)	112.42(18)	Si(6)-C(5)-Si(5)	110.65(15)
C(7)-Si(5)-C(8)	107.8(3)	C(33)-Si(9)-C(29)	114.37(19)	Si(6)-C(5)-Si(3)	115.60(16)
C(7)-Si(5)-C(6)	107.2(3)	C(35)-Si(9)-C(29)	110.6(2)	Si(5)-C(5)-Si(3)	117.74(16)
C(8)-Si(5)-C(6)	102.4(2)	C(30)-Si(10)-C(32)	108.1(3)	Si(7)-C(12)-Si(8)	109.96(14)
C(7)-Si(5)-C(5)	113.67(17)	C(30)-Si(10)-C(31)	105.3(4)	Si(7)-C(12)-Si(3)	121.53(16)
C(8)-Si(5)-C(5)	112.97(18)	C(32)-Si(10)-C(31)	103.1(3)	Si(8)-C(12)-Si(3)	118.95(14)
C(6)-Si(5)-C(5)	112.0(2)	C(30)-Si(10)-C(29)	107.6(3)	C(20)-C(19)-C(21)	109.2(3)
C(10)-Si(6)-C(11)	106.6(2)	C(32)-Si(10)-C(29)	114.3(2)	C(20)-C(19)-Si(3)	116.7(2)
C(10)-Si(6)-C(9)	103.6(2)	C(31)-Si(10)-C(29)	117.9(2)	C(21)-C(19)-Si(3)	110.2(2)
C(11)-Si(6)-C(9)	110.2(2)	C(28)-Si(11)-C(27)	106.07(18)	Si(12)-C(22)-Si(11)	111.59(17)
C(10)-Si(6)-C(5)	114.63(15)	C(28)-Si(11)-C(26)	110.0(2)	Si(12)-C(22)-Si(4)	120.13(17)
C(11)-Si(6)-C(5)	110.67(18)	C(27)-Si(11)-C(26)	104.77(19)	Si(11)-C(22)-Si(4)	114.96(17)
C(9)-Si(6)-C(5)	110.9(2)	C(28)-Si(11)-C(22)	111.62(17)	Si(9)-C(29)-Si(4)	119.13(18)
C(17)-Si(7)-C(18)	104.3(3)	C(27)-Si(11)-C(22)	114.65(15)	Si(9)-C(29)-Si(10)	110.21(17)
C(17)-Si(7)-C(16)	106.5(5)	C(26)-Si(11)-C(22)	109.46(19)	Si(4)-C(29)-Si(10)	120.1(2)
C(18)-Si(7)-C(16)	104.0(3)	C(24)-Si(12)-C(25)	108.29(19)	C(38)-C(36)-C(37)	110.1(5)
C(17)-Si(7)-C(12)	108.1(2)	C(24)-Si(12)-C(23)	107.31(19)	C(38)-C(36)-Si(4)	110.6(4)
C(18)-Si(7)-C(12)	116.72(14)	C(25)-Si(12)-C(23)	102.46(18)	C(37)-C(36)-Si(4)	111.6(7)
C(16)-Si(7)-C(12)	116.1(2)	C(24)-Si(12)-C(22)	112.89(15)	C(88)-C(86)-C(87)	110.6(6)
C(13)-Si(8)-C(15)	103.7(2)	C(25)-Si(12)-C(22)	112.87(18)	C(88)-C(86)-Si(4)	115.0(4)
C(13)-Si(8)-C(14)	107.7(3)	C(23)-Si(12)-C(22)	112.36(17)	C(87)-C(86)-Si(4)	115.1(6)
C(15)-Si(8)-C(14)	105.2(2)	C(39)-C(3)-C(4)	111.0(3)	C(37)-C(36)-Si(4)	111.6(7)
C(13)-Si(8)-C(12)	109.2(2)	C(39)-C(3)-Si(2)	117.8(2)	C(88)-C(86)-C(87)	110.6(6)
C(13)-Si(8)-C(12)	109.2(2)	C(39)-C(3)-C(4)	111.0(3)	C(88)-C(86)-Si(4)	115.0(4)
				C(87)-C(86)-Si(4)	115.1(6)

Symmetry transformations used to generate equivalent atoms: #1 -x,y,-z+3/2

Reference

1. For a recent overview, see: Power, P. P. *Chem. Rev.* **1999**, *99*, 3463.
2. Reviews: (a) Okazaki, R.; West, R. *Adv. Organomet. Chem.* **1996**, *39*, 232. (b) Weidenbruch, M. *Eur. J. Inorg. Chem.* **1999**, 373. (c) Escudie, J.; Ranaivonjatovo, H. *Adv. Organomet. Chem.* **1999**, *44*, 113. (d) Weidenbruch, M. *J. Organomet. Chem.* **2002**, *646*, 39.
3. (a) West, R.; Fink, M. J.; Michl, J. *Science* **1981**, *214*, 1343. (b) Masamune, S.; Hanzawa, Y.; Murakami, S.; Bally, T.; Blount, J. *J. Am. Chem. Soc.* **1982**, *104*, 1150. (c) Masamune, S.; Tobita, H.; Murakami, S. *J. Am. Chem. Soc.* **1983**, *105*, 6524. (d) Masamune, S.; Murakami, S. Tobita, H. *Organometallics* **1983**, *2*, 1464. (e) Watanabe, H.; Okawa, T.; Kato, M.; Nagai, Y. *J. Chem. Soc., Chem. Commun.* **1983**, 781.
4. Teramae, H. *J. Am. Chem. Soc.* **1987**, *109*, 4140.
5. (a) Nakadaira, Y.; Sato, R.; Sakurai, H. *Chem. Lett.* **1985**, 643. (b) Young, .D. J. D.; West. R. *Chem. Lett.* **1986**, 883. (c) West, R. *Angew. Chem., Int. Ed.* **1987**, *26*, 1987. (d) Weidenbruch, M.; Flintjer, B.; Pohl, S. Haase, D.; Martens, J. *J. Organomet. Chem.* **1988**, *338*, C1. (e) Weidenbruch, M; Lesch, A. *J. Organomet. Chem.* **1992**, *423*, 329. (f) Kroke, E.; Weidenbruch, M. Saak, W.; Pohl, S. *Organometallics* **1995**, *14*, 5695. (g) Dixon, E. C.; Cooke, A. J.; Baines, M. K. *Organometallics* **1997**, *16*, 5437. (h) Dixon, E. C.; Liu, W. H.; Kant, V. M. C.; Baines, M. K. *Organometallics* **1996**, *15*, 5701. (i) Iwamoto, T.; Sakurai, H.; Kira, M. *Bull. Chem. Soc. Jpn.* **1998**, *71*, 2741. (j) Ostendorf, D.; Saak, W.; Haase, D.; Weidenbruch, M. *J. Organomet. Chem.* **2001**, *636*, 7.
6. (a) Sekiguchi, A.; Zigler, S. S.; West, R. *J. Am. Chem. Soc.* **1986**, *108*, 4241. (b) Bogey, M.; Bolvin, H.; Demuynck, C.; Destombes, J. L. *Phys. Rev. Lett.* **1991**, *66*, 413. (c) Cordonnier, M.; Bogey, M.; Demuynck, C.; Destombes, J. L. *J. Chem. Phys.* **1992**, *97*, 7984. (d) Wiberg, N.; Finger, C. M. M.; Polborn, K. *Angew. Chem., Int. Ed. Engl.* **1993**, *32*, 1054. (e) Karni, M.; Apeloig, Y.; Schröder, D.; Zummack, W.; Rabezzana, R.; Schwarz, H. *Angew. Chem., Int. Ed.* **1999**, *38*, 332. (f) Pietschnig, R.; West, R.; Powell, D. R. *Organometallics* **2000**, *19*, 2724. (g) Pu, L.; Twamley, B.; Power, P. P. *J. Am. Chem. Soc.* **2000**, *122*, 3524. (h) Bibal, C.; Mazieres, S.; Gornitzka, C.; Couret, C. *Angew. Chem., Int. Ed.* **2001**, *40*, 952. (i)

Wiberg, N.; Niedermayer, W.; Fischer, G.; Nöth, H.; Sutin, M. *Eur. J. Inorg. Chem.* **2002**, 1066. (j) Stender, M.; Phillips, A. D.; Wright, R. J.; Power, P. P. *Angew. Chem., Int. Ed.* **2002**, *41*, 1785. (k) Phillips, A. D.; Wright, R. J.; Olmstead, M. M.; Power, P. P. *J. Am. Chem. Soc.* **2002**, *124*, 5930. (l) Stender, M.; Phillips, A. D.; Power, P. P. *Chem. Commun.* **2002**, 1312. (m) Pu, L.; Phillips, A. D.; Richards, A. F.; Stender, M.; Simons, R. S.; Olmstead, M. M.; Power, P. P. *J. Am. Chem. Soc.* **2003**, *125*, 11626. (n) Wiberg, N.; Vasisht, S.K.; Fischer, Gerd.; Mayer, P. *Z. Anorg. Allg. Chem.* **2004**, *630*, 1823. (o) Spikes, G. H.; Fettinger, J. C.; Power, P. P. *J. Am. Chem. Soc.* **2005**, *127*, 12232. (p) Cui, C.; Olmstead, M.; Fettinger, J. C.; Spikes, G. H.; Power, P. P. *J. Am. Chem. Soc.* **2005**, *127*, 17530. (q) Sugiyama, Y.; Sasamori, T.; Hosoi, Y.; Furukawa, Y.; Takagi, N.; Nagase, S.; Tokitoh, N. *J. Am. Chem. Soc.* **2006**, *128*, 1023.

7. (a) Sekiguchi, A.; Kinjo, R.; Ichinohe, M. *Science* **2004**, *305*, 1755. (b) Sekiguchi, A.; Ichinohe, M.; Kinjo, R. *Bull. Chem. Soc. Jpn.* **2006**, *379*, 825.
8. Calculations were carried out using the Gaussian 98 program.

Chapter 3

The First Isolable 1,2-disilabenzene: Synthesis of 1,2-bis{bis[bis(trimethylsilyl)- methyl]-isopropylsilyl}-3,5-diphenyl-1,2-disilabenzene and 1,2-bis{bis[bis(trimethyl- silyl)methyl]-isopropylsilyl}-4,5-diphenyl-1,2-disilabenzene

Summary

The first stable 1,2-disilabenzenes **33a** and **33b**, bearing an efficient steric protection group, bis[bis(trimethylsilyl)methyl]isopropylsilyl, were successfully synthesized by the reaction of disilyne **28** with phenylacetylene. 1,2-disilabenzene **33** could be isolated as yellow crystals thermally stable in the absence of air. The formation mechanism of 1,2-disilabenzenes **33** is discussed on the basis of theoretical calculation. The aromaticity of 1,2-disilabenzene **33** was discussed on the basis of its X-ray crystallography analysis and ^{1}H, ^{13}C, ^{29}Si NMR together with theoretical calculation.

Introduction

Aromatic compounds, such as benzene, naphthalene, and anthracene, play very important role in organic chemistry. Recently, much attention has been paid to silaaromatics, [4n+2]π electron ring systems containing at least one silicon atom as a ring member.[1] Because silaaromatic compounds are highly reactive and undergo ready dimerization and polymerization, there are few reports on the synthesis and isolation of silaaromatic compounds stable at room temperature. However, recently Tokitoh et al. have succeeded in the synthesis of the first stable silaanthracene,[2] silanaphthalene[3] and silabenzene[4] by taking advantage of an efficient steric protection group 2,4,6-tris[bis(trimethylsilyl)methyl]phenyl (denoted as *Tbt* hereafter) (Figure 3-1)[5].

Tbt = C_6H_2-2,4,6-[$CH(SiMe_3)_2$]$_3$

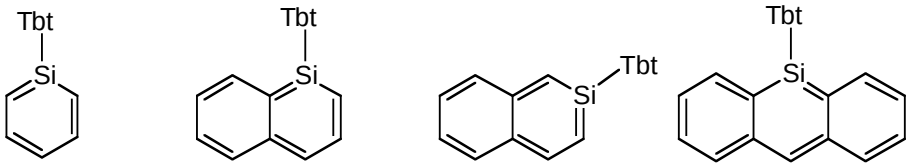

2000 **2002** **1997** **2002**

Figure 3-1. Stable ailaaromatic compounds with Tbt-group.

The considerable aromatic nature of these monosilaaromatic compounds was proved experimentally and theoretically. Meanwhile, disilabenzene having two silicon atoms as a ring members, have never been isolated as stable compound, although there are some reports of the chemical trapping of intermediary 1,4-disilabenzene and its observation by UV/vis spectroscopy in matrixes at low temperature (Scheme 3-1).[6-8] In this chapter, the successful synthesis and characterization of the first stable 1,2-disilabenzene bearing two bis[bis(trimethylsilyl)-methyl]isopropylsilyl groups from disilyne **28**,[9] is presented together with its chemical properties.

Scheme 3-1. Generation of transient 1,4-disilabenzene.

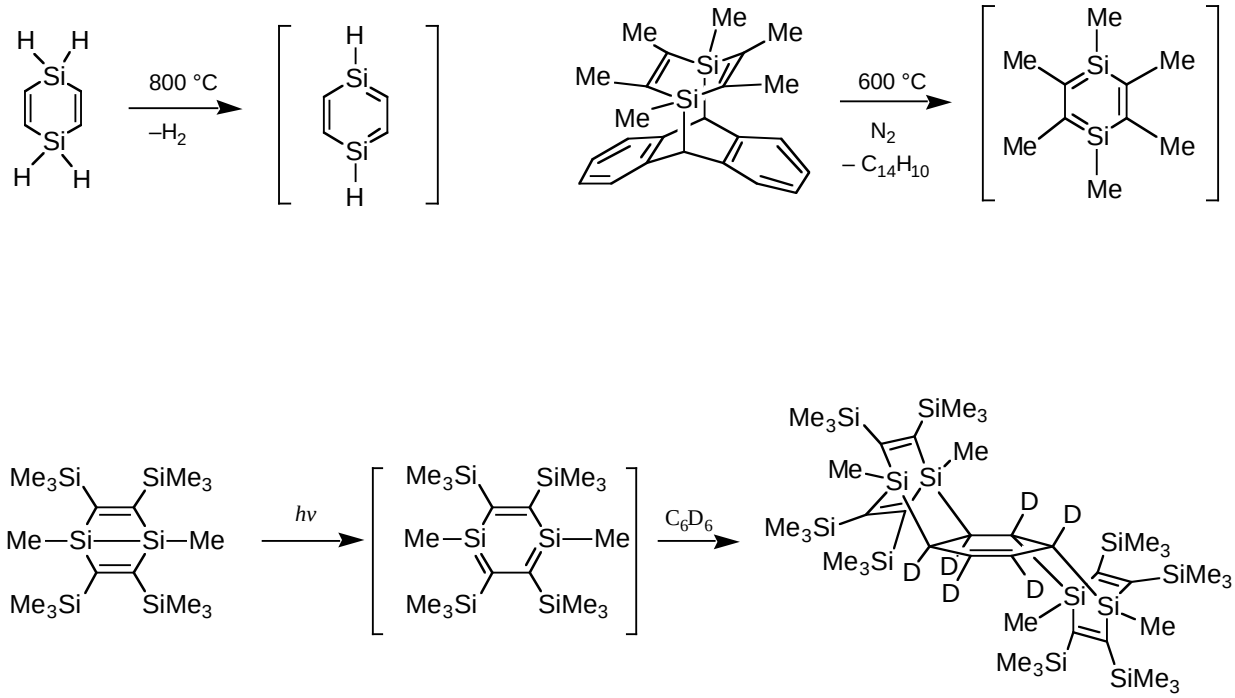

Results and Discussion

Synthesis and NMR spectra of 1,2-disilabenzene

When a dry hexane solution of disilyne **28** was treated with an excess of phenylacetylene at room temperature, the 1,2-disilabenzene **33** was obtained as mixture of two regioisomers (**33a** and **33b**; **33a** : **33b** = 4 : 6) isolated as yellow crystals (63%), which are thermally stable up to 142°C and145 °C respectively, in the absence of air (Scheme 3-2). In the ^{29}Si NMR spectrum, a low-field shifted signals (99.2 and 99.4, 106.8 ppm for **33a** and **33b** respectvely) characteristic of sp^2-Si were observed. ^{1}H and ^{13}C NMR signals of the 1,2-disilabenzene ring were assigned by 2D NMR techniques. All of the ring protons (8.47 ppm for **33a**, 8.01, 8.61 ppm for **33b**) were observed in the aromatic region. The signals of the ring carbons (147.8 and 150.6 ppm for **33a**, 141.6, 146.4, 149.6, and 161.2 ppm for **33b**) were also located in the sp^2-region (Figure 3-2a). These results indicate the aromaticity of 1,2-disilabenzene. Indeed, the carbon-carbon coupling constants in 6-memberd ring of 1,2-disilabenzene **33a** and **33b** are almost same, which shows the considerable delocalization of 6π-electron in 6-memberd ring of 1,2-disilabenzene (Figure 3-2b) .

Scheme 3-2.

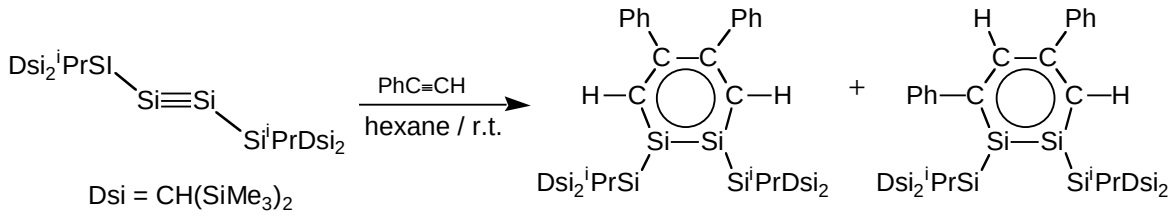

28 **33a** **33b**

(a)

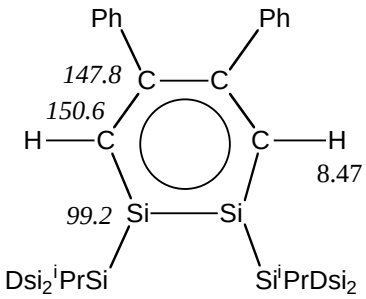

33a

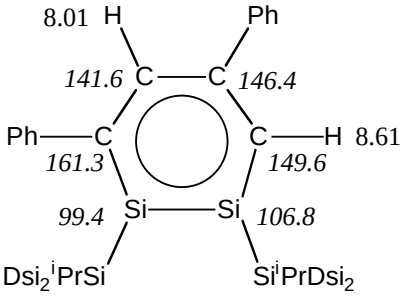

33b

(b)

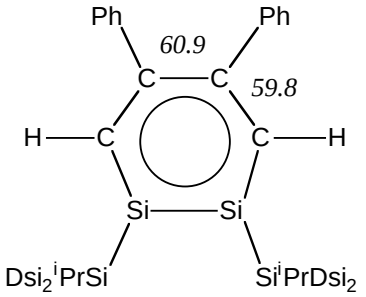

33a

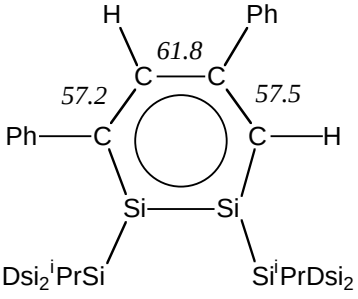

33b

Figure 3-2. (a) ^{1}H, ^{13}C, and ^{29}Si NMR chemical shifts (C_6D_6, δ) of 1,2-disilabenzenes **33a** and **33b**. (b) ^{13}C-^{13}C coupling constants of 1,2-disilabenzenes **33a** and **33b** (Hz).

Molecular Structure of 1,2-disilabenzene 33a

The single crystals of **33a** suitable for an X-ray structural analysis were obtained by recrystallization from pentane–toluene. The structure of 1,2-disilabenzene **33a** was definitely determined by X-ray crystallographic analysis at 120 K (Figure 3-3). 1,2-disilabenzene ring of **33a** is almost planar and the sums of bond angles around the two skeletal Si are 359.74 and 359.83° for Si1 and Si2, respectively. The dihedral angle between the 1,2-disilabenzene ring and each phenyl group is about 54°. The length of Si1—Si2 bond is 2.202Å, which is 6.8% longer than silicon-silicon triple bond length of precursor, disilyne.[9] The lengths of Si1—C6 and Si2—C3 bonds were found to be essentially equal to each other (1.804(4) and 1.799(5) Å, respectively),[10] and they are intermediate between those of Si—C double and single bonds (1.74 and 1.89 Å, respectively). Furthermore, the C3—C4 and C5—C6 bond lengths, that are also equal to each other (1.389(6) and 1.386(6) Å, respectively), are comparable to the C—C bond length of benzene ring (1.39—1.40 Å).[11] The C4—C5 bond length is 1.452(6) Å, which is not similar to the C—C bond length of benzene ring but is intermediate between those of C—C double and single bonds (1.34 and 1.54 Å, respectively). Thus, it has experimentally been demonstrated that 1,2-disilabenzene has a considerable contribution of 6π electron delocalization like benzene as well as monosilabenzene. Actually, the theoretical calculation at B3LYP/6-31G(d) level of the bond order (Wiberg bond index) of 1,2-disilabenzene **33a** skeleton showed the intermediate values between 1 to 2 (Si1–Si2; 1.446, Si2–C3; 1.1102, C3–C4; 1.497, C4–C5; 1.250, C5–C6; 1.501, C6–Si1; 1.107).[12]

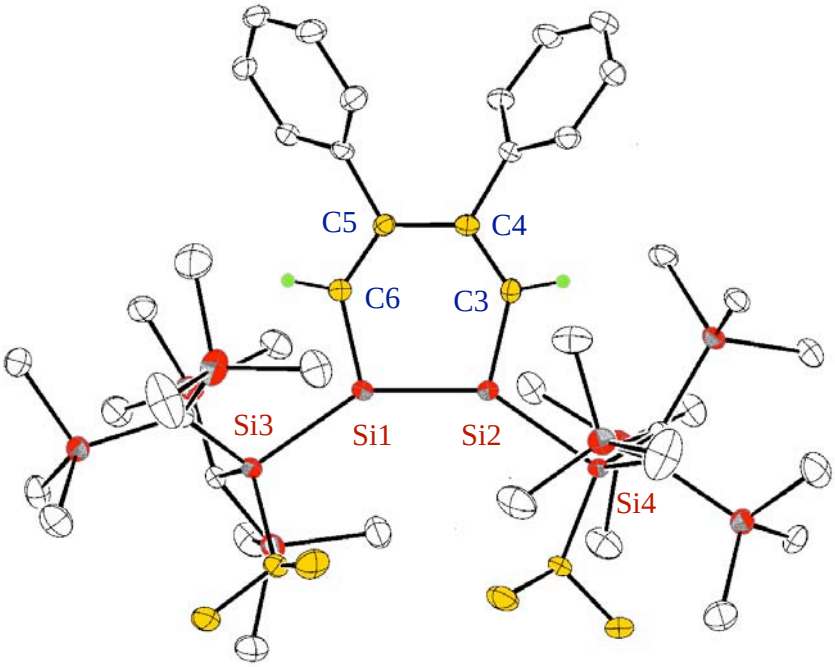

Top view

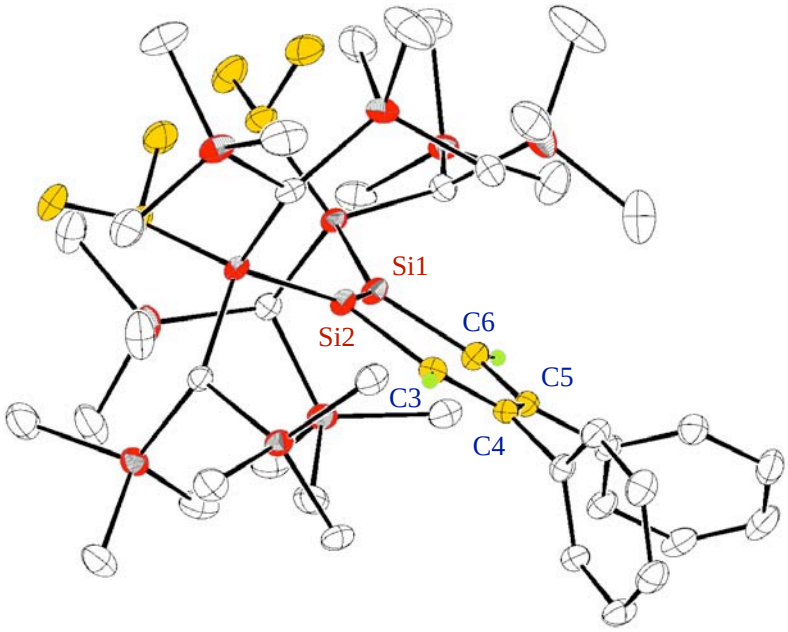

Side view

Figure 3-2. ORTEP drawing of 1,2-disilabenzene **33a**.

π-Molecular Orbitals and UV-Vis Spectrum of Disilyne

The molecular orbitals (MOs) of 1,2-disilabenzene **33a** calculated at the HF/6-31G(d) level for X-ray data presented in Figure 3-4 show two nondegenerate highest occupied π MOs (HOMO-1 **B** and HOMO **C**) and two lowest unoccupied antibonding π* MOs (LUMO **D** and LUMO+1 **E**).[12] These molecular orbitals are corresponding to those of benzene although the energy levels are very different. The aromatic nature of 6π-electron **33a** is reflected in the ultraviolet-visible absorption spectrum of **33a**, as shown in Figure 3-5. The reference spectra of benzene, silabenzene, and 1,4-disilabenzene are shown in Figure 3-6.[13] The UV-Vis spectrum of **33a** in hexane at room temperature shows two characteristic absorption bands at 427 (116) and 382 (240) nm in the visible region and two broad absorption bands at 313 (745) and 246 (2548) nm in the ultraviolet region.

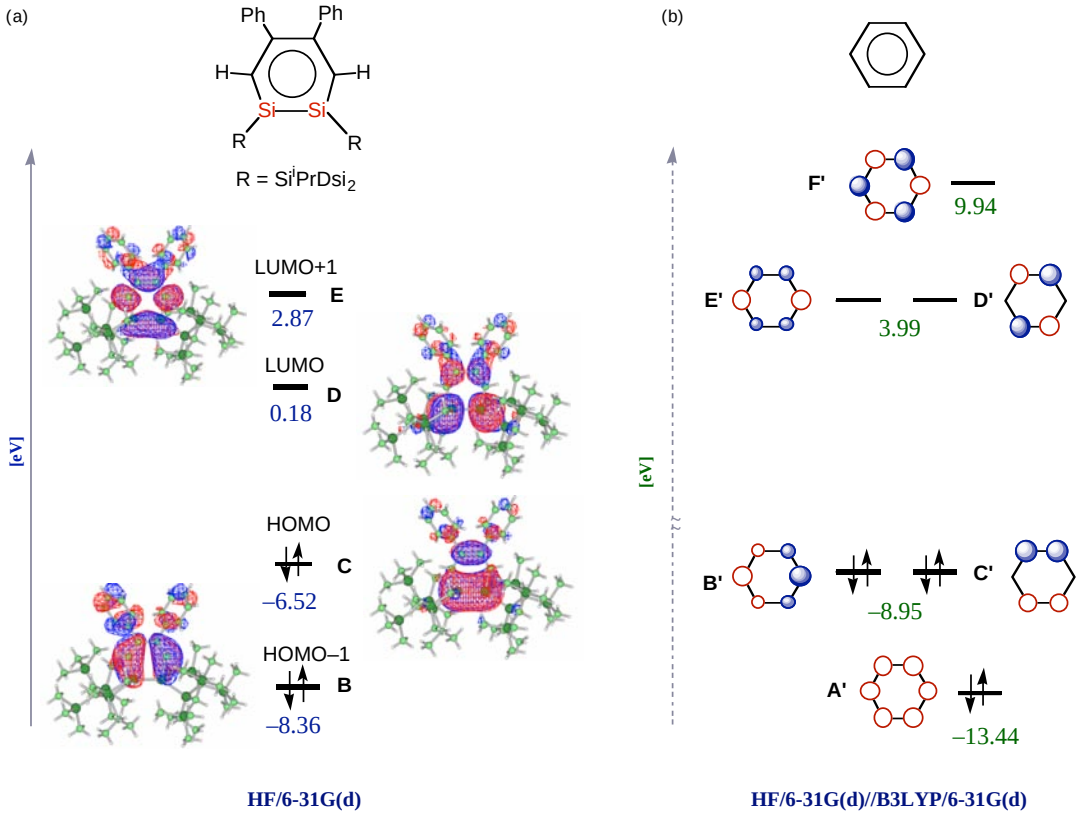

Figure 3-4. Molecular orbitals of 1,2-disilabenzene **33a** calculated at the HF/6-31G(d)//X-ray data (a) and benzene at the HF/6-31G(d)//B3LYP/6-31G(d) level (b).

Comparison of the UV-vis spectra between benzene and 1,2-disilabenzene **33a** is shown in Table 3-1. Despite the shifts to longer wavelength, the absorption maxima of 1,2-disilabenzenes cleary correspond to the *E1*, *E2*, and *B* bands of benzene. Similar relationships in UV-vis spectra are also observed for the benzene–silabenzene–1,4-disilabenzene series in low-temperature matrices as shown in Figure 3-6.

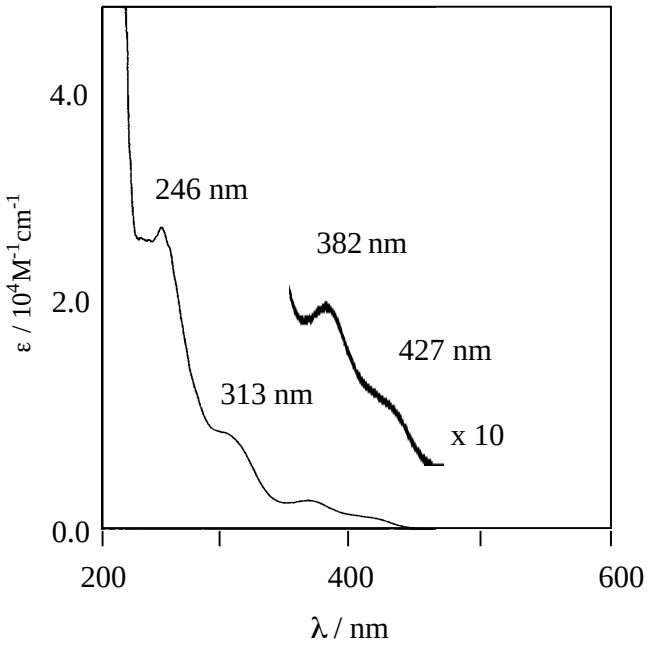

Figure 3.5. UV-Vis spectrum of 1,2-disilabenzene **33a** in hexane at room temperature.

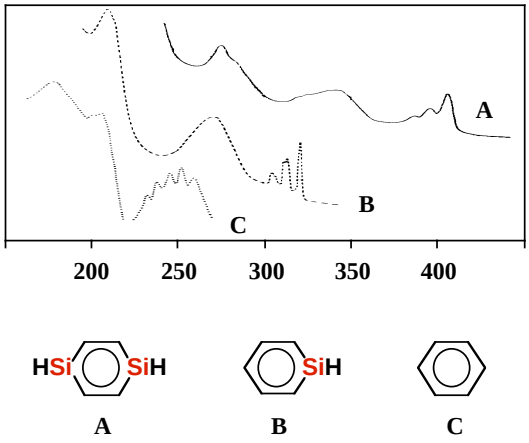

Figure 3.6. UV-Vis spectrum of 1,4-disilabenzene, monosilabenzene, and benzene in Ar matrices at 10 K.

Table 3-1. Comparison of the UV-vis spectra between benzene and 1,2-disilabenzene **33a**.

	benzene	1,2-disilabenzene **33a**
*E*1 band	184	~250
*E*2 band	204	313
B band	256	382, 427

Theoretical Study:: Aromaticity of 1,2-disilabenzene

Recently, Schleyer et al. have proposed the nucleus-independent chemical shifts (NICSs) as convenient criteria of aromaticity.[14] The refined NICSs (1) are shown in Figure 3-7.[12] All the data show the 1,2-disilabenzene rings to be aromatic although the absolute values are slightly smaller in magnitude than that of benzene (–11.1).[15] The quantitative energetic evaluation of 1,2-disilabenzene isomers along with those for benzene and silabenzene for comparison have also been carried out. The results of which are summarized in Figure 3-8. This method employed DFT-computed isodesmic isomerization energies of nonaromatic polyenes into corresponding methyl-substituted aromatic isomers.[16] The evaluations are self-consistent, and methyl groups have little effect on arene aromaticity. Theoretical results revealed that aromatic stabilization energies of 1,2-disilabenzene is about –22.5 kcal/mol, which suggest that aromatic character will be reduced by the replacement of ring carbons by two silicon atoms ($ASE_{(benzene)}$ = –35.2 kcal/mol). The degree of aromaticity would depend on the difference of energy between two bond alternation structures. Therefore, the aromaticity of 1,2-disilabenzene is about 60% of benzene or monosilabenzene.

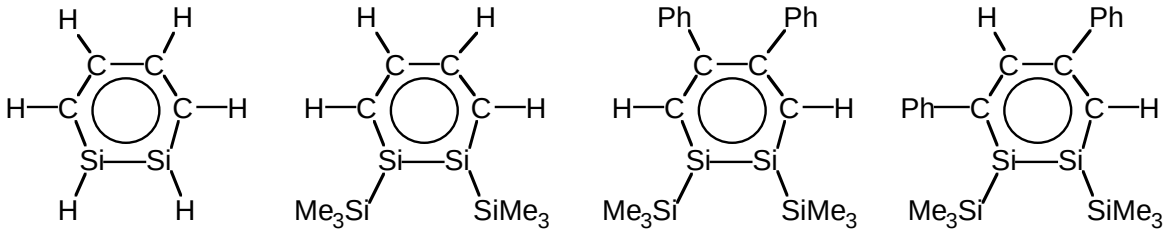

Figure 3-7. NICS (1) values (ppm) for 1,2-disilaaromatic systems calculated at the B3LYP/6-31G(d) level.

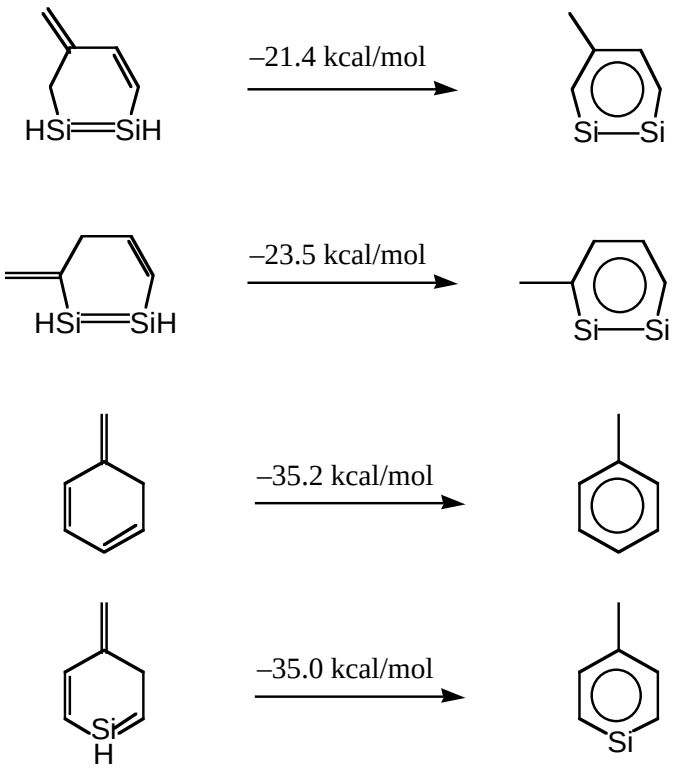

Figure 3-8. Calculated isodesmic isomerization energies (ΔH (kcal/mol), B3LYP/6-31G).

Theoretical Study: Formation Mechanism of 1,2-disilabenzene

The reaction mechanism was examined by theoretical calculations. Figure 3-9 shows the reaction mechanism of disilyne **28** with parent acetylene, together with the energies of both transition states and intermediates found by theoretical calculation of B3LYP/6-31G(d) level.[12] According to theoretical calculation, as shown in Figure 3-9, the [1+2] interaction between LUMO (in plane) of disilyne and HOMO of acetylene is first step in both reactions to afford four-membered ring intermediate (**Int2**) like 1,2-disilacyclobutadiene (Figure 3-9). Then, following the [2+4] cycloaddition reaction between the intermediate (**Int2**) and second acetylene to give 1,2-disila-Dewar benzene (**Int3**), valence isomerization of which produced 1,2-disilabenzene. The experimental ratio of regioisomers (**33a**, **33b**) depends on the difference of steric interaction between acetylene and four-membered ring of 1,2-disilacyclobutadiene intermediate (**Int2**) upon approaching the second phenylacetylene.

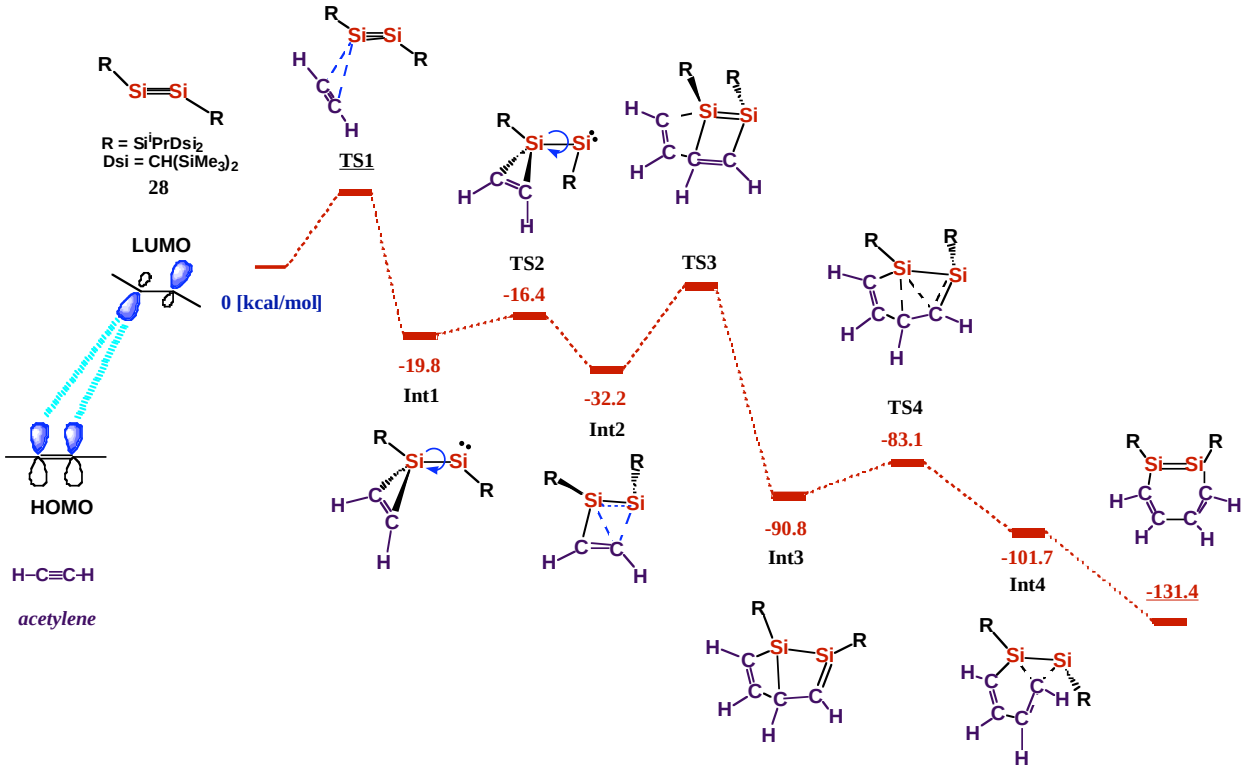

Figure 3-9. Calculated energies of transition state and intermediates (kcal/mol, B3LYP/6-31G).

Conclusion

Synthesis of the first stable 1,2-disilabenzene **33** from disilyne **28** was succeeded by taking advantage of the bis[bis(trimethylsilyl)methyl]isopropylsilyl group. The ^{1}H, ^{13}C, ^{29}Si NMR spectra of **33** indicated the aromatic nature of 1,2-disilabenzene ring. The structure of 1,2-disilabenzene **33a** was unequivocally determined by X-ray crystallography, and partial delocalization of its ring 6π-electrons was demonstrated. Furthermore, theoretical calculation supported that 1,2-disilabenzene is essentially aromatic compound although the degree of aromaticity is less than that of benzene. The reaction mechanism was supported by theoretical calculation and 1,2-disilabenzenes would be formed via valence isomerization from 1,2-disila-Dewar benzene.

Experimental Section

Synthesis of 1,2-bis{bis[bis(trimethylsilyl)methyl]-isopropylsilyl}-3,5-diphenyl-1,2-disilabenzene 33a and 1,2-bis{bis[bis(trimethylsilyl)methyl]-irosoppylsilyl}-4,5-diphenyl-1,2-disilabenzene 33b

To dry oxygen-free hexane (1.0 ml) solution of 1,1,4,4-tetrakis[bis(trimethylsilyl)methyl]-1,4-diisopropyl-tetrasila-2-yne (50 mg, 0.060 mmol), dry oxygen-free phenylacethylene (0.5 ml, 4.6 mmol) was added by vacuum transfer, and mixture was stirred at room temperature for 5 hours. After evaporation of solvent and remaining phenylacetylene, the residue was recrystallized from hexane (0.5 ml) at –30 °C to to give mixture of 1,2-bis{bis[bis(trimethylsilyl)methyl]-isopropylsilyl}-3,5-diphenyl-1,2-disila benzene **33a** and 1,2-bis{bis[bis(trimethylsilyl)methyl]-irosoppylsilyl}-4,5-diphenyl-1,2-disila benzene **33b** as yellow crystals (39 mg, 63%).

33a: Mp 142 °C (dec); ^{1}H NMR (C_6D_6, δ) 0.24 (s, 4 H, C*H*($SiMe_3$)$_2$), 0.33 (s, 36 H, Si*Me*$_3$), 0.34 (s, 36 H, Si*Me*$_3$), 1.44 (d, *J* = 7.4 Hz, 12 H, CH(C*H*$_3$)$_2$), 1.79 (sept, *J* = 7.4 Hz, 2 H, C*H*(CH_3)$_2$), 6.92 (t, *J* = 7.4 Hz, 2 H, *p*-C*H*), 7.05 (dd, *J* = 7.1 and 7.4 Hz, 4 H, *m*-C*H*), 7.35 (d, *J* = 7.1 Hz, 4 H, *o*-C*H*), 8.47 (s, 2 H, SiC*H*CPh); ^{13}C NMR (C_6D_6, δ) 5.9 (Si*Me*$_3$), 6.3 (*C*H($SiMe_3$)$_2$), 6.4 (Si*Me*$_3$), 17.6 (*C*H(CH_3)$_2$), 22.1 (CH(*C*H$_3$)$_2$), 125.6 (*p*-*C*H), 127.5 (*m*-*C*H), 130.1 (*o*-*C*H), 147.8 (*C*Ph), 149.2 (*ipso*-*C*), 150.6 (Si*C*HCPh); ^{29}Si NMR (C_6D_6, δ) 0.0 (*Si*Me_3), 0.1 (*Si*Me_3), 9.0 (*Si*^{i}PrDsi$_2$), 99.2 (*Si*Si^{i}PrDsi$_2$); HRMS: *m/z* calcd for $C_{50}H_{102}Si_{12}$ 1038.5207, found 1038.4857; UV-Vis (hexane) λ_{max} / nm (ε) 427 (116), 382 (240), 313 (745), 246 (2548).

33b: Mp 145 °C (dec); ^{1}H NMR (C_6D_6, δ) 0.20 (s, 2 H, C*H*($SiMe_3$)$_2$), 0.24 (s, 2 H, C*H*($SiMe_3$)$_2$), 0.28 (s, 18 H, Si*Me*$_3$), 0.33 (s, 18 H, Si*Me*$_3$), 0.34 (s, 18 H, Si*Me*$_3$), 0.36 (s, 18 H, Si*Me*$_3$), 1.37 (d, *J* = 7.5 Hz, 6 H, CH(C*H*$_3$)$_2$), 1.44 (d, *J* = 7.4 Hz, 6 H, CH(C*H*$_3$)$_2$), 1.92 (sept, *J* = 7.4 Hz, 1 H, C*H*(CH_3)$_2$), 1.99 (sept, *J* = 7.5 Hz, 1 H, C*H*(CH_3)$_2$), 7.10 (t, *J* = 7.3 Hz, 1 H, *p*-C*H*), 7.11 (t, *J* = 7.2 Hz, 1 H, *p*-C*H*), 7.24 (dd, *J* = 7.2 and 7.3 Hz, 2 H, *m*-C*H*), 7.30 (dd, *J* = 7.2 and 7.3 Hz, 2 H, *m*-C*H*), 7.59 (d, *J* = 7.3 Hz, 2 H, *o*-C*H*), 7.62 (d, *J* = 7.2 Hz, 2 H, *o*-C*H*), 8.01 (s, 1 H, CPhC*H*CPh), 8.61 (s, 1 H, SiC*H*CPh); ^{13}C NMR (C_6D_6, δ) 6.1 (Si*Me*$_3$), 6.46x2 (*C*H($SiMe_3$)$_2$), 6.53 (Si*Me*$_3$), 6.6 (Si*Me*$_3$), 6.8 (Si*Me*$_3$), 17.1 (*C*H(CH_3)$_2$), 19.2 (*C*H(CH_3)$_2$), 22.3 (CH(*C*H$_3$)$_2$), 22.9 (CH(*C*H$_3$)$_2$), 126.4 (*p*-*C*H), 127.7 (*p*-*C*H), 128.5 (*o*-*C*H), 128.7(*m*-*C*H), 129.6 (*m*-*C*H), 130.3 (*o*-*C*H), 141.6 (CPh*C*HCPh), 146.4 (CH*C*PhCH), 148.1 (*ipso*-*C*H), 149.6 (Si*C*HCPh), 152.2 (*ipso*-*C*H), 161.3 (Si*C*PhCH); ^{29}Si NMR (C_6D_6, δ) –0.6 (*Si*Me_3), –0.1 (*Si*Me_3), 0.0 (*Si*Me_3), 0.4 (*Si*Me_3), 6.0 (CPhSi*Si*^{i}PrDsi$_2$), 13.3 (CHSi*Si*^{i}PrDsi$_2$), 99.4 (CPh*Si*Si), 106.8 (Si*Si*CH).

X-ray Crystal Structure Determination of 33a

The single crystals of **33a** for X-ray analysis were obtained by the recrystallization from hexane. The X-ray crystallographic experiments were performed on a MacScience DIP2030 image plate diffractometer equipped with graphite-monochromatized Mo-Kα radiation (λ = 0.71070 Å). Details of crystal data and structure refinement are summarized in Table a-(**33**). The final atomic parameters, the bond lengths and the bond angles of **33** are listed in Table b-(**33**) and c-(**33**), respectively.

Appendix

Table a-(**33a**). Crystal Data and Structure Refinement for Compound **33a**.

Identification code	$(Dsi_2{}^{i}PrSi)_2Si_2C_4(Ph)_2(H)_2$
Empirical formula	$C_{50}H_{102}Si_{12}$
Formula weight	1040.40
Temperature	120.0(1) K
Wavelength	0.71070 Å
Crystal system, space group	Triclinic, P–1
Unit cell dimensions	a = 11.9640(10)Å alpha = 110.482(5) deg.
	b = 14.3110(16) Å beta = 91.712(6) deg.
	c = 20.267(2) Å gamma = 92.014(6)deg.
Volume	3245.4(6) $Å^3$
Z, Calculated density	2, 1.065 Mg/m^3
Absorption coefficient	0.269 mm^{-1}
F(000)	1140
Crystal size	0.45 x 0.25 x 0.05 mm
Theta range for data collection	2.106to 25.31 deg.
Limiting indices	0<=h<=14, –17<=k<=17, –24<=l<=24
Reflections collected / unique	25111 / 10867 [R(int) = 0.078]
Completeness to theta = 28.01	91.8 %
Absorption correction	None
Refinement method	Full-matrix least-squares on F^2
Data / restraints / parameters	10867/ 0 / 560
Goodness-of-fit on F^2	0.978
Final R indices [I>2sigma(I)]	R1 = 0.0662, wR2 = 0.1577
R indices (all data)	R1 = 0.1193, wR2 = 0.1877
Extinction coefficient	0.0072(10)
Largest diff. peak and hole	1.052 and –0.862 $e.Å^{-3}$

Table b-(**33a**). Atomic coordinates (x 10^4) and equivalent isotropic displacement parameters ($Å^2$ x 10^3) for compound.

U(eq) is defined as one third of the trace of the orthogonalized U_{ij} tensor.

	x	y	z	U(eq)
Si(1)	2385(1)	-3569(1)	7857(1)	29(1)
Si(2)	2887(1)	-5126(1)	7435(1)	27(1)
Si(3)	1870(1)	-2168(1)	7558(1)	27(1)
Si(4)	3508(1)	-6397(1)	6425(1)	25(1)
Si(5)	4314(1)	-1643(1)	7125(1)	38(1)
Si(6)	3776(1)	-774(1)	8726(1)	34(1)
Si(7)	115(1)	-360(1)	8167(1)	32(1)
Si(8)	-553(1)	-2482(1)	8245(1)	53(1)
Si(9)	882(1)	-7288(1)	6296(1)	38(1)
Si(10)	2685(1)	-8599(1)	5301(1)	39(1)
Si(11)	5012(1)	-7573(1)	7285(1)	30(1)
Si(12)	6180(1)	-5869(1)	6902(1)	34(1)
C(3)	2887(3)	-5496(3)	8197(2)	28(1)
C(4)	2666(3)	-5001(3)	8899(2)	27(1)
C(5)	2340(4)	-3973(3)	9178(2)	26(1)
C(6)	2212(4)	-3371(4)	8776(2)	30(1)
C(7)	3159(4)	-1267(3)	7786(2)	27(1)
C(8)	3985(5)	-1401(5)	6294(3)	57(2)
C(9)	4619(5)	-2995(4)	6876(3)	55(2)
C(10)	5690(4)	-916(5)	7445(4)	57(2)
C(11)	4526(4)	480(4)	8909(3)	48(1)
C(12)	4765(4)	-1664(4)	8893(3)	45(1)
C(13)	2749(4)	-489(4)	9452(3)	41(1)
C(14)	638(4)	-1630(3)	8116(2)	31(1)
C(15)	-1006(5)	-379(5)	7490(3)	54(2)
C(16)	1205(4)	559(4)	8095(3)	46(1)

C(17)	-451(5)	230(5)	9065(3)	58(2)
C(18)	-1937(5)	-2225(6)	7973(5)	93(3)
C(19)	-564(6)	-2259(6)	9229(4)	78(2)
C(20)	-506(5)	-3854(4)	7844(4)	58(2)
C(21)	1480(4)	-2572(4)	6578(2)	35(1)
C(22)	1200(5)	-1673(4)	6359(3)	53(2)
C(23)	528(5)	-3371(5)	6328(3)	53(2)
C(24)	2421(4)	-7500(3)	6132(2)	31(1)
C(25)	603(4)	-7030(5)	7242(3)	54(2)
C(26)	-45(5)	-8414(6)	5826(4)	87(3)
C(27)	321(5)	-6270(6)	6033(4)	67(2)
C(28)	2000(6)	-8464(5)	4493(3)	64(2)
C(29)	2163(5)	-9795(4)	5390(3)	59(2)
C(30)	4203(5)	-8834(4)	5142(3)	46(1)
C(31)	4921(3)	-6801(3)	6682(2)	27(1)
C(32)	3721(4)	-8318(4)	7347(3)	37(1)
C(33)	6054(4)	-8554(4)	6917(3)	42(1)
C(34)	5415(4)	-6803(4)	8226(2)	39(1)
C(35)	7489(4)	-6442(4)	7077(3)	46(1)
C(36)	5989(4)	-4739(4)	7692(3)	45(1)
C(37)	6615(4)	-5449(5)	6164(3)	56(2)
C(38)	3748(4)	-5741(4)	5768(2)	33(1)
C(39)	4302(5)	-6344(4)	5083(3)	44(1)
C(40)	2711(5)	-5267(5)	5579(3)	50(1)
C(41)	2835(4)	-5579(3)	9380(2)	28(1)
C(42)	2322(4)	-6533(4)	9212(2)	34(1)
C(43)	2554(5)	-7115(4)	9620(3)	42(1)
C(44)	3320(4)	-6779(4)	10181(3)	43(1)
C(45)	3841(4)	-5836(4)	10354(3)	41(1)
C(46)	3593(4)	-5238(4)	9960(2)	33(1)
C(47)	2083(4)	-3521(4)	9944(2)	30(1)
C(48)	1275(4)	-3963(4)	10238(3)	39(1)

C(49)	997(5)	-3503(5)	10941(3)	46(1)
C(50)	1521(5)	-2599(4)	11346(3)	48(2)
C(51)	2328(4)	-2153(4)	11064(3)	40(1)
C(52)	2607(4)	-2617(4)	10361(2)	34(1)

Table c-(**33a**). Bond lengths [Å] and angles [deg] for compound **33a**.

Si(1)-C(6)	1.804(4)	Si(8)-C(18)	1.819(6)	C(5)-C(6)	1.386(6)
Si(1)-Si(2)	2.2018(18)	Si(8)-C(20)	1.848(6)	C(5)-C(47)	1.504(6)
Si(1)-Si(3)	2.3828(18)	Si(8)-C(19)	1.907(7)	C(21)-C(23)	1.526(7)
Si(2)-C(3)	1.799(5)	Si(8)-C(14)	1.926(5)	C(21)-C(22)	1.545(7)
Si(2)-Si(4)	2.3730(16)	Si(9)-C(27)	1.858(6)	C(38)-C(40)	1.535(7)
Si(3)-C(14)	1.901(4)	Si(9)-C(25)	1.863(5)	C(38)-C(39)	1.539(6)
Si(3)-C(21)	1.903(5)	Si(9)-C(26)	1.863(7)	C(41)-C(46)	1.396(6)
Si(3)-C(7)	1.912(5)	Si(9)-C(24)	1.897(5)	C(41)-C(42)	1.400(6)
Si(4)-C(38)	1.902(5)	Si(10)-C(29)	1.871(6)	C(42)-C(43)	1.393(7)
Si(4)-C(24)	1.920(5)	Si(10)-C(30)	1.875(5)	C(43)-C(44)	1.374(7)
Si(4)-C(31)	1.921(4)	Si(10)-C(28)	1.882(6)	C(44)-C(45)	1.388(7)
Si(5)-C(8)	1.867(6)	Si(10)-C(24)	1.903(5)	C(45)-C(46)	1.392(7)
Si(5)-C(9)	1.873(5)	Si(11)-C(34)	1.876(5)	C(47)-C(52)	1.388(7)
Si(5)-C(10)	1.886(6)	Si(11)-C(33)	1.878(5)	C(47)-C(48)	1.395(7)
Si(5)-C(7)	1.912(4)	Si(11)-C(32)	1.879(5)	C(48)-C(49)	1.401(7)
Si(6)-C(12)	1.875(5)	Si(11)-C(31)	1.917(5)	C(49)-C(50)	1.381(8)
Si(6)-C(13)	1.887(5)	Si(12)-C(36)	1.862(5)	C(50)-C(51)	1.383(8)
Si(6)-C(11)	1.888(6)	Si(12)-C(35)	1.874(5)	C(51)-C(52)	1.401(6)
Si(6)-C(7)	1.901(5)	Si(12)-C(37)	1.877(6)		
Si(7)-C(16)	1.864(6)	Si(12)-C(31)	1.909(5)	C(6)-Si(1)-Si(2)	102.68(16)
Si(7)-C(17)	1.876(5)	C(3)-C(4)	1.389(6)	C(6)-Si(1)-Si(3)	112.25(16)
Si(7)-C(15)	1.883(6)	C(4)-C(5)	1.452(6)	Si(2)-Si(1)-Si(3)	144.81(7)
Si(7)-C(14)	1.912(5)	C(4)-C(41)	1.495(6)	C(3)-Si(2)-Si(1)	103.00(15)

C(3)-Si(2)-Si(4)	112.22(15)	C(13)-Si(6)-C(7)	116.5(2)	C(30)-Si(10)-C(24)	114.3(2)
Si(1)-Si(2)-Si(4)	144.61(7)	C(11)-Si(6)-C(7)	109.8(2)	C(28)-Si(10)-C(24)	111.9(2)
C(14)-Si(3)-C(21)	111.5(2)	C(16)-Si(7)-C(17)	105.1(3)	C(34)-Si(11)-C(33)	110.4(2)
C(14)-Si(3)-C(7)	112.6(2)	C(16)-Si(7)-C(15)	103.9(3)	C(34)-Si(11)-C(32)	104.0(2)
C(21)-Si(3)-C(7)	109.9(2)	C(17)-Si(7)-C(15)	108.2(3)	C(33)-Si(11)-C(32)	103.2(2)
C(14)-Si(3)-Si(1)	106.08(15)	C(16)-Si(7)-C(14)	115.7(2)	C(34)-Si(11)-C(31)	113.3(2)
C(21)-Si(3)-Si(1)	110.38(16)	C(17)-Si(7)-C(14)	107.1(2)	C(33)-Si(11)-C(31)	107.8(2)
C(7)-Si(3)-Si(1)	106.07(15)	C(15)-Si(7)-C(14)	116.1(3)	C(32)-Si(11)-C(31)	117.7(2)
C(38)-Si(4)-C(24)	115.8(2)	C(18)-Si(8)-C(20)	103.7(3)	C(36)-Si(12)-C(35)	107.1(3)
C(38)-Si(4)-C(31)	108.8(2)	C(18)-Si(8)-C(19)	107.4(4)	C(36)-Si(12)-C(37)	108.2(3)

C(24)-Si(4)-C(31)	110.8(2)	C(20)-Si(8)-C(19)	102.9(3)	C(35)-Si(12)-C(37)	100.9(2)
C(38)-Si(4)-Si(2)	104.09(15)	C(18)-Si(8)-C(14)	114.3(3)	C(36)-Si(12)-C(31)	112.9(2)
C(24)-Si(4)-Si(2)	109.27(14)	C(20)-Si(8)-C(14)	120.5(2)	C(35)-Si(12)-C(31)	111.7(2)
C(31)-Si(4)-Si(2)	107.55(14)	C(19)-Si(8)-C(14)	107.0(3)	C(37)-Si(12)-C(31)	115.2(2)
C(8)-Si(5)-C(9)	107.7(3)	C(27)-Si(9)-C(25)	108.7(3)	C(4)-C(3)-Si(2)	133.2(4)
C(8)-Si(5)-C(10)	102.5(3)	C(27)-Si(9)-C(26)	105.5(4)	C(3)-C(4)-C(5)	123.8(4)
C(9)-Si(5)-C(10)	106.5(3)	C(25)-Si(9)-C(26)	103.4(3)	C(3)-C(4)-C(41)	115.8(4)
C(8)-Si(5)-C(7)	113.1(2)	C(27)-Si(9)-C(24)	114.5(2)	C(5)-C(4)-C(41)	120.4(4)
C(9)-Si(5)-C(7)	112.2(2)	C(25)-Si(9)-C(24)	110.8(2)	C(6)-C(5)-C(4)	124.1(4)
C(10)-Si(5)-C(7)	114.2(2)	C(26)-Si(9)-C(24)	113.2(3)	C(6)-C(5)-C(47)	116.5(4)
C(12)-Si(6)-C(13)	106.1(2)	C(29)-Si(10)-C(30)	101.5(3)	C(4)-C(5)-C(47)	119.3(4)
C(12)-Si(6)-C(11)	109.9(2)	C(29)-Si(10)-C(28)	109.5(3)	C(5)-C(6)-Si(1)	133.2(3)
C(13)-Si(6)-C(11)	102.4(2)	C(30)-Si(10)-C(28)	108.8(3)	Si(6)-C(7)-Si(3)	119.4(2)
C(12)-Si(6)-C(7)	111.7(2)	C(29)-Si(10)-C(24)	110.3(3)	Si(6)-C(7)-Si(5)	110.8(2)
Si(3)-C(7)-Si(5)	114.6(2)	Si(12)-C(31)-Si(4)	118.7(2)	C(44)-C(45)-C(46)	120.3(5)
Si(3)-C(14)-Si(7)	120.2(2)	Si(11)-C(31)-Si(4)	121.3(2)	C(45)-C(46)-C(41)	120.9(5)
Si(3)-C(14)-Si(8)	121.3(2)	C(40)-C(38)-C(39)	108.8(4)	C(52)-C(47)-C(48)	118.8(4)
Si(7)-C(14)-Si(8)	111.4(2)	C(40)-C(38)-Si(4)	114.7(3)	C(52)-C(47)-C(5)	119.9(4)
C(23)-C(21)-C(22)	109.7(4)	C(39)-C(38)-Si(4)	116.5(3)	C(48)-C(47)-C(5)	121.2(4)
C(23)-C(21)-Si(3)	114.1(4)	C(46)-C(41)-C(42)	118.0(4)	C(47)-C(48)-C(49)	120.5(5)
C(22)-C(21)-Si(3)	111.8(4)	C(46)-C(41)-C(4)	121.5(4)	C(50)-C(49)-C(48)	119.8(5)
Si(9)-C(24)-Si(10)	113.8(2)	C(42)-C(41)-C(4)	120.1(4)	C(49)-C(50)-C(51)	120.4(5)
Si(9)-C(24)-Si(4)	120.6(2)	C(43)-C(42)-C(41)	120.6(5)	C(50)-C(51)-C(52)	119.7(5)
Si(10)-C(24)-Si(4)	117.8(2)	C(44)-C(43)-C(42)	120.7(5)	C(47)-C(52)-C(51)	120.8(5)
Si(12)-C(31)-Si(11)	108.5(2)	C(43)-C(44)-C(45)	119.5(5)		

Symmetry transformations used to generate equivalent atoms: #1 -x,y,-z+3/2

Referenc

1. (a) Raabe, G.; Michl, J. *Chem. Rev.* **1985**, *85*, 419. (b) Raabe, G.; Michl, J. In *The Chemistry of Organic Silicon Compounds*; Patai, S., Rappoport, Z., Eds.; Wiley: New York, 1989; p1102-1108. (c) Apeloig, Y. In *The Chemistry of Organic Silicon Compounds*; Patai, S., Rappoport, Z., Eds.; Wiley: New York, 1989; pp 151-166. (d) Brook, A. G.; Brook, M. A. *Adv. Organomet. Chem.* **1996**, *39*, 71. (e) Apeloig, Y.; Karni, M. In *The Chemistry of Organic Silicon Compounds*; Rappoport, Z., Appeloig, Y., Eds.; Wiley: New York, 1998; Vol. 2.
2. Takeda, N.; Shinohara, A.; Tokitoh, N. *Organometallics* **2002**, *21*, 256.
3. (a) Takeda, N.; Shinohara, A.; Tokitoh, N. *Organometallics* **2002**, *21*, 4024 (b) Shinohara, A.; Takeda, N.; Sasamori, T.; Tokitoh, N. *Bull. Chem. Soc. Jpn.* **2005**, *78*, 977. (c) Tokitoh, N.; Wakita, K.; Okazaki, R.; Nagase, S.; Schleyer, P. v. R.; Jiao, H. *J. Am. Chem. Soc.* **1997**, *119*, 6951. (d) Wakita, K.; Tokitoh, N.; Okazaki, R.; Nagase, S.; Schleyer, P. v. R.; Jiao, H. *J. Am. Chem. Soc.* **1999**, *121*, 11336. (e) Wakita, K.; Tokitoh, N.; Okazaki, R. *Bull. Chem. Soc. Jpn.* **2000**, *73*, 2157.
4. (a) Wakita, K.; Tokitoh, N.; Okazaki, R.; Nagase, S. *Angew. Chem., Int. Ed.* **2000**, *39*, 634. (b) Wakita, K.; Tokitoh, N.; Okazaki, R.; Takagi, N.; Nagase, S. *J. Am. Chem. Soc.* **2000**, *122*, 5648.
5. (a) Okazaki, R.; Unno, M.; Inamoto, N. *Chem. Lett.* **1987**, 2293. (b) Okazaki, R.; Tokitoh, N.; Matsumoto, T. In *Synthetic Methods of Organometallic and Inorganic Chemistry*; Herrmann, W. A., Ed.; Thieme: New York, 1996; Vol. 2, pp 260-269.
6. Maier, G.; Schottler, K.; Reisenauer, H. P.; *Tetrahedron Lett.* **1985**, *26*, 4039.
7. Rich, J. D.; West, R.; *J. Am. Chem. Soc.* **1982**, *104*, 6884.
8. Kabe, Y.; Ohkubo, K.; Ishikawa, H.; Ando, W.; *J. Am. Chem. Soc.* **2000**, *122*, 3775.
9. (a) Sekiguchi, A.; Kinjo, R.; Ichinohe, M. *Science* **2004**, *305*, 1755; (b) Sekiguchi, A.; Ichinohe, M.; Kinjo, R. *Bull. Chem. Soc. Jpn* **2006**, *79*, 825.
10. (a) Wiberg, N.; Wagner, G.; Müller, G. *Angew. Chem., Int. Ed. Engl.* **1985**, *24*, 229. (b) Gutowsky, H. S.; Chen, J.; Hajduk, P. J.; Keen, J. D.; Chuang, C.; Emilsson, T. *J. Am. Chem. Soc.* **1991**, *113*, 4747.
11. Minkin, V. J.; Glukhovtsev, M. N.; Simkin, Y. B. *Aromaticity and*

Antiaromaticity; Electronic and Structural Aspects; Wiley: New York, 1994.

12. Calculations were carried out using the Gaussian 98 program.
13. Maier, G.; Schöttler, K. Reisenauer, H. P. *Tetrahedron Lett.* **1985**, *26*, 4079.
14. Schleyer, P. v. R.; Maerker, C.; Dransfeld, A.; Jiao, H.; Hommes, N. J. R. v. E. *J. Am. Chem. Soc.* **1996**, *118*, 12669.
15. Baldridge, K. K.; Uzan, O.; Martin, J. M. L. *Organometallics* **2000**, *19*, 1477.
16. Schleyer, P. v. R.; Pühlhofer, F. *Org. Lett.* **2002**, *4*, 2873.

Chapter 4

trans-1,1,4,4-tetrakis[bis(trimethylsilyl)methyl]-1,4-diisopropyl-2-lithio-2-tetrasilene: A New Route to the Disilenide Ion by the Reduction of a Disilyne

Summary

The reaction of 1,1,4,4-tetrakis[bis(trimethylsilyl)methyl]-1,4-diisopropyl-2-tetrasilyne with an equivalent amount of *tert*-butyllithium (^{t}BuLi) in tetrahydrofuran produces *trans*-1,1,4,4-tetrakis[bis(trimethylsilyl)methyl]-1,4-diisopropyl-2-lithio-2-tetrasilene, the product of the formal addition of LiH across the Si≡Si triple bond of disilyne through a single electron transfer reaction. The solvent-separated ion pair of the disilenide; tris(l,2-dimethoxyethane)lithium(I)*trans*-1,1,4,4-tetrakis[bis-(trimethylsilyl)methyl]-1,4-diisopropyl-2-tetrasilene-2-yl-2-ide, was characterized by X-ray crystallography. The bulky Si^{i}Pr[CH(SiMe$_3$)$_2$]$_2$ groups are arranged in the *trans* fashion with a silicon–silicon double bond length of 2.2034(9).

Introduction

The chemistry of anion species of heavier Group 14 elements (E = Si, Ge, Sn), which are the heavier analogues of carbanions, has attracted considerable attention because of their unique structures and reactivity. The anionic species of heavier group 14 elements are very useful synthetic groups in both organometallic and organic chemistry. Particularly, since the discovery of triphenylsilyllithium by the reaction of hexaphenyldisilane with lithium metal in 1954 (Scheme 4-1),[1] the chemistry of sp^3-silyl anions has been greatly developed during the past decade.[2]

Scheme 4-1.

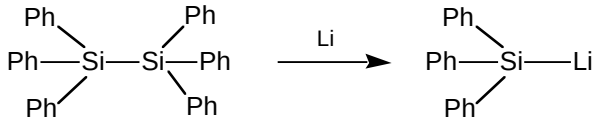

In contrast, the chemistry of disilenides, that is, silicon analogues of vinylic anions, has remained poorly explored because of the synthetic difficulties. In 1997, Weidenbruch et al. reported the first disilenide: tris(2,4,6-triisopropylphenyl)disilenyllithium **34**, as a key intermediate for formation of tetrasilabutadiene (Scheme 4-2).[3] However, tris(2,4,6-triisopropylphenyl)disilenyllithium **34** could not be isolated, or characterized at that time. A couple of years ago, Scheschkewitz reported on the isolation and structural characterization of tris(2,4,6-triisopropylphenyl)disilenyllithium **34** by means of a simplified synthetic protocol: reaction of bis(2,4,6-triisopropylphenyl)dichlorosilane with required amount of lithium powder (Scheme 4-3).[4]

Scheme 4-2.

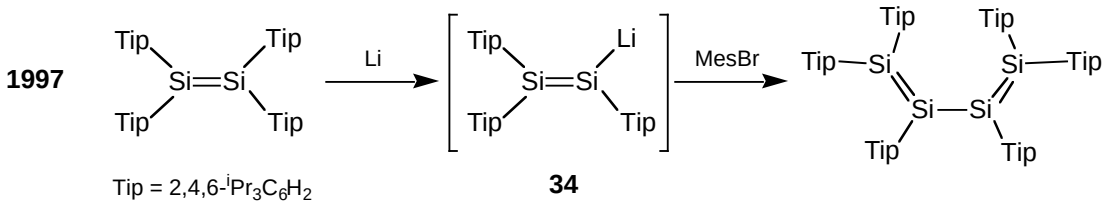

Scheme 4-3.

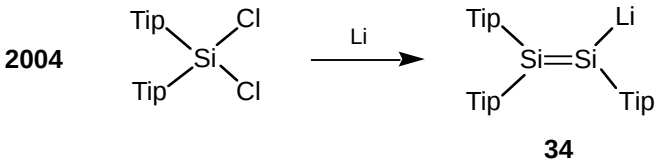

34

On the other hand, recently, Sekiguchi et al. have succeeded to isolate novel disilenylanion **35** by the reaction of tetrasilabutadiene with ^{t}BuLi, which causes the cleavage of the central Si-Si bond connecting two Si=Si double bond units (Scheme 4-4).[5]

Scheme 4-4.

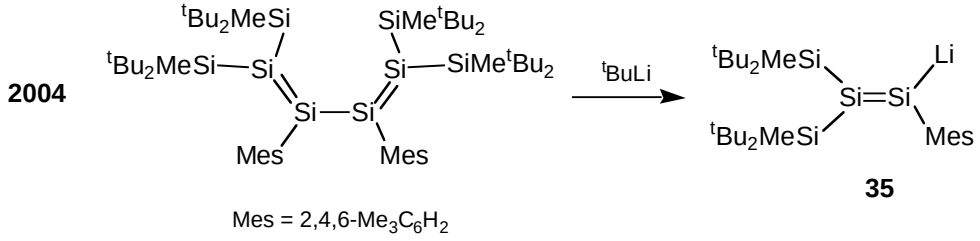

35

Mes = 2,4,6-$Me_3C_6H_2$

Furthermore, Sekiguchi et al reported the reaction of disilene bearing four $^{t}Bu_2MeSi$ groups with metal naphthalenide (M = Li, Na, K) in THF by the elimination of one $^{t}Bu_2MeSi$ group to afford novel disilenide **36a-c** (Scheme 4-5).[6]

Scheme 4-5.

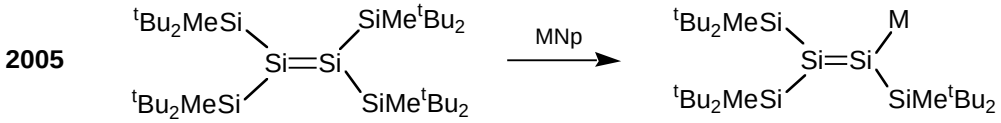

36a (M = Li)
36b (M = Na)
36c (M = K)

In this chapter, the reduction of disilyne **28** with ^{t}BuLi, leading to isolation of the disilenyllithium is reported. This provides a new route to the disilenide derivatives by the formal addition of LiH to the silicon–silicon triple bond.

Results and Discussion

Synthesis and NMR spectra of disilenide 37

The reaction of disilyne **28** [7] with an equivalent amount of ^{t}BuLi in dry THF at –78 °C resulted in the immediate development of a red color. Disilenyllithium **37** was isolated as air- and moisture-sensitive red crystals in 82% isolated yield (Scheme 4-6). The disilenide ion was also obtained as a solvent-separated ion pair **38** by the addition of 1,2-dimethoxyethane (DME) to **37**, and purified by recrystallization from pentane, benzene and DME at –30 °C.

Scheme 4-6.

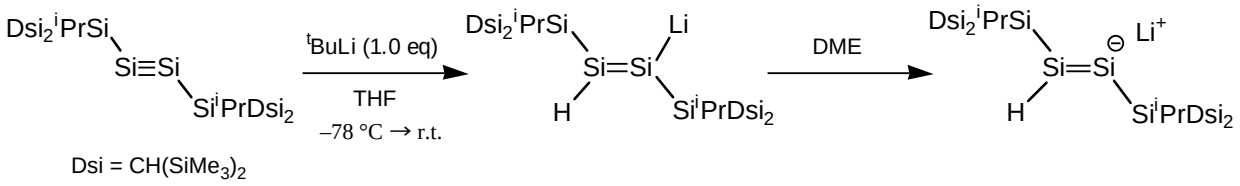

28 **37** **38**

The present method provides an entirely new method for the preparation of disilenide derivatives by taking advantage of the reactivity of the silicon–silicon triple bond. The formation of **37** can be rationalized by assuming an initial single electron transfer process involving intermediate formation of the anion radical of **28** and *tert*-butyl radical as a key radical pair, followed by fast hydrogen abstraction by the anion radical of **28** with the formation of disilenyllithium.[8] Indeed, the simultaneous formation of an equivalent amount of isobutene as the sole side product was observed by ^{1}H and ^{13}C NMR spectroscopy. Therefore, disilenyllithium **37** is the product of a formal 1,2-addition of lithium hydride across the Si≡Si triple bond of **28**.

The disilenyllithium **37** was fully characterized spectroscopically. Eight signals at –0.8, –0.74, –0.7, –0.5, 2.3, 12.8, 124.7, and 165.0 ppm were observed in the ^{29}Si NMR spectrum. The last two were assigned as follows: the peak at 165.0 ppm corresponds to the Li-substituted sp^2-Si atom, and the peak at 124.7 ppm corresponds to the H-substituted sp^2-Si atom (Chart 4-1). The

characteristic lower shifted signal of the Li-substituted sp^2-Si resulted from a paramagnetic effect, which was observed in the other disilenides (Chart 4-2).[3-6] Unexpectedly, the Si(sp^2)–H coupling constant of 155 Hz is smaller than the typical Si(sp^3)–H coupling constant (av. 190 Hz),[9] because of the severe steric congestion of the bulky Si substituents. In the ^{1}H NMR spectrum, the signal due to hydrogen on the sp^2-silicon atom appeared at 7.10 ppm; this is obviously the result of the deshielding effect of the Si=Si π-electrons.

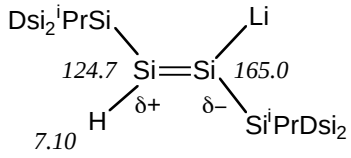

37

Chart 4-1. ^{1}H and ^{29}Si NMR shifts (C_6D_6, δ) of disilenide **37**.

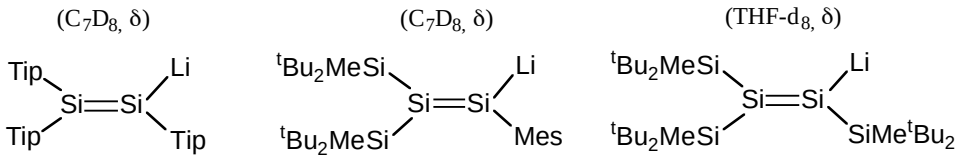

34 **35** **36**

Chart 4-2. ^{29}Si NMR shifts of disilenides **34**, **35**, **36**.

Molecular Structure of disilenide 38

The molecular structure of the solvent-separated ion pair of disilenide **38** determined by X-ray crystallographic analysis is shown in Figure 4-1.[11] The lithium counter cation is coordinated by three DME molecules. Consequently, the distance between the lithium ion and Si1 is greater than 7 Å, showing no interactions between them. The four Si atoms (Si4, Si2, Si1, Si3) are almost coplanar and the bulky $Si^{i}Pr[CH(SiMe_3)_2]_2$ groups at Si=Si are arranged in the *trans* orientation, due to their extreme bulkiness. The Si=Si double bond length is 2.2034(9) Å, which is elongated by 7% relative to the precursor disilyne **28** (2.0622(9) Å).[7,10] The bond lengths of Si1-Si3 and Si2-Si4 are 2.4201(8) Å and 2.3642(8) Å, respectively. The high p-character lengthens Si1-Si3 bond, which is elongated by 0.06 Å relative to Si2-Si4 bond length. Indeed, the bond angle of Si1–Si2–Si4 is 121.45(3)°, whereas Si2–Si1–Si3 is significantly contracted to 102.69(3)°, due to the influence of the negative charge on the Si1 atom.

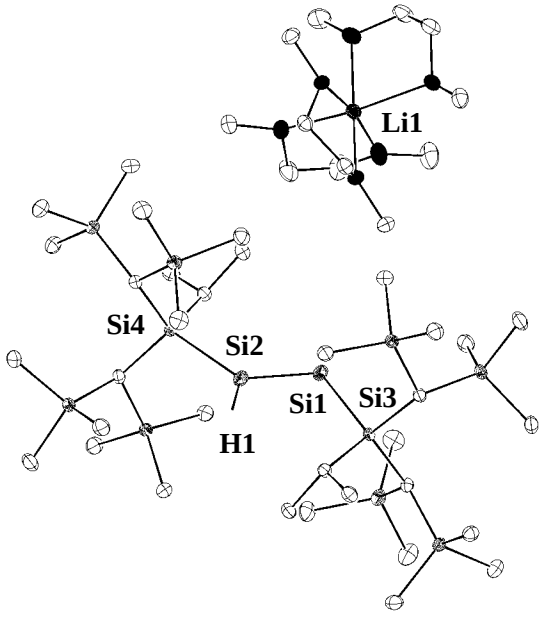

Figure 4-1. ORTEP drawing of disilenide **38**.

Molecular Orbitals of Disilenide 38

The molecular orbitals (MOs) of disilenide **38** calculated at the HF/6-31G(d) level from X-ray data presented in Figure 4-2 show localized lone-pair electrons on sp^2-silicon atom (HOMO-1), Si=Si π MO (HOMO), and Si=Si antibonding π* MO (LUMO).[11] The silicon-silicon double bond nature of disilenide **37** is reflected in the ultraviolet-visible absorption spectrum, as shown in Figure 4-3. The UV-Vis spectrum of **37** in hexane at room temperature shows characteristic absorption bands at 390(ε 5440) nm in the visible region and two shoulders at 302(ε 1430) and 268(ε 3380) nm in the ultraviolet region (Figure 4-3). The absorption band with maximum of 390 nm is assigned to π -π* transition. No n--π* transition was observed.

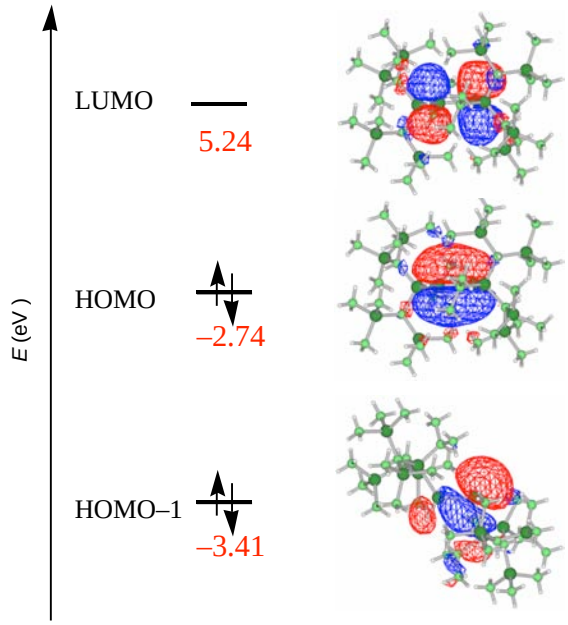

Figure 4-2. Molecular Orbitals of disilenide **38** calculated at the HF/6-31G(d) from X-ray data.

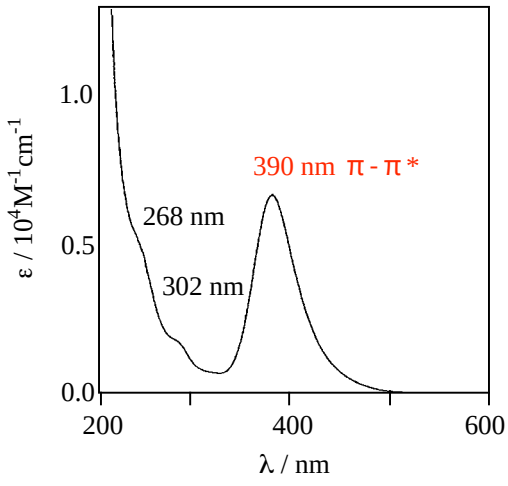

Figure 4-3 UV-Vis spectrum of disilenide **38** in hexane at room temperature.

Reactivity of disilenide 37

The reactivity of disilenide **37** is quite interesting owing to limited number of examples.[12] The reaction of disilenide **37** with cyclopentadiene in hexane was examined. The generation of dihidrodisilene **39** was confirmed by direct observation in ^{1}H and ^{29}Si NMR spectra and its trapping reaction with MeOH (Scheme 4-7).[13]

Scheme 4-7.

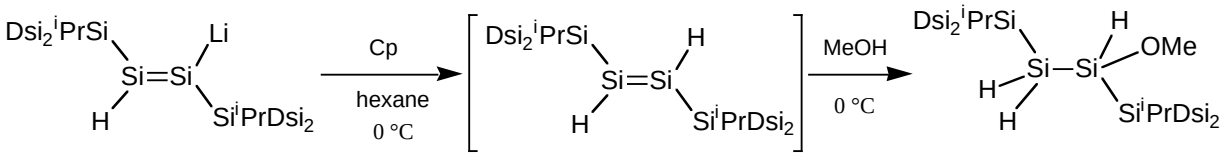

37 **39** **40**

A signal of 101.3 ppm in ^{29}Si NMR spectrum is assigned to H-substituted sp^2-Si atom (Chart 4-3). The Si(sp^2)-H coupling constant of 179 Hz is bigger than that of disilenide **37** (155 Hz). In ^{1}H NMR spectrum, the signal of hydrogen on sp^2-silicon atom is low-field shifted at 5.46 ppm, that is apparently the result of the deshielding by ring current effect of Si=Si π-electrons. Full characterization of NMR spectra has not been accomplished because dihydrodisilene **39** is not stable at room temperature and decomposition occurs gradually. Finally, MeOH trapping reaction of dihydrodisilene **39** at 0 °C resulted in formation of trihydromethoxydisilane **40**, which was completely characterized by ^{1}H, ^{13}C and ^{29}Si NMR spectra.

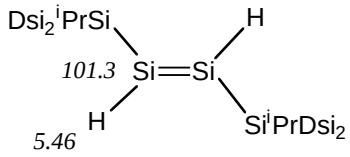

39

Chart 4-3. ^{1}H and ^{29}Si NMR shifts (C_6D_6, δ) of dihydrodisilene **39**.

Conclusion

The novel disilenide **37** was synthesized by the reaction of disilyne **28** with *tert*-butyllithium in hexane. In this reaction, the formal 1,2-addition of lithium hydride across the Si≡Si triple bond occurred. X-ray crystallography of disilenylanion species **38**, which was formed by mixing of disilenide **37** with DME, revealed the molecular structure of solvent-separated sp^2-silyl anion species. The reaction of disilenylide **37** with cyclopentadiene in hexane proceeded cleanly to give dihydrodisilene **39**, which is not stable at ambient temperature.

Experimental Section

Synthesis of 1,1,4,4-tetrakis[bis(trimethylsilyl)methyl]-1,4-diisopropyl-2-lithium-3-hydro tetrasila-2-ene 37.

To a mixture of 1,1,4,4-tetrakis[bis(trimethylsilyl)methyl]-1,4-diisopropyl-tetrasila-2-yne (200 mg, 0.172 mmol) and ^{t}BuLi (15 mg, 0.234 mmol), dry oxygen-free THF (2.0 ml) was added by vacuum transfer, and then the reaction mixture was allowed to warm from –78 °C to room temperature with stirring overnight. After evaporation of solvent, the reaction mixture was washed with dry hexane (0.5 ml), and the residue was recrystallized at –30 °C to give 1,1,4,4-tetrakis[bis(trimethylsilyl)methyl]-1,4-diisopropyl-2-lithium-3-hydrotetrasila -2-ene as red crystals (119 mg, 82%); Mp 92 °C (dec); ^{1}H NMR (C_6D_6, δ) 0.22 (s, 2 H, C*H*($SiMe_3$)$_2$), 0.24 (s, 2 H, C*H*($SiMe_3$)$_2$), 0.47 (s, 18 H, Si*Me*$_3$), 0.50 (s, 18 H, Si*Me*$_3$), 0.51 (s, 18 H, Si*Me*$_3$), 0.54 (s, 18 H, Si*Me*$_3$), 1.53 (d, *J* = 7.2 Hz, 6 H, CH*Me*$_2$), 1.72 (d, *J* = 7.2 Hz, 6 H, CH*Me*$_2$), 1.77 (sept, *J* = 7.2 Hz, 1 H, C*H*Me$_2$), 1.88 (sept, *J* = 7.2 Hz, 1 H, C*H*Me$_2$), 7.10 (s, 1 H, =Si*H*); ^{13}C NMR (C_6D_6, δ) 5.8 (Si*Me*$_3$), 6.0 (Si*Me*$_3$), 6.3 (Si*Me*$_3$), 6.7 (Si*Me*$_3$), 7.7 (C*H*(Si*Me*$_3$)$_2$), 8.3 (C*H*(Si*Me*$_3$)$_2$), 18.26 (C*H*Me$_2$), 18.34 (C*H*Me$_2$), 23.5 (CH*Me*$_2$), 23.8 (CH*Me*$_2$); ^{29}Si NMR (C_6D_6, δ) –0.8 (*Si*Me$_3$), –0.74 (*Si*Me$_3$), –0.70 (*Si*Me$_3$), –0.5 (*Si*Me$_3$), 2.3 (*Si* ^{i}PrDsi$_2$), 12.8 (*Si* ^{i}PrDsi$_2$), 124.7 (=*Si*H), 165.0 (=*Si*Li).

Reaction of 1,1,4,4-tetrakis[bis(trimethylsilyl)methyl]-1,4-diisopropyl-2-lithium-3-hydro tetrasila-2-ene 37 with cyclopentadiene.

To 1,1,4,4-tetrakis[bis(trimethylsilyl)methyl]-1,4-diisopropyl-2-lithium-3-hydro tetrasila-2-ene (36 mg, 0.043 mmol), dry oxygen-free hexane (1.0 ml) was added by vacuum transfer, then cyclopentadiene (0.5 ml) was added by syringe at 0 °C. The reaction mixture was stirred for 20 minutes. After evaporation of remaining cyclopentadiene and solvent, the C_6D_6 (400 µl) was added. The ^{1}H and ^{29}Si NMR spectra indicated the formation of 1,1,4,4-tetrakis[bis(trimethylsilyl)methyl]-1,4-diisopropyl-2,3-dihydrotetrasila-2-ene **39**. Since the decomposition occurs even at room temperature, isolation and full characterization of dihydrodisilene **39** has not been succeeded yet.

1,1,4,4-tetrakis[bis(trimethylsilyl)methyl]-1,4-diisopropyl-2,3-dihydrotetrasila-2-ene; ^{1}H NMR (C_6D_6, δ) 0.04 (s, 4 H, C*H*($SiMe_3$)$_2$), 0.31 (s, 36 H, Si*Me*$_3$), 0.39 (s, 36 H, Si*Me*$_3$), 1.35 (d, *J*=7.1 Hz, 12 H, CH*Me*$_2$), 1.55 (sept, 2 H, C*H*Me_2), 5.47 (s, 2 H, =Si*H*); ^{29}Si NMR (C_6D_6, δ) –0.2 (*Si*Me_3), –0.1 (*Si*Me_3), 15.1 (*Si*^{i}PrDsi$_2$), 101.3 (=*Si*).

Trapping Reaction of 1,1,4,4-tetrakis[bis(trimethylsilyl)methyl]-1,4-diisopropyl-2,3-dihydro tetrasila-2-ene 39 with MeOH.

To 1,1,4,4-tetrakis[bis(trimethylsilyl)methyl]-1,4-diisopropyl-2-lithium-3-hydro tetrasila-2-ene (36 mg, 0.043 mmol), dry oxygen-free hexane (1.0 ml) was added by vacuum transfer, then cyclopentadiene (0.5 ml) was added by syringe at 0 °C. The reaction mixture was stirred for 10 minutes. After the reaction, oxygen-free MeOH

(0.5 ml) was added by syringe at 0 °C and then the reaction mixture was allowed to warm from 0 °C to room temperature with stirring. After evaporation of solvent, the reaction mixture was washed with dry hexane (0.5 ml), and the residue was recrystallized at 0 °C to give 1,1,4,4-tetrakis[bis(trimethylsilyl)methyl]-1,4-diisopropyl-2-methoxy-2,3,3-trihydrotetrasilane as colorless crystals (49 mg, 65%); 1,1,4,4-tetrakis[bis(trimethylsilyl)methyl]-1,4-diisopropyl-2-methoxy-2,3,3-trihydrotetrasilane; Mp. 127-129 °C; ^{1}H NMR (C_6D_6, δ) 0.30 (s, 9 H, *Si*Me_3), 0.31 (s, 9 H, *Si*Me_3), 0.336 (s, 9 H, *Si*Me_3), 0.342 (s, 9 H, *Si*Me_3), 0.36 (s, 9 H, *Si*Me_3), 0.37 (s, 9 H, *Si*Me_3), 0.38 (s, 9 H, *Si*Me_3), 0.41 (s, 9 H, *Si*Me_3), 1.29 (d, *J* = 7.2 Hz, 3 H, CH*Me*$_2$), 1.31 (d, *J* = 7.2 Hz, 3 H, CH*Me*$_2$), 1.35 (d, *J* = 7.3 Hz, 3 H, CH*Me*$_2$), 1.40 (d, *J* = 7.3 Hz, 3 H, CH*Me*$_2$), 1.50 (sept, *J* = 7.2 Hz, 1 H, C*H*Me_2), 1.54 (spet, *J* = 7.3 Hz, 1 H, C*H*Me_2), 3.44 (d, *J* = 5.7 Hz, 1 H, Si*H*H), 3.49 (s, 3 H, O*Me*), 5.88 (dd, *J* = 5.8 and 9.4 Hz, 1 H, SiH*H*), 5.88 (d, *J* = 9.4 Hz, 1 H, Si*H*OMe); ^{13}C NMR (C_6D_6, δ) 5.20 (Si*Me*$_3$), 5.22 (Si*Me*$_3$), 5.26 (Si*Me*$_3$), 5.29 (Si*Me*$_3$), 5.38 (Si*Me*$_3$), 5.41 (Si*Me*$_3$), 5.45 (Si*Me*$_3$), 5.54 (C*H*(SiMe$_3$)$_2$), 5.55 (Si*Me*$_3$), 6.2 (C*H*(SiMe$_3$)$_2$), 7.9 (C*H*(SiMe$_3$)$_2$), 8.0 (C*H*(SiMe$_3$)$_2$), 17.75 (C*H*Me_2), 17.79 (C*H*Me_2), 21.2 (CH*Me*$_2$), 21.7 (CH*Me*$_2$), 21.8 (CH*Me*$_2$), 21.9 (CH*Me*$_2$), 56.9 (O*Me*); ^{29}Si NMR (C_6D_6, δ) –96.5 (*Si*H_2), –0.4 (*Si*Me_3), –0.2 (*Si*Me_3), –0.14 (*Si*Me_3), –0.11 (*Si*Me_3), 0.0 (*Si*Me_3), 0.2 (*Si*Me_3), 0.4 (*Si*Me_3), 0.6 (*Si*Me_3), 4.4 (*Si*^{i}PrDsi$_2$), 8,1 (*Si*HOMe), 10.7 (*Si*^{i}PrDsi$_2$).

X-ray Crystal Structure Determination of 38

The single crystals of **38** for X-ray analysis were obtained by the recrystallization from hexane. The X-ray crystallographic experiments were performed on a MacScience DIP2030 image plate diffractometer equipped with graphite-monochromatized Mo-Kα radiation (λ = 0.71070 Å). Details of crystal data and structure refinement are summarized in Table a-**38**. The final atomic parameters, the bond lengths and the bond angles of **38** are listed in Table b-**38** and c-**38**, respectively.

Appendix

Table a-(**38**). Crystal Data and Structure Refinement for Compound **38**.

Identification code	$[(Dsi_2{}^{i}PrSi)(H)Si{=}Si^{-}(Si^{i}PrDsi_2)][Li^{+}(dme)_3]$
Empirical formula	$C_{52}H_{127}LiO_6Si_{12}$
Formula weight	1192.56
Temperature	120.0(1) K
Wavelength	0.71070 Å
Crystal system, space group	Monoclinic, P21/c
Unit cell dimensions	a = 25.3480(6)Å alpha = 90 deg.
	b = 13.8790(4) Å beta = 114.4791(10) deg.
	c = 23.1990(7) Å gamma = 90deg.
Volume	7416.0(4) $Å^3$
Z, Calculated density	4, 1.068 Mg/m^3
Absorption coefficient	0.248 mm^{-1}
F(000)	2632
Crystal size	0.25 x 0.20 x 0.15 mm
Theta range for data collection	2.14 to 28.02 deg.
Limiting indices	–33<=h<=30, –18<=k<=0, 0<=l<=30
Reflections collected / unique	77815 / 17684 [R(int) = 0.0460]
Completeness to theta = 28.01	98.5 %
Absorption correction	None
Refinement method	Full-matrix least-squares on F^2
Data / restraints / parameters	17684/ 0 / 641
Goodness-of-fit on F^2	1.049
Final R indices [I>2sigma(I)]	R1 = 0.0494, wR2 = 0.1349
R indices (all data)	R1 = 0.0648, wR2 = 0.1456
Extinction coefficient	0.0021(2)
Largest diff. peak and hole	1.989 and –0.893 $e.Å^{-3}$

Table b-(**38**). Atomic coordinates (x 10^4) and equivalent isotropic displacement parameters ($Å^2$ x 10^3) for compound.

U(eq) is defined as one third of the trace of the orthogonalized U_{ij} tensor.

	x	y	z	U(eq)
Si(1)	7965(1)	3323(1)	6319(1)	30(1)
Si(2)	7212(1)	2348(1)	5928(1)	29(1)
Si(3)	8744(1)	2342(1)	6291(1)	19(1)
Si(4)	6274(1)	2859(1)	5781(1)	20(1)
Si(5)	8978(1)	1537(1)	7694(1)	23(1)
Si(6)	9805(1)	3122(1)	7593(1)	25(1)
Si(7)	9700(1)	2329(1)	5636(1)	23(1)
Si(8)	8718(1)	3936(1)	5242(1)	27(1)
Si(9)	6056(1)	3468(1)	4350(1)	22(1)
Si(10)	5403(1)	1674(1)	4536(1)	25(1)
Si(11)	5278(1)	2648(1)	6360(1)	26(1)
Si(12)	6430(1)	1387(1)	6941(1)	26(1)
O(1)	7224(1)	7594(1)	9004(1)	39(1)
O(2)	8305(1)	6874(1)	9307(1)	33(1)
O(3)	7703(1)	7608(1)	7931(1)	43(1)
O(4)	6676(1)	6802(1)	7680(1)	36(1)
O(5)	7784(1)	5427(1)	8106(1)	28(1)
O(6)	7264(1)	5408(1)	8881(1)	28(1)
C(1)	9292(1)	2107(1)	7163(1)	22(1)
C(2)	8370(1)	653(2)	7308(1)	29(1)
C(3)	8677(1)	2478(2)	8061(1)	31(1)
C(4)	9556(1)	800(2)	8328(1)	33(1)
C(5)	9426(1)	4313(2)	7457(1)	36(1)
C(6)	10196(1)	2959(2)	8480(1)	39(1)
C(7)	10438(1)	3227(2)	7372(1)	33(1)
C(8)	9156(1)	2996(1)	5852(1)	22(1)
C(9)	10165(1)	1420(2)	6243(1)	29(1)
C(10)	10246(1)	3182(2)	5561(1)	34(1)

C(11)	9368(1)	1664(2)	4857(1)	34(1)
C(12)	9069(1)	4393(2)	4722(1)	45(1)
C(13)	8647(1)	5050(2)	5666(1)	43(1)
C(14)	7987(1)	3529(2)	4666(1)	37(1)
C(15)	8469(1)	1102(1)	5916(1)	22(1)
C(16)	8903(1)	262(2)	6078(1)	28(1)
C(17)	8116(1)	1153(2)	5194(1)	28(1)
C(18)	5759(1)	2864(1)	4890(1)	22(1)
C(19)	6554(1)	4522(2)	4685(1)	29(1)
C(20)	6473(1)	2605(2)	4075(1)	28(1)
C(21)	5425(1)	3987(2)	3649(1)	33(1)
C(22)	5944(1)	669(2)	4820(1)	34(1)
C(23)	5057(1)	1621(2)	3642(1)	39(1)
C(24)	4760(1)	1369(2)	4705(1)	37(1)
C(25)	5915(1)	2125(1)	6239(1)	22(1)
C(26)	4755(1)	3372(2)	5672(1)	34(1)
C(27)	4799(1)	1665(2)	6444(1)	39(1)
C(28)	5504(1)	3421(2)	7091(1)	36(1)
C(29)	6070(1)	815(2)	7422(1)	39(1)
C(30)	7054(1)	2069(2)	7541(1)	35(1)
C(31)	6711(1)	331(2)	6649(1)	37(1)
C(32)	6419(1)	4176(2)	6058(1)	25(1)
C(33)	6776(1)	4261(2)	6777(1)	32(1)
C(34)	5912(1)	4892(2)	5835(1)	32(1)
C(41)	6745(1)	8241(2)	8767(2)	54(1)
C(42)	7714(1)	8012(2)	9516(1)	47(1)
C(43)	8155(1)	7239(2)	9796(1)	45(1)
C(44)	8744(1)	6151(2)	9550(1)	39(1)
C(45)	8190(1)	8220(2)	8121(2)	58(1)
C(46)	7231(1)	7920(2)	7399(1)	54(1)
C(47)	6761(1)	7218(2)	7178(1)	51(1)
C(48)	6158(1)	6256(2)	7497(1)	39(1)

C(49)	8194(1)	5415(2)	7829(1)	36(1)
C(50)	7775(1)	4527(2)	8400(1)	29(1)
C(51)	7258(1)	4526(2)	8560(1)	28(1)
C(52)	6853(1)	5388(2)	9157(1)	36(1)
C(53)	7947(1)	7981(2)	11289(1)	44(1)
C(54)	7979(1)	6990(2)	11253(1)	42(1)
C(55)	7481(1)	6458(2)	10920(1)	43(1)
C(56)	6955(1)	6928(2)	10624(1)	48(1)
C(57)	6926(1)	7918(2)	10661(1)	49(1)
C(58)	7422(1)	8449(2)	10994(1)	49(1)
Li(1)	7496(2)	6604(3)	8479(2)	29(1)

Table c-(**38**). Bond lengths [Å] and angles [deg] for compound **38**.

Si(1)-C(6)	1.804(4)	Si(8)-C(18)	1.819(6)	C(5)-C(6)	1.386(6)
Si(1)-Si(2)	2.2018(18)	Si(8)-C(20)	1.848(6)	C(5)-C(47)	1.504(6)
Si(1)-Si(3)	2.3828(18)	Si(8)-C(19)	1.907(7)	C(21)-C(23)	1.526(7)
Si(2)-C(3)	1.799(5)	Si(8)-C(14)	1.926(5)	C(21)-C(22)	1.545(7)
Si(2)-Si(4)	2.3730(16)	Si(9)-C(27)	1.858(6)	C(38)-C(40)	1.535(7)
Si(3)-C(14)	1.901(4)	Si(9)-C(25)	1.863(5)	C(38)-C(39)	1.539(6)
Si(3)-C(21)	1.903(5)	Si(9)-C(26)	1.863(7)	C(41)-C(46)	1.396(6)
Si(3)-C(7)	1.912(5)	Si(9)-C(24)	1.897(5)	C(41)-C(42)	1.400(6)
Si(4)-C(38)	1.902(5)	Si(10)-C(29)	1.871(6)	C(42)-C(43)	1.393(7)
Si(4)-C(24)	1.920(5)	Si(10)-C(30)	1.875(5)	C(43)-C(44)	1.374(7)
Si(4)-C(31)	1.921(4)	Si(10)-C(28)	1.882(6)	C(44)-C(45)	1.388(7)
Si(5)-C(8)	1.867(6)	Si(10)-C(24)	1.903(5)	C(45)-C(46)	1.392(7)
Si(5)-C(9)	1.873(5)	Si(11)-C(34)	1.876(5)	C(47)-C(52)	1.388(7)
Si(5)-C(10)	1.886(6)	Si(11)-C(33)	1.878(5)	C(47)-C(48)	1.395(7)
Si(5)-C(7)	1.912(4)	Si(11)-C(32)	1.879(5)	C(48)-C(49)	1.401(7)

Si(2)-Si(1)-Si(3)	102.69(3)	C(6)-Si(6)-C(1)	114.69(10)	C(26)-Si(11)-C(28)	107.51(11)
Si(1)-Si(2)-Si(4)	121.45(3)	C(10)-Si(7)-C(11)	105.69(11)	C(26)-Si(11)-C(27)	102.49(11)
C(15)-Si(3)-C(1)	106.65(9)	C(10)-Si(7)-C(9)	103.57(10)	C(28)-Si(11)-C(27)	106.51(11)
C(15)-Si(3)-C(8)	110.43(8)	C(11)-Si(7)-C(9)	106.07(10)	C(26)-Si(11)-C(25)	114.95(9)
C(1)-Si(3)-C(8)	108.28(8)	C(10)-Si(7)-C(8)	111.20(10)	C(28)-Si(11)-C(25)	113.22(10)
C(15)-Si(3)-Si(1)	111.79(6)	C(11)-Si(7)-C(8)	114.21(10)	C(27)-Si(11)-C(25)	111.31(10)
C(1)-Si(3)-Si(1)	107.65(6)	C(9)-Si(7)-C(8)	115.15(9)	C(30)-Si(12)-C(31)	109.44(11)
C(8)-Si(3)-Si(1)	111.80(6)	C(14)-Si(8)-C(13)	109.93(12)	C(30)-Si(12)-C(29)	103.93(11)
C(32)-Si(4)-C(18)	107.68(9)	C(14)-Si(8)-C(12)	103.78(12)	C(31)-Si(12)-C(29)	103.64(12)
C(32)-Si(4)-C(25)	112.53(8)	C(13)-Si(8)-C(12)	103.45(13)	C(30)-Si(12)-C(25)	115.39(10)
C(18)-Si(4)-C(25)	108.93(8)	C(14)-Si(8)-C(8)	114.94(10)	C(31)-Si(12)-C(25)	109.82(10)
C(32)-Si(4)-Si(2)	101.31(7)	C(13)-Si(8)-C(8)	109.09(10)	C(29)-Si(12)-C(25)	113.84(10)
C(18)-Si(4)-Si(2)	110.17(6)	C(12)-Si(8)-C(8)	114.95(10)	C(41)-O(1)-C(42)	111.7(2)

C(25)-Si(4)-Si(2)	115.79(6)	C(19)-Si(9)-C(20)	105.14(10)	C(41)-O(1)-Li(1)	127.79(19)
C(2)-Si(5)-C(4)	103.50(10)	C(19)-Si(9)-C(21)	103.98(11)	C(42)-O(1)-Li(1)	110.91(18)
C(2)-Si(5)-C(3)	105.21(10)	C(20)-Si(9)-C(21)	110.21(10)	C(44)-O(2)-C(43)	110.96(19)
C(4)-Si(5)-C(3)	110.67(10)	C(19)-Si(9)-C(18)	117.04(9)	C(44)-O(2)-Li(1)	121.28(17)
C(2)-Si(5)-C(1)	116.42(9)	C(20)-Si(9)-C(18)	112.09(9)	C(43)-O(2)-Li(1)	107.21(17)
C(4)-Si(5)-C(1)	109.42(9)	C(21)-Si(9)-C(18)	108.02(9)	C(46)-O(3)-C(45)	114.2(2)
C(3)-Si(5)-C(1)	111.29(10)	C(22)-Si(10)-C(24)	109.31(11)	C(46)-O(3)-Li(1)	114.11(18)
C(5)-Si(6)-C(7)	108.76(11)	C(22)-Si(10)-C(23)	107.04(11)	C(45)-O(3)-Li(1)	128.24(19)
C(5)-Si(6)-C(6)	106.81(12)	C(24)-Si(10)-C(23)	100.06(11)	C(47)-O(4)-C(48)	114.70(19)
C(7)-Si(6)-C(6)	100.70(10)	C(22)-Si(10)-C(18)	110.55(10)	C(47)-O(4)-Li(1)	109.99(18)
C(5)-Si(6)-C(1)	112.15(10)	C(24)-Si(10)-C(18)	113.84(10)	C(48)-O(4)-Li(1)	129.12(18)
C(7)-Si(6)-C(1)	112.94(9)	C(23)-Si(10)-C(18)	115.37(10)	C(50)-O(5)-C(49)	111.31(17)
C(50)-O(5)-Li(1)	113.78(15)	Si(10)-C(18)-Si(4)	116.54(10)	O(3)-Li(1)-O(5)	92.84(15)
C(49)-O(5)-Li(1)	129.13(17)	Si(9)-C(18)-Si(4)	115.44(10)	O(6)-Li(1)-O(5)	77.29(14)
C(51)-O(6)-C(52)	111.32(17)	Si(11)-C(25)-Si(12)	113.62(10)	O(3)-Li(1)-O(1)	98.13(17)
C(51)-O(6)-Li(1)	112.89(15)	Si(11)-C(25)-Si(4)	120.07(11)	O(6)-Li(1)-O(1)	92.12(15)
C(52)-O(6)-Li(1)	127.16(17)	Si(12)-C(25)-Si(4)	115.97(10)	O(5)-Li(1)-O(1)	168.4(2)
Si(6)-C(1)-Si(5)	110.46(9)	C(34)-C(32)-C(33)	110.29(17)	O(3)-Li(1)-O(4)	77.80(14)
Si(6)-C(1)-Si(3)	117.27(10)	C(34)-C(32)-Si(4)	119.11(15)	O(6)-Li(1)-O(4)	97.70(16)
Si(5)-C(1)-Si(3)	115.73(10)	C(33)-C(32)-Si(4)	112.32(15)	O(5)-Li(1)-O(4)	96.93(16)
Si(7)-C(8)-Si(8)	113.65(10)	C(58)-C(53)-C(54)	120.5(3)	O(1)-Li(1)-O(4)	89.02(15)
Si(7)-C(8)-Si(3)	121.10(10)	C(53)-C(54)-C(55)	120.1(3)	O(3)-Li(1)-O(2)	92.27(16)
Si(8)-C(8)-Si(3)	115.56(10)	C(56)-C(55)-C(54)	119.4(3)	O(6)-Li(1)-O(2)	94.51(15)
C(17)-C(15)-C(16)	109.46(16)	C(57)-C(56)-C(55)	120.2(3)	O(5)-Li(1)-O(2)	97.75(16)
C(17)-C(15)-Si(3)	112.86(14)	C(56)-C(57)-C(58)	120.4(3)	O(1)-Li(1)-O(2)	78.22(14)
C(16)-C(15)-Si(3)	118.78(14)	C(53)-C(58)-C(57)	119.4(3)	O(4)-Li(1)-O(2)	162.6(2)
Si(10)-C(18)-Si(9)	110.31(10)	O(3)-Li(1)-O(6)	168.7(2)		

Symmetry transformations used to generate equivalent atoms.

Reference

1. Brook, A. G.; Gilman, H. *J. Am. Chem. Soc.* **1954**, *76*, 278.
2. Recent reviews: (a) Tamao, K.; Kawachi, A. *Adv. Organomet. Chem*. **1995**, *38*, 1; (b) Lickiss, P. D.; Smith, C. M. *Coord. Chem. Rev.* **1995**, *145*, 75; (c) Belzner, J.; Dehner, U. *The Chemistry of Organic Silicon Compounds Vol. 2, Part 1* (Eds. : Rappoport, Z.; Apeloig, Y.), Wiley, Chichester **1998**, 779; (d) Sekiguchi, A.; Lee, V. Ya; Nanjo, M. *Coord. Chem. Rev.* **2000**, *210*, 11. (e) Lerner, H.-W. *Coord. Chem. Rev.* **2005**, 249, 789.
3. Weidenbruch, M.; Willms, S.; Saak, W.; Henkel, G. *Angew. Chem. Int. Ed. Engl.* **1997**, *22*, 36.
4. Scheschkewitz, D. *Angew. Chem. Int. Ed. Engl.* **2004**, *43*, 2965.
5. Ichinohe, M.; Sanuki, K.; Inoue, S.; Sekiguchi, A. *Organometallics* **2004**, *23*, 3088.
6. Inoue, S.; Ichinohe, M.; Sekiguchi, A. *Chem. Lett.* **2005**, *34*, 1564.
7. (a) Sekiguchi, A.; Kinjo, R.; Ichinohe, M. *Science* **2004**, *305*, 1755; (b) Sekiguchi, A.; Ichinohe, M.; Kinjo, R. *Bull. Chem. Soc. Jpn* **2006**, *79*, 825.
8. A similar pathway was observed in the reaction of disilenes with ^{t}BuLi, see: (a) Lee, V. Ya; Sekiguchi, A. *Chem. Lett.* **2004**, *33*, 84. (b) Sekiguchi, A.; Inoue, S.; Ichinohe, M.; Arai, Y. *J. Am. Chem. Soc.* **2004**, *126*, 9626.
9. Williams, E. A. In *The Chemistry of Organic Silicon Compounds*; Patai, S.; Rappoport, Z., Eds.; Wiley: Chichester, U. K., 1989, Part 1, Chapter 8.
10. The Si=Si bond lengths of disilenyllithium derivatives: 2.192(1) Å for $Tip_2Si=Si(Tip)Li$ (ref. 4), 2.2092(7) Å for $(^{t}Bu_2MeSi)_2Si=Si(Mes)Li$ (ref. 5), and 2.1983(18) Å for $(^{t}Bu_2MeSi)_2Si=Si(SiMe^{t}Bu_2)Li$ (ref. 6).
11. Calculations were carried out using the Gaussian 98 program. 1
12. (a) T. Nguyen, D. Scheschkewitz, *J. Am. Chem. Soc.* **2005**, 127,10174. (b) Scheschkewitz, D. *Angew. Chem. Int. Ed.* **2005**, 44, 2954. (c) Abersfelder, K.; Güclü, D.; Scheschkewitz, D. *Angew. Chem. Int. Ed. Engl.* **2006**, *45*, 1643.
13. (a) Sekiguchi, A.; Maruki, I.; Sakurai, H. *J. Am. Chem. Soc.* **1993**, *115*, 11460. (b) Budaraju, J.; Powell, D. R.; West, R. *Main Group Met. Chem.* **1996**, *19*, 531. (c) Apeloig, Y.; Nakash, M. *J. Am. Chem. Soc.* **1996,** *118*, 9798. (d) De Young, D. J.; Fink, M. J.; West, R. Michl, J. *Main Group Met. Chem.* **1987**, *10*, 19. (e) Apeloig, Y.; Nakash, M. *Organometallics* **1998**, *17*, 1260.

Chapter 5

One Electron Reduction of Disilyne with Alkali Metals: Synthesis, Characterization of the First Isolable Disilyne Anion Radicals and Silicon Vinyl Radical

Summary

The reaction of 1,1,4,4-tetrakis[bis(trimethylsilyl)methyl]-1,4-diisopropyl-2-tetrasilyne with an equivalent amount of alkali metals (Li, Na, K, KC_8) in tetrahydrofuran produces alkali metal salt of 1,1,4,4-tetrakis[bis(trimethylsilyl)methyl]-1,4-diisopropyl-2-tetrasilyne anion radical, the product of the one electron reduction of disilyne. One of the solvent-separated ion pairs of the disilyne anion radical; tetrakis(l,2-dimethoxyethane)potassium(I)1,1,4,4-tetrakis[bis(trimethylsilyl)methyl]-1,4-diisopropyl-2-tetrasilyne anion radical, was characterized by X-ray crystallography, which showed a trans bent structure with bend angle of 113.4°. The central silicon-silicon bond length is 2.1728(14). An electron spin resonance (ESR) study indicates delocalization of the unpaired electron between the two central silicon atoms. On the other hand, the reduction of disilyne with an equivalent amount of sodium in toluene produces 1,1,4,4-tetrakis[bis(trimethylsilyl)methyl]-1,4-diisopropyl-3-sodio-2-tetrasilene-2-yl, which is the first isolable silicon vinyl radical.

Introduction

The chemistry of silyl radical species has been the subject of extensive studies because of the unusual chemical and physical properties.[1] Especially, anion radical species of disilene, alkene analogue of heavier group 14 elements, have been paid much attention since much less is known about their chemical properties. In 1985, Weidenbruch et al. have first reported ESR spectra of tetra-*tert*-butyldisilene and tetramesityldisilene anion radicals, which were generated during reduction of the corresponding 1,1-dichlorosilanes but not by direct reduction of the corresponding disilenes with alkali metals (Scheme 5-1).[2]

Scheme 5-1.

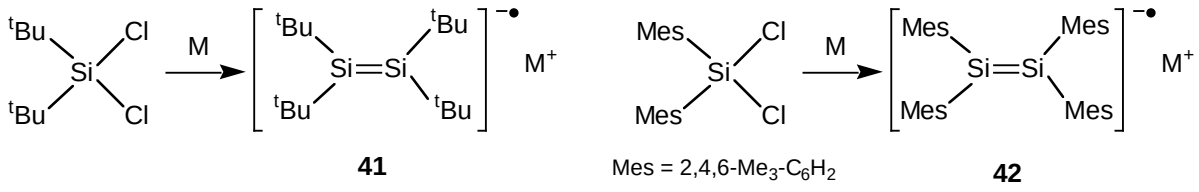

41 Mes = 2,4,6-Me_3-C_6H_2 **42**

In 2000, Kira et al. reported the direct method to generate the disilene anion radicals from corresponding disilenes. The structure of these anion radical species was characterized by ESR spectroscopy (Scheme 5-2).[3] In 2004, Sekiguchi et al. first revealed the structure of disilene anion radical, which was prepared by direct reduction of corresponding disilene with *tert*-butyllithium (Scheme 5-3).[4] The interesting feature of disilene anion radical is that one of the central silicon atoms has radical character, whereas the other silicon atom has silyl anion character. The ESR study indicates that rapid spin exchange occurs between central silicon atoms on the ESR time scale.

Scheme 5-2.

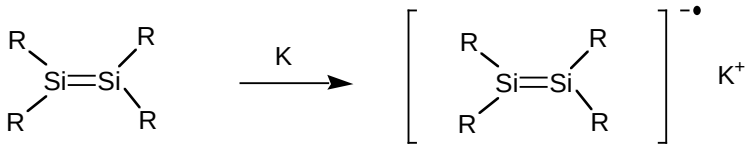

43 (R = $SiMe^iPr_2$)
44 (R = Si^tBuMe_2)
45 (R = Si^iPr_3)

Scheme 5-3.

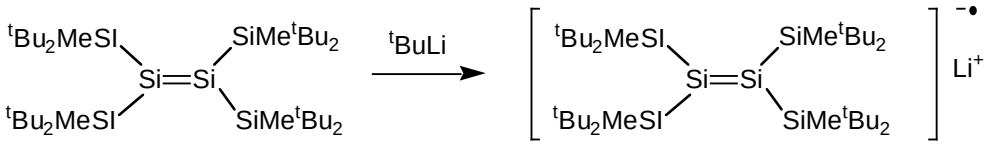

46

On the other hand, chemistry of anion radical of disilyne, alkyne analogue of heavier group 14 elements, has not been reported so far even as transient species although anion radical species of germanium and tin alkyne analogues have been reported by Power et al. in 2000 (Chart 5-1).[5]

Chart 5-1.

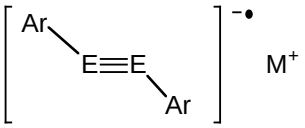

47 (E = Ge, Ar = C_6H_3-2,6-(C_6H_2-2,4,6-$^iPr_3$)$_2$, M = Na)
48 (E = Ge, Ar = C_6H_3-2,6-(C_6H_3-2,6--$^iPr_2$)$_2$, M = K)
49 (E = Sn, Ar = C_6H_3-2,6-(C_6H_2-2,4,6-$^iPr_3$)$_2$, M = Na)
50 (E = Sn, Ar = C_6H_3-2,6-(C_6H_2-2,4,6-$^iPr_3$)$_2$, M = K)
51 (E = Sn, Ar = C_6H_3-2,6-(C_6H_3-2,6-$^iPr_2$)$_2$, M = K)

Disilyne has characteristic structure and the geometry around the silicon–silicon triple bond is not linear, but *trans*-bent, which results in splitting of the two occupied MOs (π_{in} for HOMO–1 and π_{out} for HOMO) and splitting of the two unoccupied MOs (π^*_{in} for LUMO and π^*_{out} for LUMO+1) as shown in chapter 1.[6] Upon bending, the energy of the HOMO is raised, whereas the energy of the LUMO is significantly lowered. Therefore, it is expected that the disilyne **28** is prone to easy reduction of its low-lying LUMO. In this chapter, the one electron reduction of disilyne **28** with alkali metals is reported. It represents the first example of the stable compounds of such class, which has been fully characterized including X-ray crystallography.

Results and Discussion

Synthesis and EPR spectra of disilyne anion radicals 52

The anion radical of disilyne **28** was obtained by one electron reduction with alkali metals. Thus, the reaction of disilyne **28** with an equivalent amount of lithium, sodium, and KC_8 or potassium metal in THF produced the disilyne anion radical **52a-c** (Scheme 5-4). Especially, potassium salt of disilyne anion radical **52c** was isolated by recrystallization from pentane and DME as dark brown crystals in 63% isolated yield. These products were characterized by EPR spectroscopy, and X-ray crystallography for **52c**.

Scheme 5-4.

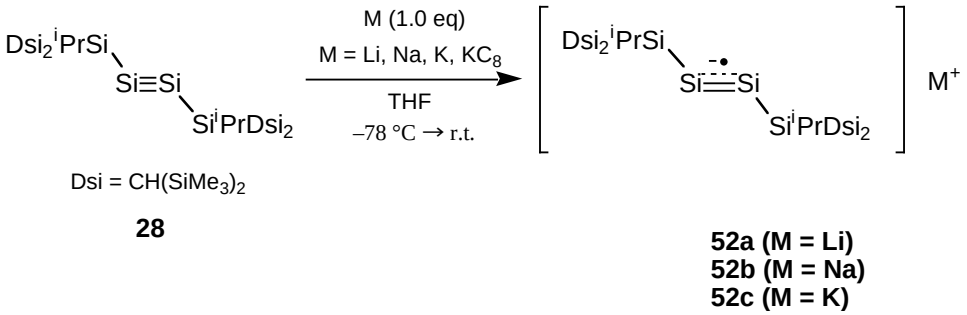

The EPR spectra of **52a-c** showed the same signal, indicating that the **52a-c** were metal free disilyne anion radical species. Figure 5-1 shows the EPR spectrum of **52c** in 2-methyl-THF solvent. It showed a triplet signal with a *g* value of 1.99962 (hfcc = 0.23 mT), which is one of the smallest values for silyl radicals, due to the high *s*-character of the SOMO of **52c**.[6] The triplet splitting of the signal arises from coupling with the two δ-H of isopropyl groups. The signal is accompanied by the two pairs of satellite signals (3.92 and 2.24 mT), due to coupling of the unpaired electron with the α- and β-^{29}Si nuclei, respectively. The magnitude of the spin coupling by the α-^{29}Si nuclei is smaller than that in the tris(di-*tert*-butylmethylsilyl)silyl radical (5.80 mT),[1r] implying delocalization of unpaired electron between central silicon atoms. The magnitude of the spin coupling by the β-^{29}Si nuclei, however, is the largest for all observed silyl-

substituted silyl radicals. The EPR spectrum of **52a-c** was also measured in 2-methyl-THF at glass matrix condition (100 K). Expectedly, the low symmetry of disilyne anion radical **52a-c** caused the three axes anisotropy of *g*-factor, g_{xx} = 2.00907, g_{yy} = 2.00340, g_{zz} = 2.198763 (Figure 5-2).

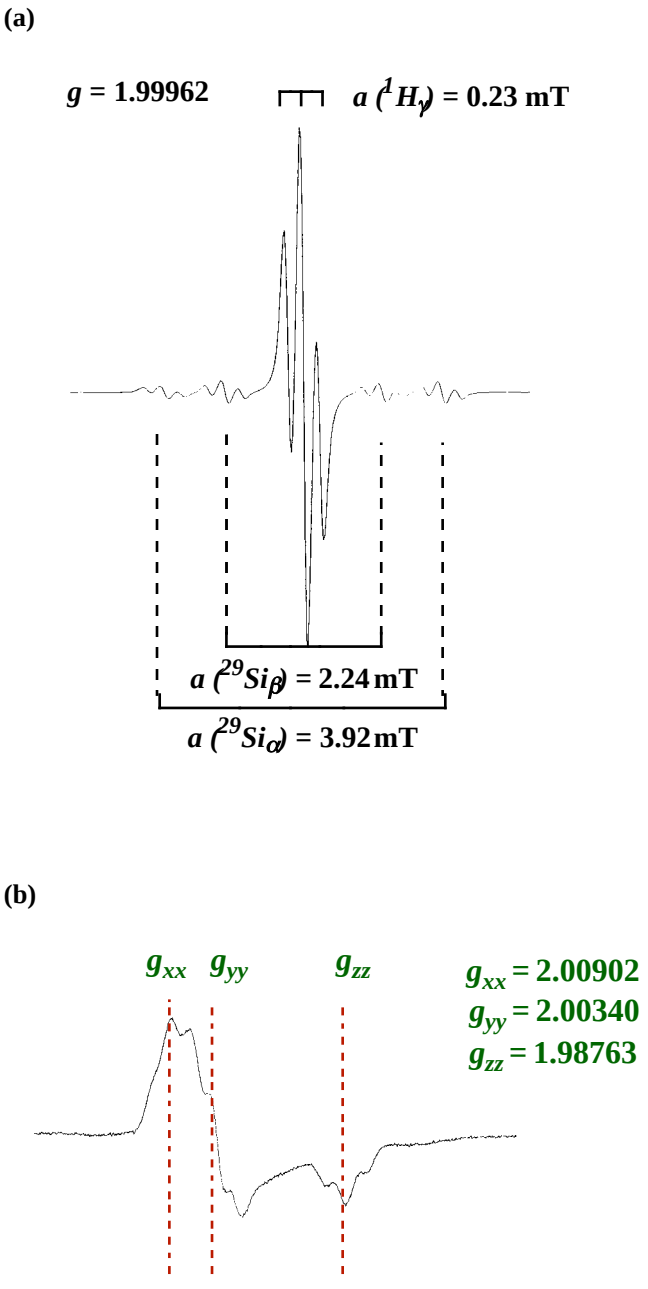

Figure 5-1. (a) The EPR spectrum of anion radical **52c** in 2-Me-THF at ambient temperature, and (b)100 K.

Molecular Structure of disilyne anion radical 52c

X-ray crystallography unambiguously revealed the *trans*-bent structure of disilyne anion radical **52c** (Figure 5-2). The counter cation, potassium, is solvated by four DME molecules and the distance between Si1 and K1 is greater than 11 Å, showing that anion radical **52c** is free. The central Si–Si bond length is 2.1728(14) Å, which is 5% longer than that of disilyne **28** (2.0622(9) Å)[6] because of the partial rehybridization of the central Si atoms. The bond lengths of Si1-Si3 and Si2-Si4 are 2.3639(13) Å and 2.3714(13) Å, respectively. The characteristic bond angles (112.84(6) and 113.97(6)°) of the tetrasilane unit are smaller than the corresponding bond angle (137.44°) of **28** due to the influence of the negative charge on the central silicon atoms. These bond angles are found to be essentially equal to each other, indicating the delocalization of the unpaired electron between the two central silicon atoms.

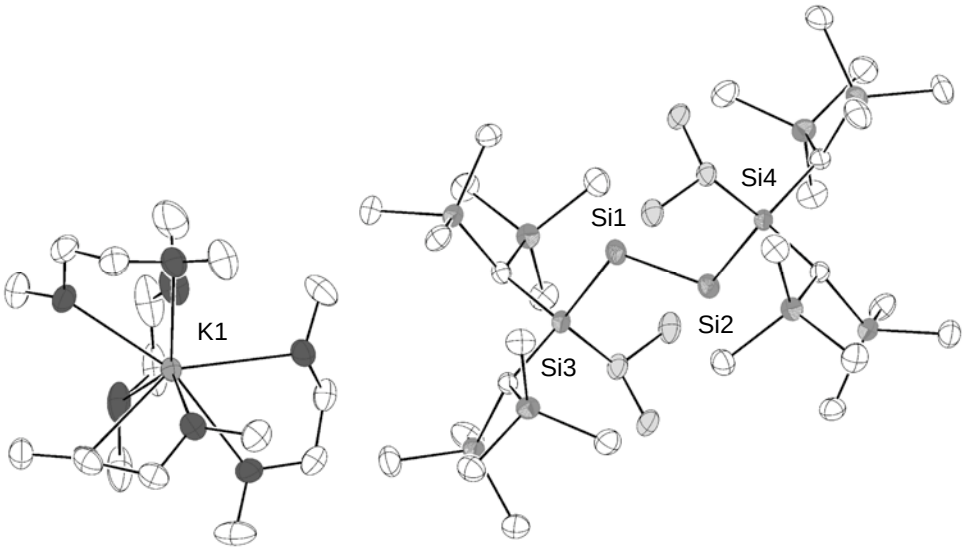

Figure 5-2. ORTEP drawing of disilyne anion radical **52c**.

Molecular Orbitals of Disilyne Anion Radical 52c

A DFT calculation on disilyne anion radical **52c** at the UB3LYP/6-31G(d) level showed two sets of π MOs (Figure 5-3). The SOMO is corresponding to the asymmetrical π*-orbital, LUMO of disilyne **28**, which indicates the delocalization of unpaired electron between central silicon atoms. The presence of the two nondegenerate π and two π* MOs, including SOMO, in **52c** is reflected in the UV-spectrum of **52c**, which shows four absorption bands: 237 (ε 14781), 292 (ε 4891), 403 (ε 2036), 713 (ε 48) nm (Figure 5-4). The very weak absorption band with maximum of 713 nm (ε 48) is assigned to the formally forbidden HOMO to SOMO and SOMO to LUMO electronic transitions, which is responsible for the dark-brownish color of disilyne anion radical **52c**. This absorption band is red-shifted comparing to HOMO to LUMO absorption band with maximum of 690 nm (e 14) of disilyne **28**.

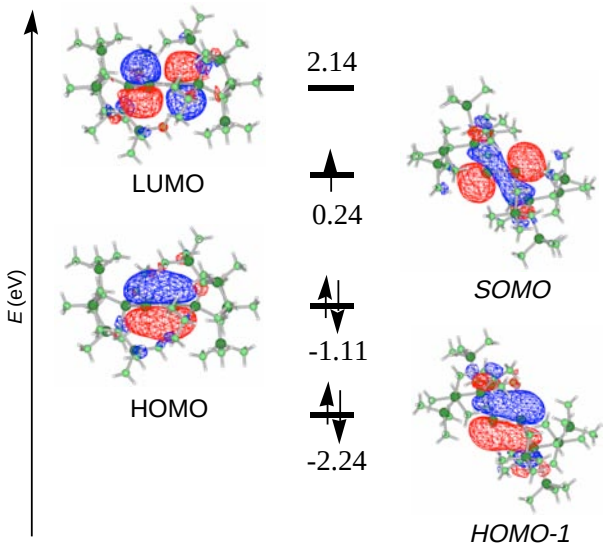

Figure 5-3. Molecular Orbitals of disilyne anion radica **52c** calculated at the UB3LYP/6-31G(d) from X-ray data

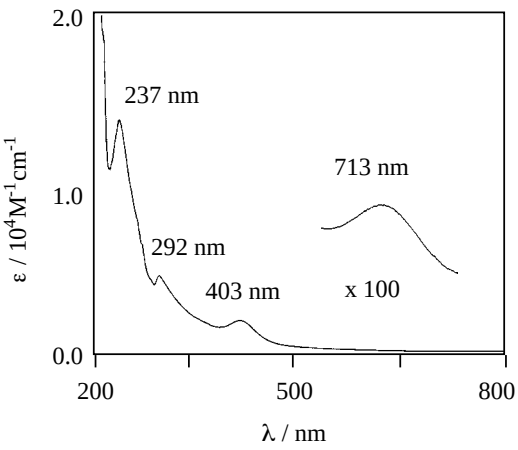

Figure 5-4 UV-Vis spectrum of disilyne anion radical **52c** in hexane at room temperature.

Synthesis and EPR spectra of disilyne anion radical 53

One electron reduction of disilyne **28** in THF gave metal free disilyne anion radical **52a-c**. To examine whether metal interacting anion radical species could be obtained or not when the reduction is conducted in non-polar solvent, the one electron reduction of disilyne with potassium in toluene was performed. The reaction of disilyne **28** with an equivalent amount of potassium metal in toluene at room temperature, produced the disilyne anion radical **53** (Scheme 5-5). The product was isolated by recrystallization from toluene as dark brown crystals in 57% isolated yield (Figure 5-5), and was characterized by both EPR spectroscopy and X- ray crystallography.

Scheme 5-5.

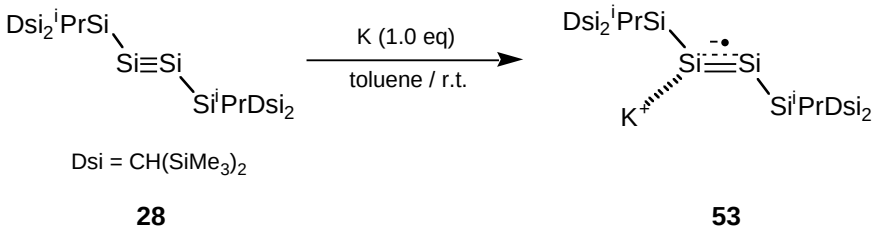

Dsi = $CH(SiMe_3)_2$

28 **53**

EPR spectrum of anion radical species **53** showed the sextet signal at g = 2.00003, which is almost the same as that of disilyne anion radicals **52a-c** (g = 1.99962) (Figure 5-6). The simulation result with coupling constants of 1.85, 1.12, 2.62 and 4.02 mT for ^{1}H, ^{39}K, ^{41}K, and $^{29}Si_{\alpha}$, respectively, well agrees with experimental spectrum.

The sextet splitting of the signal arises mainly from coupling with the two δ-H of isopropyl groups and ^{41}K. The signal is accompanied by one pair of satellite signals (4.02 mT), due to coupling of the unpaired electron with the α-^{29}Si nuclei. The magnitude of the spin coupling by the α-^{29}Si nuclei is similar to that of anion radical species **52a-c** (3.92 mT),[14] indicating delocalization of unpaired electron between the central silicon atoms.

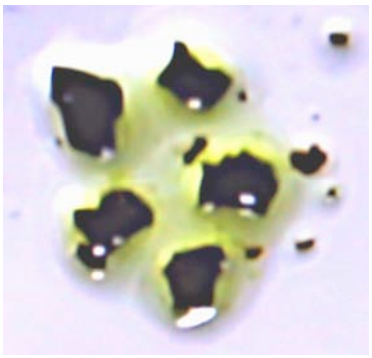

Figure 5-5. Crystals of disilyne anion radical **53**.

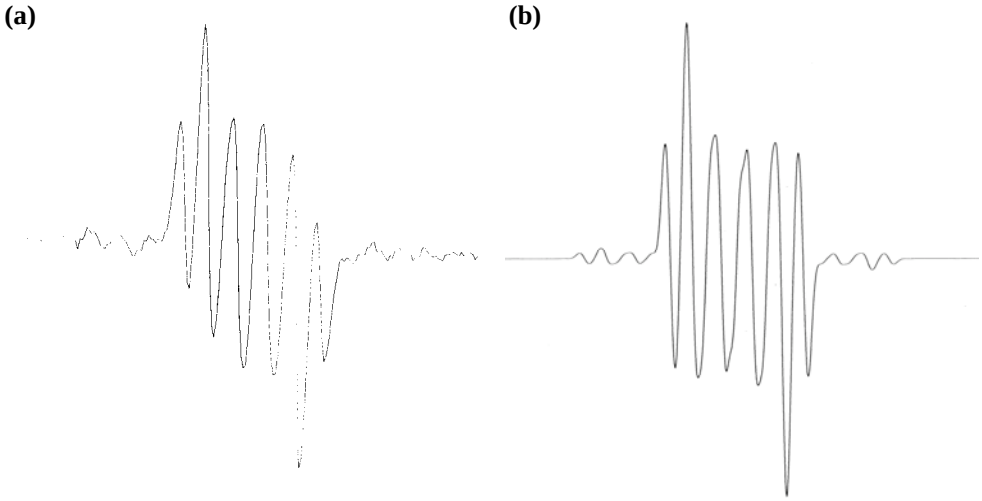

Figure 5-6. (a) The EPR spectrum of disilyne anion radical **53** in toluene at ambient temperature. (b) Simulation EPR spectrum fof **53**.

Molecular Structure of disilyne anion radical 53

X-ray crystallography disclosed the *trans*-bent anion radical structure of **53** (Figure 5-7). Counter cation, potassium, is solvated by one toluene molecule and distance between Si1 and K1 is 3.4042(15)Å, showing their interaction to each other. The central Si–Si bond length is 2.1617(15) Å, which is 5% longer than that of disilyne **28** and almost the same as that of metal-free disilyne anion radical **52c**. The bond lengths of Si1-Si3 and Si2-Si4 are 2.3637(16) Å and 2.3712(16) Å, respectively. The characteristic bond angles (118.76 ° and 112.73 °) of tetrasilane unit are smaller than the corresponding bond angle (137.44°) of **28**, and these angles are similar to that of metal-free disilyne anion radical **52c**, indicating the delocalization of the unpaired electron between the two central silicon atoms.

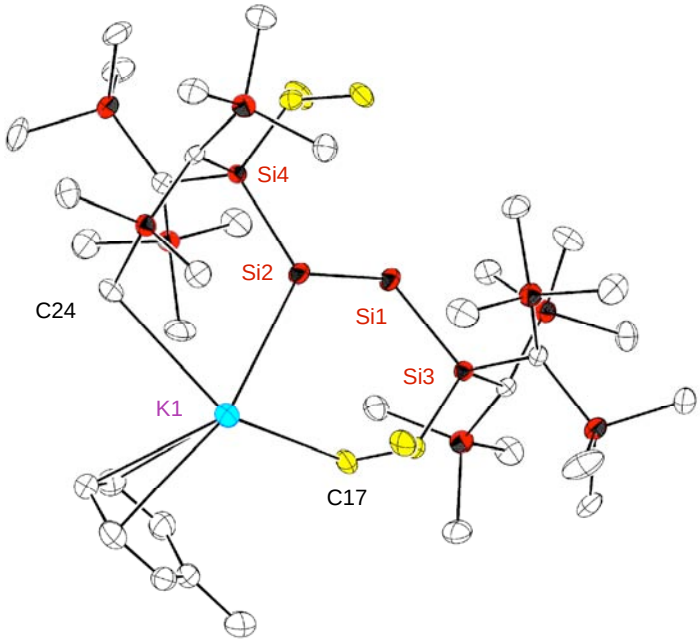

Figure 5-7. ORTEP drawing of disilyne anion radical **53**.

Molecular Orbitals of Disilyne Anion Radical 53

A DFT calculation on disilyne anion radical **53** at the UB3LYP/6-31G(d) level showed two sets of π MOs (Figure 5-8). The SOMO is corresponding to the asymmetrical π*-orbital, LUMO of disilyne **28**, which indicates the delocalization of unpaired electron between the central silicon atoms. The presence of the two nondegenerate π and two π* MOs, including SOMO, in **53** is reflected in the UV-spectrum, which shows five absorption bands: 283 (ε 6014), 330 (ε 8320), 388 (ε 9369), 478 (ε 408), 682 (ε 12) nm (Figure 5-9). The very weak absorption band with maximum of 682 nm (ε 12) is assigned to the formally forbidden HOMO to SOMO and SOMO to LUMO+3 electronic transitions, which is responsible for the dark-brownish color of disilyne anion radical **53**. This absorption band is red-shifted comparing to HOMO to LUMO absorption band with maximum of 690 nm (e 14) of disilyne **28**.

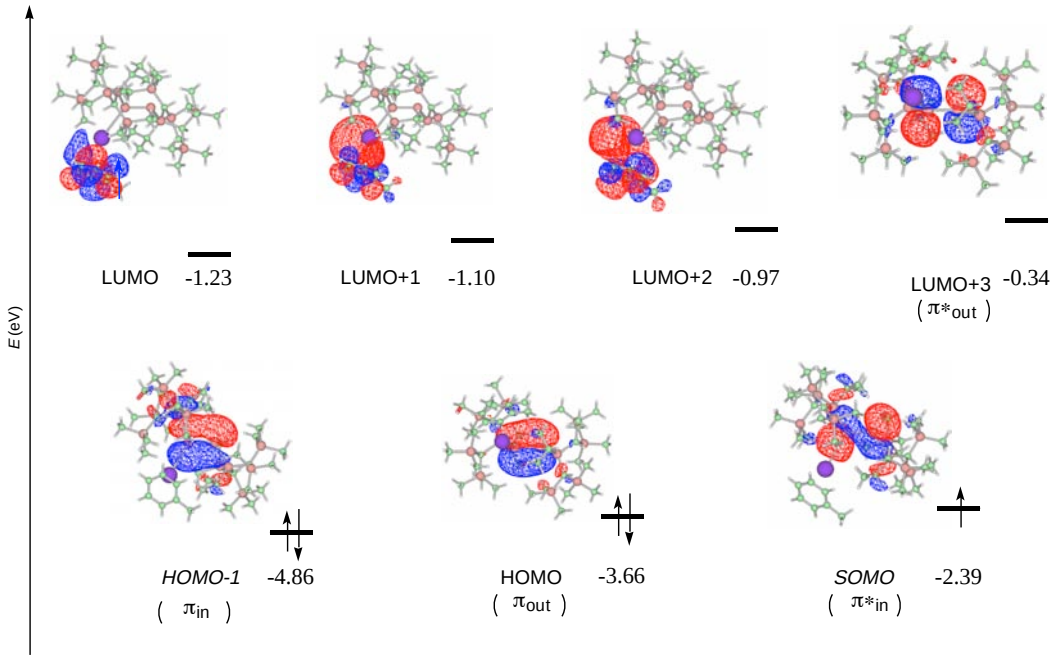

Figure 5-8. Molecular Orbitals of disilyne anion radical **53** calculated at the UB3LYP/6-31G(d) from X-ray data.

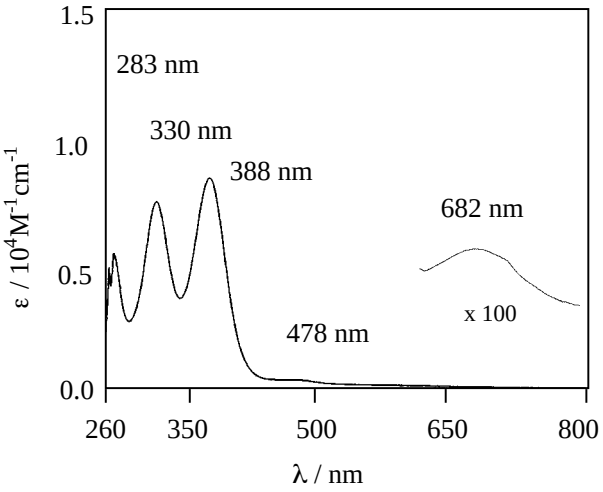

Figure 5-9. UV-Vis spectrum of disilyne anion radical **53** in hexane at room temperature.

Synthesis and EPR spectra of Silicon Vinyl Radical 54

One electron reduction of disilyne **28** with potassium even in toluene gave disilyne anion radical **53** where unpaired electron delocalized between the central silicon atoms. To examine whether metal bonded silicon vinyl radical species could be obtained or not when the reduction is conducted with sodium as reductant, the one electron reduction of disilyne with sodium in toluene was examined. The reaction of disilyne **28** with an equivalent amount of sodium metal in toluene at room temperature, produced the silicon vinyl radical **54** (Scheme 5-6). The product was isolated by recrystallization from toluene as red crystals in 64% isolated yield (Figure 5-10). The product was characterized by EPR spectroscopy.

Scheme 5-6.

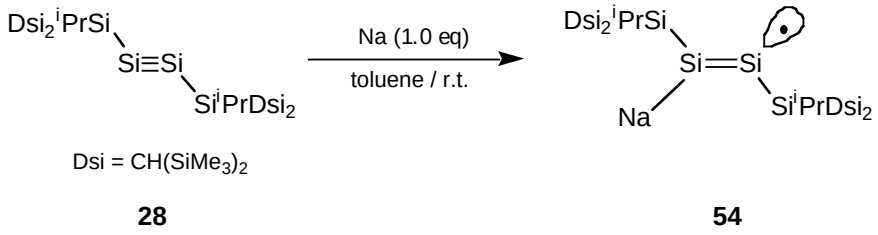

Dsi = $CH(SiMe_3)_2$

28 **54**

EPR spectrum of anion radical species **54** showed the quartet signal at g = 1.99958, which value is slightly smaller than that of disilyne anion radicals **52a-c** (g = 1.99962) (Figure 5-11). The simulation result with coupling constants of 2.14, 2.27, 9.12 and 18.2 mT for ^{1}H, ^{1}H, ^{23}Na, ^{29}Si, respectively, well agrees with experimental spectrum.

The quartet splitting of the signal arises mainly from coupling with the ^{23}Na. The signal is accompanied by one pair of satellite signals (18.2 mT), due to coupling of the unpaired electron with the α-^{29}Si nuclei. The magnitude of the spin coupling by the α-^{29}Si nuclei is bigger than that of anion radical species **52a-c** and **53** (3.92 and 4.02 mT, respectively), indicating localization of unpaired electron on one unsaturated (sp^2) silicon atom (so-called *vinyl radical*).

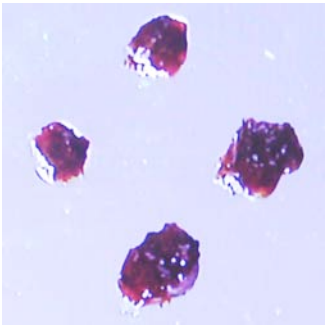

Figure 5-10. Crystals of silicon vinyl radical **54**.

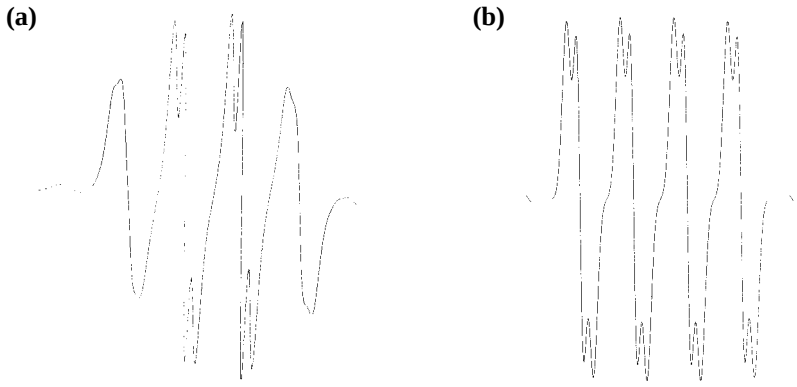

Figure 5-11. (a) The EPR spectrum of disilyne anion radical **54** in toluene at ambient temperature. (b) Simulation EPR spectrum of **54**.

UV-Vis Spectrum of Silicon Vinyl Radical 54

The presence of only one set of π and π* MOs is reflected in the UV-spectrum, which shows two absorption bands: 309 (ε 1450), 397 (ε 7980) nm (Figure 5-12). The characteristic absorption band with maximum of 397 nm (ε 7980) is assigned to HOMO to LUMO electronic transition, which is responsible for the red color of **54**. This absorption band is slightly red-shifted comparing to HOMO to LUMO transition absorption band with maximum of 390 nm (e 5440) of disilenide **38**.

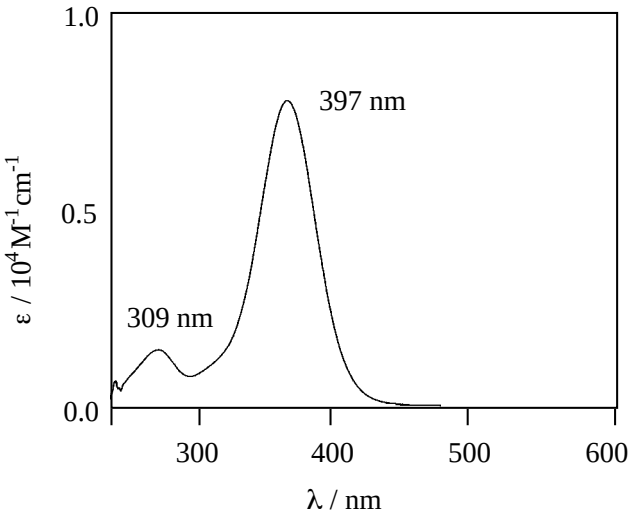

Figure5-12 UV-Vis spectrum of disilyne anion radical **54** in toluene at room temperature.

Conclusion

The first stable disilyne anion radicals **52a-c** and **53** were synthesized by the reaction of disilyne **28** with alkali metals (Li, Na, K, KC_8) in THF or potassium in toluene. In this reaction, the one electron reduction of disilyne **28** occurred. X-ray crystallography of anion radical species **52c** revealed the molecular structure of solvent-separated disilyne anion radical species. On the other hand, X-ray crystallography of anion radical species **53** revealed the molecular structure of potassium interacting disilyne anion radical species. According to spectroscopy and theoretical calculation, it was found that unpaired electron in both of **52c** and **53** is delocalized between the central silicon atoms.

The reaction of disilyne **28** with sodium in toluene produced the first isolable silicon vinyl radical **54**. The vinyl radical species **54** was characterized by EPR and UV-Vis spectra, which indicated that the unpaired electron is localized on sp^2-silicon atom.

Experimental Section

Synthesis of 1,1,4,4-tetrakis[bis(trimethylsilyl)methyl]-1,4-diisopropyltetrasila-2-ene Anion Radical 52c.

Dry oxygen-free THF (2.0 ml) was added by vacuum transfer to a mixture of 1,1,4,4-tetrakis[bis(trimethylsilyl)methyl]-1,4-diisopropyltetrasila-2-yne **28** (50 mg, 0.060 mmol) and KC_8 (8.1 mg, 0.060 mmol), and then the reaction mixture was allowed to warm from –78 °C to room temperature with stirring overnight. After evaporation of solvent, dry pentane (0.5ml) was added to the reaction mixture, and residue was recrystallized from pentane-DME mixed solvent (4:1) at –30 °C to give the anion radical **52c** as dark brown crystals (47 mg, 63%). Mp. 121 °C (dec); ESR (Me-THF) g = 1.99962, $a(^{29}Si_{\alpha})$ = 3.92 mT, $a(^{29}Si_{\beta})$ = 2.24 mT, $a(^{1}H_{\gamma})$ = 0.23 mT; UV-Vis (hexane) λ_{max}/nm (ε) 237 (14800), 292 (4890), 403 (2040), 713 (50).

Synthesis of Potassium interacting 1,1,4,4-tetrakis[bis(trimethylsilyl)methyl]-1,4-diisopropyltetrasila-2-ene Anion Radical 53.

Dry oxygen-free toluene (1.2 ml) was added by vacuum transfer to a mixture of 1,1,4,4-tetrakis[bis(trimethylsilyl)methyl]-1,4-diisopropyltetrasila-2-yne **28** (50 mg, 0.060 mmol) and potassium (2.3 mg, 0.060 mmol), and then the reaction mixture was stirred for 24 hours. After the reaction, anion radical species **53** was obtained as dark brown crystals by recrystallization from toluene at room temperature (30 mg, 57%). Mp. 117 °C (dec); ESR (toluene) g = 2.00003, $a(^{29}Si_{\alpha})$ = 4.02 mT, $a(^{39}K)$ = 1.22 mT, $a(^{41}K)$ = 2.62 mT, $a(^{1}H_{\gamma})$ = 1.85 mT; UV-Vis (toluene) λ_{max}/nm (ε) 283 (6014), 330 (8320), 388 (9369), 682 (12).

Synthesis of 1,1,4,4-tetrakis[bis(trimethylsilyl)methyl]-1,4-diisopropyltetrasila-3-sodio-2-ene-2-yl 54.

Dry oxygen-free toluene (1.2 ml) was added by vacuum transfer to a mixture of 1,1,4,4-tetrakis[bis(trimethylsilyl)methyl]-1,4-diisopropyltetrasila-2-yne **28** (100 mg, 0.120 mmol) and sodium (2.8 mg, 0.120 mmol), and then the reaction mixture was stirred for 24 hours. After the reaction, silicon vinyl radical species **54** was obtained as red crystals by recrystallization from toluene at room temperature (66 mg, 64%). Mp. 115 °C (dec); ESR (toluene) g = 1.99958, $a(^{29}Si_{\alpha})$ = 18.2 mT, $a(^{23}Na)$ = 9.12 mT, $a(^{1}H_{\gamma})$ = 2.27 mT, $a(^{1}H_{\delta})$ = 2.14 mT; UV-Vis (toluene) λ_{max}/nm (ε) 309 (1450), 397 (7980).

Xray Crystal Structure Determination of 52c

The single crystals of **52c** for X-ray analysis were obtained by the recrystallization from hexane. The X-ray crystallographic experiments were performed on a MacScience DIP2030 image plate diffractometer equipped with graphite-monochromatized Mo-Kα radiation (λ = 0.71070 Å). Details of crystal data and structure refinement are summarized in Table a-**52c**. The final atomic parameters, the bond lengths and the bond angles of **52c** are listed in Tables b-**52c** and c-**52c**, respectively.

Appendix

Table a-(**52**). Crystal Data and Structure Refinement for Compound **52c**.

Identification code	$[Dsi_2{}^{i}PrSiSi{\equiv}SiSi{}^{i}PrDsi_2]^{\bullet-}[K^{+}(dme)_4]$
Empirical formula	$C_{50}H_{130}KO_8Si_{12}$
Formula weight	1235.72
Temperature	120.0(1) K
Wavelength	0.71070 Å
Crystal system, space group	Monoclinic, P21/c
Unit cell dimensions	a = 11.1710(8)Å alpha = 90 deg.
	b = 22.1790(12) Å beta = 93.542(4) deg.
	c = 31.4580(19) Å gamma = 90deg.
Volume	7779.2(8) $Å^3$
Z, Calculated density	4, 1.055 Mg/m^3
Absorption coefficient	0.292 mm^{-1}
F(000)	2724
Crystal size	0.25 x 0.25x 0.20 mm
Theta range for data collection	2.11to 27.98 deg.
Limiting indices	0<=h<=14, 0<=k<=29, –41<=l<=41
Reflections collected / unique	81605/ 18045 [R(int) = 0.065]
Completeness to theta = 28.01	96.2 %
Absorption correction	None
Refinement method	Full-matrix least-squares on F^2
Data / restraints / parameters	18045/ 0 / 641
Goodness-of-fit on F^2	0.984
Final R indices [I>2sigma(I)]	R1 = 0.0712, wR2 = 0.1798
R indices (all data)	R1 = 0.1229, wR2 = 0.2145
Extinction coefficient	0.0021(3)
Largest diff. peak and hole	1.046 and –0.480 $e.Å^{-3}$

Table b-(**52c**). Atomic coordinates (x 10^4) and equivalent isotropic displacement parameters ($Å^2$ x 10^3) for compound.

U(eq) is defined as one third of the trace of the orthogonalized U_{ij} tensor.

	x	y	z	U(eq)
K(1)	-5006(1)	7605(1)	8782(1)	39(1)
Si(1)	759(1)	2303(1)	8851(1)	44(1)
Si(2)	-775(1)	2843(1)	8626(1)	44(1)
Si(3)	726(1)	1306(1)	8586(1)	32(1)
Si(4)	-667(1)	3851(1)	8878(1)	34(1)
Si(5)	-1146(1)	928(1)	9315(1)	43(1)
Si(6)	-219(1)	-86(1)	8712(1)	43(1)
Si(7)	3352(1)	1195(1)	9074(1)	38(1)
Si(8)	3239(1)	1192(1)	8084(1)	40(1)
Si(9)	1256(1)	4144(1)	8145(1)	42(1)
Si(10)	470(1)	5206(1)	8734(1)	44(1)
Si(11)	-3269(1)	4004(1)	8378(1)	38(1)
Si(12)	-3172(1)	4017(1)	9368(1)	43(1)
O(1)	-3001(3)	7751(1)	9365(1)	61(1)
O(2)	-4189(3)	6641(1)	9325(1)	59(1)
O(3)	-6975(3)	7440(2)	9255(1)	85(1)
O(4)	-5810(4)	8563(2)	9300(1)	81(1)
O(5)	-6904(3)	7880(1)	8206(1)	60(1)
O(6)	-6054(3)	6698(1)	8221(1)	62(1)
O(7)	-4078(2)	8559(1)	8298(1)	50(1)
O(8)	-3120(2)	7385(1)	8279(1)	56(1)
C(1)	24(3)	695(1)	8940(1)	36(1)
C(2)	-518(4)	1434(2)	9748(1)	59(1)
C(3)	-2494(3)	1310(2)	9060(1)	59(1)
C(4)	-1738(4)	265(2)	9622(1)	62(1)
C(5)	-1817(4)	-254(2)	8526(1)	61(1)

C(6)	281(4)	-660(2)	9124(1)	58(1)
C(7)	665(4)	-292(2)	8247(1)	62(1)
C(8)	2380(3)	1042(1)	8569(1)	33(1)
C(9)	2536(4)	1255(2)	9575(1)	54(1)
C(10)	4392(4)	539(2)	9180(1)	55(1)
C(11)	4234(3)	1908(2)	9051(1)	49(1)
C(12)	2597(4)	757(2)	7613(1)	50(1)
C(13)	4827(4)	897(2)	8141(1)	58(1)
C(14)	3355(4)	2018(2)	7959(1)	53(1)
C(15)	-96(3)	1263(2)	8028(1)	39(1)
C(16)	213(4)	1763(2)	7716(1)	48(1)
C(17)	-1466(3)	1242(2)	8053(1)	52(1)
C(18)	102(3)	4428(1)	8517(1)	36(1)
C(19)	584(4)	3628(2)	7727(1)	52(1)
C(20)	2562(3)	3747(2)	8412(1)	57(1)
C(21)	1916(4)	4775(2)	7826(1)	57(1)
C(22)	2097(4)	5318(2)	8915(1)	61(1)
C(23)	78(4)	5778(2)	8312(1)	66(1)
C(24)	-408(4)	5472(2)	9188(2)	69(1)
C(25)	-2300(3)	4152(1)	8882(1)	34(1)
C(26)	-4154(3)	3287(2)	8401(1)	48(1)
C(27)	-2454(3)	3946(2)	7874(1)	50(1)
C(28)	-4329(4)	4663(2)	8271(1)	54(1)
C(29)	-4764(3)	4314(2)	9310(1)	57(1)
C(30)	-2542(4)	4460(2)	9837(1)	56(1)
C(31)	-3305(4)	3192(2)	9495(1)	56(1)
C(32)	135(3)	3898(2)	9438(1)	46(1)
C(33)	1505(3)	3892(2)	9420(1)	57(1)
C(34)	-215(4)	3417(2)	9755(1)	55(1)
C(51)	-2038(5)	8145(3)	9284(2)	86(2)
C(52)	-2631(4)	7269(2)	9630(2)	71(1)
C(53)	-3683(4)	6888(2)	9712(1)	65(1)

C(54)	-5069(5)	6197(2)	9389(2)	84(2)
C(55)	-7936(6)	7053(3)	9113(2)	115(2)
C(56)	-7365(7)	7898(3)	9507(2)	108(3)
C(57)	-6331(7)	8280(3)	9657(2)	106(3)
C(58)	-4854(7)	8967(2)	9428(2)	121(3)
C(59)	-7786(4)	8320(2)	8295(2)	74(1)
C(60)	-7354(4)	7441(2)	7906(2)	72(1)
C(61)	-6386(4)	7007(2)	7834(1)	67(1)
C(62)	-5349(5)	6196(2)	8151(2)	85(2)
C(63)	-4857(4)	9038(2)	8179(2)	69(1)
C(64)	-3519(4)	8317(2)	7940(1)	59(1)
C(65)	-2574(4)	7878(2)	8082(1)	59(1)
C(66)	-2266(4)	6928(2)	8402(2)	69(1)

Table c-(**52c**). Bond lengths [Å] and angles [deg] for compound **52c**.

K(1)-O(8)	2.754(3)	Si(6)-C(7)	1.870(4)	Si(11)-C(25)	1.893(3)
K(1)-O(3)	2.756(3)	Si(6)-C(6)	1.878(4)	Si(11)-C(28)	1.899(4)
K(1)-O(5)	2.770(3)	Si(6)-C(5)	1.881(4)	Si(12)-C(30)	1.872(4)
K(1)-O(1)	2.824(3)	Si(6)-C(1)	1.889(3)	Si(12)-C(31)	1.882(4)
K(1)-O(7)	2.840(3)	Si(7)-C(11)	1.867(4)	Si(12)-C(25)	1.887(3)
K(1)-O(2)	2.850(3)	Si(7)-C(9)	1.873(4)	Si(12)-C(29)	1.895(4)
K(1)-O(4)	2.857(3)	Si(7)-C(10)	1.879(4)	O(1)-C(52)	1.404(5)
K(1)-O(6)	2.876(3)	Si(7)-C(8)	1.899(3)	O(1)-C(51)	1.421(5)
K(1)-C(61)	3.529(4)	Si(8)-C(12)	1.873(4)	O(2)-C(54)	1.415(5)
Si(1)-Si(2)	2.1728(14)	Si(8)-C(14)	1.881(4)	O(2)-C(53)	1.422(5)
Si(1)-Si(3)	2.3639(13)	Si(8)-C(8)	1.883(3)	O(3)-C(56)	1.375(6)
Si(2)-Si(4)	2.3714(13)	Si(8)-C(13)	1.889(4)	O(3)-C(55)	1.425(7)
Si(3)-C(15)	1.932(3)	Si(9)-C(20)	1.861(4)	O(4)-C(58)	1.432(7)
Si(3)-C(8)	1.942(3)	Si(9)-C(19)	1.867(4)	O(4)-C(57)	1.440(7)
Si(3)-C(1)	1.948(3)	Si(9)-C(21)	1.899(4)	O(5)-C(60)	1.427(5)
Si(4)-C(32)	1.930(3)	Si(9)-C(18)	1.899(3)	O(5)-C(59)	1.427(5)
Si(4)-C(25)	1.944(3)	Si(10)-C(23)	1.867(4)	O(6)-C(62)	1.389(5)
Si(4)-C(18)	1.947(3)	Si(10)-C(24)	1.880(4)	O(6)-C(61)	1.424(5)
Si(5)-C(3)	1.866(4)	Si(10)-C(22)	1.887(4)	O(7)-C(63)	1.410(5)

Si(5)-C(2)	1.867(4)	Si(10)-C(18)	1.891(3)	O(7)-C(64)	1.426(5)
Si(5)-C(1)	1.888(3)	Si(11)-C(26)	1.875(4)	O(8)-C(65)	1.415(5)
Si(5)-C(4)	1.900(4)	Si(11)-C(27)	1.880(4)	O(8)-C(66)	1.429(5)
C(15)-C(16)	1.534(5)	C(32)-C(33)	1.536(5)	C(60)-C(61)	1.475(6)
C(15)-C(17)	1.538(5)	C(52)-C(53)	1.483(6)	C(64)-C(65)	1.485(6)
C(32)-C(34)	1.529(5)	C(56)-C(57)	1.486(9)		

O(8)-K(1)-O(3)	161.97(10)	O(1)-K(1)-O(6)	139.04(9)	C(25)-Si(4)-Si(2)	107.32(10)
O(8)-K(1)-O(5)	104.22(9)	O(7)-K(1)-O(6)	109.90(8)	C(18)-Si(4)-Si(2)	116.16(10)
O(3)-K(1)-O(5)	77.19(10)	O(2)-K(1)-O(6)	86.93(9)	C(3)-Si(5)-C(2)	107.3(2)
O(8)-K(1)-O(1)	77.83(9)	O(4)-K(1)-O(6)	137.72(11)	C(3)-Si(5)-C(1)	115.22(17)
O(3)-K(1)-O(1)	106.94(11)	O(8)-K(1)-C(61)	76.02(10)	C(2)-Si(5)-C(1)	112.15(17)
O(5)-K(1)-O(1)	160.63(10)	O(3)-K(1)-C(61)	94.88(13)	C(3)-Si(5)-C(4)	105.9(2)
O(8)-K(1)-O(7)	60.48(8)	O(5)-K(1)-C(61)	41.74(10)	C(2)-Si(5)-C(4)	102.8(2)
O(3)-K(1)-O(7)	135.93(9)	O(1)-K(1)-C(61)	151.56(11)	C(1)-Si(5)-C(4)	112.53(18)
O(5)-K(1)-O(7)	77.03(8)	O(7)-K(1)-C(61)	89.00(10)	C(7)-Si(6)-C(6)	103.0(2)
O(1)-K(1)-O(7)	87.78(8)	O(2)-K(1)-C(61)	109.33(10)	C(7)-Si(6)-C(5)	104.3(2)
O(8)-K(1)-O(2)	89.02(9)	O(4)-K(1)-C(61)	128.71(11)	C(6)-Si(6)-C(5)	108.4(2)
O(3)-K(1)-O(2)	79.23(9)	O(6)-K(1)-C(61)	22.91(9)	C(7)-Si(6)-C(1)	116.74(17)
O(5)-K(1)-O(2)	139.51(9)	Si(2)-Si(1)-Si(3)	113.97(6)	C(6)-Si(6)-C(1)	109.29(17)
O(1)-K(1)-O(2)	59.04(8)	Si(1)-Si(2)-Si(4)	112.84(6)	C(5)-Si(6)-C(1)	114.26(18)
O(7)-K(1)-O(2)	140.00(9)	C(15)-Si(3)-C(8)	111.13(15)	C(11)-Si(7)-C(9)	104.98(18)
O(8)-K(1)-O(4)	137.57(11)	C(15)-Si(3)-C(1)	107.44(15)	C(11)-Si(7)-C(10)	109.93(18)
O(3)-K(1)-O(4)	60.04(12)	C(8)-Si(3)-C(1)	102.89(14)	C(9)-Si(7)-C(10)	103.52(18)
O(5)-K(1)-O(4)	87.38(9)	C(15)-Si(3)-Si(1)	111.26(11)	C(11)-Si(7)-C(8)	113.24(16)
O(1)-K(1)-O(4)	78.95(10)	C(8)-Si(3)-Si(1)	107.30(10)	C(9)-Si(7)-C(8)	115.73(16)
O(7)-K(1)-O(4)	83.66(10)	C(1)-Si(3)-Si(1)	116.53(10)	C(10)-Si(7)-C(8)	108.92(17)
O(2)-K(1)-O(4)	108.42(9)	C(32)-Si(4)-C(25)	110.91(15)	C(12)-Si(8)-C(14)	111.40(18)
O(8)-K(1)-O(6)	79.66(9)	C(32)-Si(4)-C(18)	107.49(16)	C(12)-Si(8)-C(8)	111.16(16)
O(3)-K(1)-O(6)	86.04(11)	C(25)-Si(4)-C(18)	103.09(14)	C(14)-Si(8)-C(8)	112.75(16)
O(5)-K(1)-O(6)	59.13(9)	C(32)-Si(4)-Si(2)	111.55(12)	C(12)-Si(8)-C(13)	102.03(18)
C(14)-Si(8)-C(13)	106.32(19)	C(31)-Si(12)-C(29)	105.8(2)	C(65)-O(8)-K(1)	118.8(2)
C(8)-Si(8)-C(13)	112.59(16)	C(25)-Si(12)-C(29)	113.24(16)	C(66)-O(8)-K(1)	119.5(2)
C(20)-Si(9)-C(19)	107.32(19)	C(52)-O(1)-C(51)	112.1(4)	Si(5)-C(1)-Si(6)	113.55(17)
C(20)-Si(9)-C(21)	105.6(2)	C(52)-O(1)-K(1)	119.4(2)	Si(5)-C(1)-Si(3)	119.11(17)
C(19)-Si(9)-C(21)	103.37(18)	C(51)-O(1)-K(1)	122.2(3)	Si(6)-C(1)-Si(3)	118.33(17)
C(20)-Si(9)-C(18)	115.00(17)	C(54)-O(2)-C(53)	112.9(4)	Si(8)-C(8)-Si(7)	110.69(16)
C(19)-Si(9)-C(18)	112.25(16)	C(54)-O(2)-K(1)	114.1(3)	Si(8)-C(8)-Si(3)	120.14(16)
C(21)-Si(9)-C(18)	112.45(17)	C(53)-O(2)-K(1)	108.7(2)	Si(7)-C(8)-Si(3)	114.78(16)
C(23)-Si(10)-C(24)	102.5(2)	C(56)-O(3)-C(55)	111.5(5)	C(16)-C(15)-C(17)	108.6(3)
C(23)-Si(10)-C(22)	107.7(2)	C(56)-O(3)-K(1)	120.3(4)	C(16)-C(15)-Si(3)	115.6(2)
C(24)-Si(10)-C(22)	105.5(2)	C(55)-O(3)-K(1)	121.4(3)	C(17)-C(15)-Si(3)	111.9(2)
C(23)-Si(10)-C(18)	109.06(17)	C(58)-O(4)-C(57)	112.6(4)	Si(10)-C(18)-Si(9)	112.57(17)
C(24)-Si(10)-C(18)	116.71(18)	C(58)-O(4)-K(1)	111.7(3)	Si(10)-C(18)-Si(4)	118.92(17)
C(22)-Si(10)-C(18)	114.40(17)	C(57)-O(4)-K(1)	106.1(3)	Si(9)-C(18)-Si(4)	118.75(16)
C(26)-Si(11)-C(27)	105.02(18)	C(60)-O(5)-C(59)	112.2(3)	Si(12)-C(25)-Si(11)	110.78(17)
C(26)-Si(11)-C(25)	112.95(16)	C(60)-O(5)-K(1)	120.4(2)	Si(12)-C(25)-Si(4)	118.90(16)
C(27)-Si(11)-C(25)	115.87(16)	C(59)-O(5)-K(1)	122.2(3)	Si(11)-C(25)-Si(4)	114.99(16)
C(26)-Si(11)-C(28)	109.57(18)	C(62)-O(6)-C(61)	111.8(4)	C(34)-C(32)-C(33)	108.2(3)
C(27)-Si(11)-C(28)	103.48(18)	C(62)-O(6)-K(1)	116.4(3)	C(34)-C(32)-Si(4)	115.8(3)
C(25)-Si(11)-C(28)	109.41(16)	C(61)-O(6)-K(1)	105.2(2)	C(33)-C(32)-Si(4)	112.0(3)
C(30)-Si(12)-C(31)	111.96(19)	C(63)-O(7)-C(64)	111.5(3)	O(1)-C(52)-C(53)	109.3(4)
C(30)-Si(12)-C(25)	111.61(17)	C(63)-O(7)-K(1)	117.7(3)	O(2)-C(53)-C(52)	110.3(4)
C(31)-Si(12)-C(25)	112.14(16)	C(64)-O(7)-K(1)	109.5(2)	O(3)-C(56)-C(57)	109.7(5)
C(30)-Si(12)-C(29)	101.47(18)	C(65)-O(8)-C(66)	111.6(3)	O(4)-C(57)-C(56)	110.1(4)
O(5)-C(60)-C(61)	108.4(4)	O(6)-C(61)-K(1)	51.85(18)	O(7)-C(64)-C(65)	110.4(3)

O(6)-C(61)-C(60)	109.7(4)	C(60)-C(61)-K(1)	84.9(2)	O(8)-C(65)-C(64)	108.7(3)

Symmetry transformations used to generate equivalent atoms.

X-ray Crystal Structure Determination of 53

The single crystals of **53** for X-ray analysis were obtained by the recrystallization from hexane. The X-ray crystallographic experiments were performed on a MacScience DIP2030 image plate diffractometer equipped with graphite-monochromatized Mo-Kα radiation (λ = 0.71070 Å). Details of crystal data and structure refinement are summarized in Table a-**53**. The final atomic parameters, the bond lengths and the bond angles of **53** are listed in Tables b-**53** and c-**53**, respectively.

Appendix

Table a-(**38**). Crystal Data and Structure Refinement for Compound **53**.

Identification code	$[Dsi_2{}^{i}PrSiSi{\equiv}SiSi^{i}PrDsi_2]^{\cdot-}[K^{+}(toluene)_1]$
Empirical formula	$C_{41}H_{98}KSi_{12}$
Formula weight	967.37
Temperature	150.0(1) K
Wavelength	0.71070 Å
Crystal system, space group	Triclinic, P-1
Unit cell dimensions	a = 10.5260(7)Å alpha = 91.714(5) deg.
	b = 11.8840(13) Å beta = 89.729(5) deg.
	c = 25.435(3) Å gamma = 106.927(5)deg.
Volume	3042.5(5) $Å^3$
Z, Calculated density	2, 1.056 Mg/m^3
Absorption coefficient	0.349 mm^{-1}
F(000)	1062
Crystal size	0.10 x 0.10 x 0.10 mm
Theta range for data collection	2.17 to 28.07 deg.
Limiting indices	0<=h<=13, –15<=k<=14, –33<=l<=33
Reflections collected / unique	32067/ 12699 [R(int) = 0.0000]
Completeness to theta = 28.01	58.8 %
Absorption correction	None
Refinement method	Full-matrix least-squares on F^2
Data / restraints / parameters	12699/ 0 / 488
Goodness-of-fit on F^2	0.889
Final R indices [I>2sigma(I)]	R1 = 0.0555, wR2 = 0.1309
R indices (all data)	R1 = 0.1345, wR2 = 0.1524
Extinction coefficient	0.0040(4)
Largest diff. peak and hole	0.563 and –0.392 $e.Å^{-3}$

Table b-(**53**). Atomic coordinates (x 10^4) and equivalent isotropic displacement parameters ($Å^2$ x 10^3) for compound.

U(eq) is defined as one third of the trace of the orthogonalized U_{ij} tensor.

	x	y	z	U(eq)
K(1)	6554(1)	4439(1)	2599(1)	47(1)
Si(1)	1871(1)	2578(1)	2217(1)	34(1)
Si(2)	3447(1)	2577(1)	2759(1)	33(1)
Si(3)	2430(1)	3183(1)	1348(1)	26(1)
Si(4)	2642(1)	1812(1)	3586(1)	25(1)
Si(5)	1322(1)	5478(1)	1288(1)	36(1)
Si(6)	-699(1)	2954(1)	1220(1)	32(1)
Si(7)	2910(1)	2389(1)	138(1)	35(1)
Si(8)	2695(1)	520(1)	1020(1)	35(1)
Si(9)	3770(1)	-501(1)	3602(1)	35(1)
Si(10)	5733(1)	2004(1)	3819(1)	32(1)
Si(11)	2057(1)	2458(1)	4814(1)	34(1)
Si(12)	2241(1)	4397(1)	3966(1)	34(1)
C(1)	1090(3)	3878(3)	1121(2)	28(1)
C(2)	1469(4)	5772(4)	2014(2)	46(1)
C(3)	2753(4)	6452(4)	932(2)	49(1)
C(4)	-92(4)	6012(4)	1048(2)	48(1)
C(5)	-1457(4)	3396(4)	1838(2)	41(1)
C(6)	-1705(4)	3116(4)	636(2)	47(1)
C(7)	-1004(4)	1335(4)	1271(2)	50(1)
C(8)	2357(3)	1949(3)	832(1)	28(1)
C(9)	3102(4)	3947(4)	-43(2)	50(1)
C(10)	1588(5)	1514(5)	-327(2)	62(2)
C(11)	4561(5)	2195(6)	-35(2)	77(2)
C(12)	2486(5)	-529(4)	430(2)	58(1)
C(13)	1446(4)	-318(4)	1498(2)	48(1)

C(14)	4365(4)	659(5)	1312(2)	61(2)
C(15)	4184(3)	4278(4)	1326(2)	32(1)
C(16)	5252(3)	3619(4)	1322(2)	44(1)
C(17)	4543(4)	5223(4)	1774(2)	42(1)
C(18)	3933(3)	1072(3)	3825(2)	28(1)
C(19)	3825(4)	-697(4)	2865(2)	48(1)
C(20)	2240(4)	-1566(4)	3870(2)	48(1)
C(21)	5121(4)	-1062(4)	3886(2)	50(1)
C(22)	6612(4)	1766(4)	3197(2)	44(1)
C(23)	6643(4)	1718(4)	4405(2)	49(1)
C(24)	6020(4)	3645(4)	3876(2)	40(1)
C(25)	2622(3)	2983(3)	4129(2)	29(1)
C(26)	1885(5)	881(4)	4957(2)	53(1)
C(27)	3394(5)	3309(5)	5287(2)	65(2)
C(28)	410(4)	2638(5)	5004(2)	56(1)
C(29)	2415(5)	5416(4)	4566(2)	60(1)
C(30)	568(4)	4250(4)	3675(2)	58(1)
C(31)	3488(5)	5300(4)	3508(2)	54(1)
C(32)	910(3)	693(4)	3555(2)	33(1)
C(33)	-224(4)	1257(4)	3628(2)	50(1)
C(34)	587(4)	-113(4)	3066(2)	45(1)
C(50)	7719(5)	7507(4)	2347(2)	49(1)
C(51)	8836(5)	7133(4)	2407(2)	50(1)
C(52)	9113(4)	6701(4)	2881(2)	50(1)
C(53)	8263(4)	6627(4)	3298(2)	47(1)
C(54)	7140(4)	6975(5)	3235(2)	55(1)
C(55)	6856(4)	7399(4)	2765(2)	50(1)
C(56)	7466(5)	8044(5)	1845(2)	75(2)

Table c-(**53**). Bond lengths [Å] and angles [deg] for compound **53**.

K(1)-Si(2)	3.4042(15)	Si(10)-C(23)	1.868(4)	C(15)-Si(3)-C(1)	111.93(17)
Si(1)-Si(2)	2.1617(15)	Si(10)-C(22)	1.884(4)	C(8)-Si(3)-Si(1)	116.05(13)
Si(1)-Si(3)	2.3637(16)	Si(10)-C(24)	1.885(4)	C(15)-Si(3)-Si(1)	110.62(13)
Si(2)-Si(4)	2.3712(16)	Si(10)-C(18)	1.896(4)	C(1)-Si(3)-Si(1)	106.20(12)
Si(3)-C(8)	1.923(4)	Si(11)-C(28)	1.867(4)	C(32)-Si(4)-C(18)	110.25(17)
Si(3)-C(15)	1.925(4)	Si(11)-C(26)	1.876(5)	C(32)-Si(4)-C(25)	107.96(16)
Si(3)-C(1)	1.929(4)	Si(11)-C(27)	1.888(5)	C(18)-Si(4)-C(25)	104.71(17)
Si(4)-C(32)	1.919(4)	Si(11)-C(25)	1.903(4)	C(32)-Si(4)-Si(2)	113.85(13)
Si(4)-C(18)	1.930(4)	Si(12)-C(31)	1.862(4)	C(18)-Si(4)-Si(2)	104.61(11)
Si(4)-C(25)	1.935(4)	Si(12)-C(30)	1.871(4)	C(25)-Si(4)-Si(2)	114.99(13)
Si(5)-C(3)	1.861(4)	Si(12)-C(25)	1.896(4)	C(3)-Si(5)-C(2)	111.6(2)
Si(5)-C(2)	1.867(4)	Si(12)-C(29)	1.895(5)	C(3)-Si(5)-C(1)	111.93(18)
Si(5)-C(1)	1.880(4)	C(15)-C(17)	1.542(5)	C(2)-Si(5)-C(1)	111.17(19)
Si(5)-C(4)	1.890(4)	C(15)-C(16)	1.546(5)	C(3)-Si(5)-C(4)	101.4(2)
Si(6)-C(7)	1.865(5)	C(32)-C(34)	1.523(6)	C(2)-Si(5)-C(4)	107.4(2)
Si(6)-C(6)	1.874(4)	C(32)-C(33)	1.538(5)	C(1)-Si(5)-C(4)	112.95(19)
Si(6)-C(5)	1.889(4)	C(50)-C(51)	1.383(6)	C(7)-Si(6)-C(6)	104.6(2)
Si(6)-C(1)	1.903(4)	C(50)-C(55)	1.379(6)	C(7)-Si(6)-C(5)	104.2(2)
Si(7)-C(11)	1.867(4)	C(50)-C(56)	1.504(6)	C(6)-Si(6)-C(5)	109.29(18)
Si(7)-C(9)	1.874(5)	C(51)-C(52)	1.388(6)	C(7)-Si(6)-C(1)	116.99(17)
Si(7)-C(10)	1.876(5)	C(52)-C(53)	1.374(6)	C(6)-Si(6)-C(1)	108.60(19)
Si(7)-C(8)	1.898(4)	C(53)-C(54)	1.373(6)	C(5)-Si(6)-C(1)	112.67(18)
Si(8)-C(13)	1.869(4)	C(54)-C(55)	1.379(6)	C(11)-Si(7)-C(9)	102.9(2)
Si(8)-C(14)	1.873(4)			C(11)-Si(7)-C(10)	111.0(3)
Si(8)-C(12)	1.892(5)	Si(2)-Si(1)-Si(3)	118.76(6)	C(9)-Si(7)-C(10)	103.1(2)
Si(8)-C(8)	1.908(4)	Si(1)-Si(2)-Si(4)	112.73(6)	C(11)-Si(7)-C(8)	113.7(2)
Si(9)-C(20)	1.875(4)	Si(1)-Si(2)-K(1)	120.40(6)	C(9)-Si(7)-C(8)	117.71(18)
Si(9)-C(19)	1.886(4)	Si(4)-Si(2)-K(1)	122.56(5)	C(10)-Si(7)-C(8)	107.9(2)
Si(9)-C(21)	1.893(4)	C(8)-Si(3)-C(15)	107.68(16)	C(13)-Si(8)-C(14)	106.2(2)
Si(9)-C(18)	1.896(4)	C(8)-Si(3)-C(1)	104.26(17)	C(13)-Si(8)-C(12)	103.5(2)
C(14)-Si(8)-C(12)	107.0(2)	C(24)-Si(10)-C(18)	115.80(16)	Si(6)-C(1)-Si(3)	115.6(2)
C(13)-Si(8)-C(8)	111.89(17)	C(28)-Si(11)-C(26)	103.6(2)	Si(7)-C(8)-Si(8)	112.52(18)
C(14)-Si(8)-C(8)	116.4(2)	C(28)-Si(11)-C(27)	110.7(2)	Si(7)-C(8)-Si(3)	117.9(2)
C(12)-Si(8)-C(8)	110.84(19)	C(26)-Si(11)-C(27)	103.6(2)	Si(8)-C(8)-Si(3)	121.3(2)
C(20)-Si(9)-C(19)	110.1(2)	C(28)-Si(11)-C(25)	114.01(19)	Si(12)-C(25)-Si(11)	113.04(18)
C(20)-Si(9)-C(21)	101.4(2)	C(26)-Si(11)-C(25)	117.66(18)	Si(12)-C(25)-Si(4)	121.1(2)
C(19)-Si(9)-C(21)	107.1(2)	C(27)-Si(11)-C(25)	106.8(2)	Si(11)-C(25)-Si(4)	118.1(2)
C(20)-Si(9)-C(18)	112.10(18)	C(31)-Si(12)-C(30)	106.7(2)	C(51)-C(50)-C(55)	118.2(4)
C(19)-Si(9)-C(18)	113.1(2)	C(31)-Si(12)-C(25)	111.84(18)	C(51)-C(50)-C(56)	121.0(5)
C(21)-Si(9)-C(18)	112.22(19)	C(30)-Si(12)-C(25)	116.8(2)	C(55)-C(50)-C(56)	120.7(5)
C(23)-Si(10)-C(22)	110.10(19)	C(31)-Si(12)-C(29)	102.3(2)	C(50)-C(51)-C(52)	121.2(4)
C(23)-Si(10)-C(24)	102.3(2)	C(30)-Si(12)-C(29)	106.6(2)	C(53)-C(52)-C(51)	120.0(4)
C(22)-Si(10)-C(24)	104.84(19)	C(25)-Si(12)-C(29)	111.5(2)	C(54)-C(53)-C(52)	118.8(5)
C(23)-Si(10)-C(18)	110.76(19)	Si(5)-C(1)-Si(6)	111.73(17)	C(53)-C(54)-C(55)	121.5(4)
C(22)-Si(10)-C(18)	112.39(18)	Si(5)-C(1)-Si(3)	118.3(2)	C(50)-C(55)-C(54)	120.2(4)

Symmetry transformations used to generate equivalent atoms.

Reference

1. For examples of Group 14 radicals, see: (a) Bennett, S. W.; Eaborn, C.; Hudson, A.; Jackson, R. A.; Root, K. D. J. *J. Chem. Soc. (A)* **1970**, 348. (b) Cotton, J. D.; Cundy, C. S.; Harris, D. H.; Hudson, A.; Lappert, M. F.; Lednor, P. W. *J. Chem. Soc., Chem. Commun.* **1974**, 651. (c) Hudson, A.; Lappert, M. F.; Lednor, P. W. *J. Chem. Soc., Dalton Trans.* **1976**, 2369. (d) Gynane, M. J. S.; Lappert, M. F.; Riley, P. I.; Rivie彳re, P.; Riviére-Baudet, M. *J. Organomet. Chem.* **1980**, *202*, 5. (e) Sakurai, H.; Umino, H.; Sugiyama, H. *J. Am. Chem. Soc.* **1980**, *102*, 6837. (f) McKinley, A. J.; Karatsu, T.; Wallraff, G. M.; Miller, R. D.; Sooriyakumaran, R.; Michl, J. *Organometallics* **1988**, *7*, 2567. (g) McKinley, A. J.; Karatsu, T.; Wallraff, G. M.; Thompson, D. P.; Miller, R. D.; Michl, J. *J. Am. Chem. Soc.* **1991**, *113*, 2003. (h) Kyushin, S.; Sakurai, H.; Betsuyaku, T.; Matsumoto, H. *Organometallics* **1997**, *16*, 6, 5386. (i) Olmstead M. M.; Pu, L.; Simons, R. S.; Power, P. P. *Chem. Commun.* **1997**, 1595. (j) Kyushin, S.; Sakurai, H.; Matsumoto, H. *Chem. Lett.* **1998**, 107. (k) Kira, M.; Obata, T.; Kon, I.; Hashimoto, H.; Ichinohe, M.; Sakurai, H.; Kyushin, S.; Matsumoto, H. *Chem. Lett.* **1998**, 1097. (l) Apeloig, Y.; Bravo-Zhivotovskii, D.; Yuzefovich, M.; Bendikov, M.; Shames, A. I. *Appl. Magn. Reson.* **2000**, *18*, 425. (m) Sekiguchi, A.; Matsuno, T.; Ichinohe, M. *J. Am. Chem. Soc.* **2001**, *123*, 12436. (n) Matsuno, T.; Ichinohe, M.; Sekiguchi, A. *Angew. Chem., Int. Ed.* **2002**, *41*, 1575. (o) Sekiguchi, A.; Fukawa, T.; Nakamoto, M.; Lee, V. Ya.; Ichinohe, M. *J. Am. Chem. Soc.* **2002**, *124*, 9865. (p) Ishida, S.; Iwamoto, T.; Kira, M. *J. Am. Chem. Soc.* **2003**, *125*, 3212. (q) Tumanskii, B.; Pine, P.; Apeloig, Y.; Hill, J. N.; West, R. *J. Am. Chem. Soc.* **2004**, *126*, 7786.: see the review; (r) Sakurai, H. *Free Radicals*; Kochi, J. K., Ed.; John Wiley & Sons Ltd.: New York, 1973; Vol. II. (s) Chatgilialoglu, C. *Chem. Rev.* **1995**, *95*, 1229. (t) Iley, J. In *The Chemistry of Organic Germanium, Tin and Lead Compounds*; Patai, S., Rappoport, Z., Eds.; John Wiley & Sons Ltd.: Chichester, 1995; Chapter 5. (u) Power P. P. *Chem. Rev.* **2003**, *103*, 789. (v) Lee, V. Ya.; Fukawa, T.; Nakamoto, M.; Sekiguchi, A.; Tumanskii, B. L.; Karni, M.; Apeloig, Y. *J. Am. Chem. Soc.* **2006**, *128*, 11643.
2. (a) Weidenbruch, M.; Kramer, K.; Schaéfer, A.; Blum, J. K. *Chem. Ber.* **1985**, *118*, 107. (b) Weidenbruch, M.; Thom, K.-L. *J. Organomet. Chem.* **1986**, *308*, 177.

3. Kira, M.; Iwamoto, T. *J. Organomet. Chem.* **2000**, *611*, 236.
4. Sekiguchi, A.; Inoue, S.; Ichinohe, M.; Arai, Y. *J. Am. Chem. Soc.* **2004**, *126*, 9626.
5. Pu, L.; Phillips, A. D.; Richards, A. F.; Stender, M.; Simons, R. S.; Olmstead, M. M.; Power. P. P. *J. Am. Chem. Soc.* **2003**, *125*, 11626.
6. (a) Sekiguchi, A.; Kinjo, R.; Ichinohe, M. *Science* **2004**, *305*, 1755. (b) Sekiguchi, A.; Kinjo, R.; Ichinohe, M. *Bull. Chem. Soc. Jpn.* **2006**, *79*, 825. (c) Frenking, G.; Krapp, A.; Nagase, S.; Takagi, N.; Sekiguchi, A. *ChemPhysChem*. **2006**, *7*, 799. (d) Kravchenko, V.; Kinjo, R.; Sekiguchi, A.; Ichinohe, M.; West, R.; Balazs, Y. S.; Schmidt, A.; Karni, M.; Apeloig, Y. *J. Am. Chem. Soc. 128*, 14472, **2006**.

List of Publications

(1) ‘An Isolable Disilyne Anion Radical and a New Route to the Disilenide Ion upon Reduction of a Disilyne’
R. Kinjo, M. Ichinohe, A. Sekiguchi, *J. Am. Chem. Soc. 129*, 26, **2007**.

(2) ‘A Solid-State ^{29}Si NMR Study of RSiSiR - A Tool for Analyzing the Nature of the Si-Si Bond’
V. Kravchenko, R. Kinjo, A. Sekiguchi, M. Ichinohe, R. West, Y. S. Balazs, A. Schmidt, M. Karni, and Y. Apeloig, *J. Am. Chem. Soc. 128*, 14472, **2006**.

(3) ‘The Chemistry of Disilyne with a Genuine Si–Si Triple Bond: Synthesis, Structure, and Reactivity’
A. Sekiguchi, M. Ichinohe, and R. Kinjo, *Bull. Chem. Soc. Jpn (Account), 79*, 825, **2006**.

(4) ’The First Stable Silicon-Silicon Triple Bond Species’
A. Sekiguchi, R. Kinjo, M. Ichinohe, *Science 305*, 1755, **2004**.

(5) ‘The First Stable Methyl-Substituted Disilene: Synthesis, Crystal Structure, a Regiospecific MeLi Addition’
M. Ichinohe, R. Kinjo, A. Sekiguchi, *Organometallics 22*, 4621, **2003**.

(6) ‘Tetrasilatetrahedranide: A Silicon Cage Anion’
M. Ichinohe, M. Toyoshima, R. Kinjo, A. Sekiguchi, *J. Am. Chem. Soc.* 125, 13328, **2003**.

Acknowledgement

The studies described in this dissertation have been carried out under the direction of Professor Akira Sekiguchi at the Department of Chemistry, Graduated School of Pure and Applied Sciences, University of Tsukuba. These works were supported by Research Fellowships of the Japan Society for the Promotion of Science for Young Scientist and 21st century COE (Center of Excellence) program.

The author sincerely wishes to express great thanks to Professor Akira Sekiguchi for his continuing guidance and valuable discussions and encouragement throughout the course of studies. Grateful acknowledgement is made to Professor Yoshio Kabe, Associate Professor Masaaki Ichinohe, Dr. Masaaki Nakamoto, and Norio Nakata for their helpful discussions and suggestions. The author would express his sincerest gratitude to Dr. Vladimir Ya. Lee for his continuing advice and kindly discussions, and for reading the entire text in his original form and making of helpful suggestions.

The author is very grateful to Dr. Norihisa Fukaya, Dr. Tadahiro Matsuno, Dr. Yutaka Ishida for their passionate discussions, helpful suggestions, and kindness. The author would express his appreciation to Dr. Masanobu Tanaka, Dr. Takashi Tanaka, Dr. Tomohide Fukawa, Mr. Yuuichi Hayata, Ms. Rika Izumi for their helpful discussions.

The author really respects Mr. Masaaki Toyoshima for his discovery of tetrasilatetrahedorane, which opened the root to prepare the disilyne. The author would express his honest gratitude to special rival, Mr. Tomoyasu Honda, for his continuing effort to establish his chemistry.

The author is grateful to Mr. Yasuyuki Murakami, Mr. Takeshi Matsumoto, Ms. Kaori Sanuki, Mr. Shigeyoshi Inoue, Mr. Toru Oikawa, Mr. Kazunori Takanashi, Mr. Masayasu Igarashi, Mr. Kousuke Shimizu, Mr. Hiroyuki Yasuda for their helpful, daily discussions, and friendship. The author would express appreciation to Mr. Hideki Yamauchi for his helpful and special friendship. The author thanks to all members of Professor Sekiguchi's group for their kind assistance.

The author wishes to thank to Professor Shigeru Nagase and Dr. Nozomi Takagi for helpful discussions about the theoretical investigations and collaborations. The author wishes to thank Professor Yitzhak Apeloig, Dr. Victoria Kravchenko, Dr. Yael S. Balazs, Dr. Asher Schmidt, Dr. Miriam Karni (Technion-Isreal Institute of Technology), and Robert West (University of Wisconsin) for discussion and collaborations in solid ^{29}Si NMR measurement and calculation.

The author thanks to all his friends for their kind assistance and continuous encouragement and support. Finally, the author would like to thank his parents Mr. Hiroyoshi Kinjo and Ms. Sumiko Kinjo, and his brother Mr. Yuuki Kinjo and Syo Kinjo, and his home island, Okinawa very much for their kindly continuous encouragement and support in all his life, and providing the very comfortable environment to concentrate on research.

February, 2007

Rei KINJO